DEVELOPMENT OF AN ACID-BASE-NEUTRAL SEPARATION SCHEME AND ITS APPLICATION TO ALTERNATIVE FUEL MIXTURES

Fernando M. Lanças, E.M. Soares, H.S. Karam
Universidade de São Paulo
Instituto de Física e Química de São Carlos
13560 - São Carlos (SP) - BRASIL

and

Harold M. McNair
Virgina Polytechnic Institute and State University
Blacksburg, VA, 24061 - U.S.A.

INTRODUCTION

Alternative fuels, such as solvent-refined coal (SRC), shale oil, and biomass, are gaining more importance as energy sources, as the scarcity of crude oil increases. Fractionation of these fuels into acidic, basic and neutral components is a generally accepted method of separation that has been widely applied for the characterization of coal-derived liquids (1-6) and shale oil (7,8). Various schematics have been utilized for this kind of separation, among which aqueous extraction (1,7,10,11), ion exchange chromatography (6,9, 12) and selective isolation of N-containing compounds by HCl-precipitation (2,3,5) or organometallic-coordination chromatography (6,12,13) have been the most commonly used.

Many of these schematics possess a number of disadvantages and/or limitations. The limited solubility of the protonated bases in the aqueous acid (aqueous acid extraction) (11,14) and the selective precipitation of the aromatic bases by HCl (HCl precipitation)   (15)   are just examples. The work by several authors (10,11,14,15) demonstrates that the basic fractions generated by different base isolation methods are not identical, and in some cases posses significant structural differences (15).

The inadequacy of the existing methods, in their present form, suggested to us that there is a need for a general and integrated acid base-neutral separation schematic. Such a schematic should be applicable to various kinds of liquid fuels, should avoid any extraction or precipitation steps and rely instead on chromatography. We have undertaken the development of this separation scheme using a large number of standards that represent the various chemical classes generally found in liquid fuels.

One "silica gel modified with KOH" column and one cation exchange resin column were employed for the fractionation. Mixtures of the various standards, as well as the alternative fuels, were separated into acids, bases and neutrals fractions which were then characterized by Gas Chromatography/Mass Spectrometry (GC/MS).

EXPERIMENTAL

Preparation of the packing materials for column-chromatography

Amberlyst 15, the cation-exchanger utilized, and the silica treated with KOH, were prepared according to the literature (9,16). In this work, 20 gm of the

cation-exchange resin,slurried in tetrahydrofuran; and 20 gm of the KOH trea-
ted silica, slurried in isopropanol-chloroform mixture, each was mechanically
stirred for 30 minutes before being introduced into a 500 x 11 mm I.D. glass
colunm fitted with a teflon stopcock and a piece of glass wool to retain the
packing material. The modified silica column was then washed with 100 ml of
chloroform while the resin column with 100 ml of n-hexane, each solvent of
which serving as a first eluent.

Fractionation of standard mixtures on both columns

Separate mixtures of acids, bases and neutrals standards were prepared so as
to contain 300 mg/ml of tetrahydrofuran. The composition of these standards
appears in Table 1. The retention behaviour of the separate mixtures, on both
columns, was monitored gravimetrically (and later studied by GC/MS) by injec-
ting 1 ml of each mixture on each of the two columns and collecting fractions
in vials of 5 ml each. Fractions were evaporated to constant weight by placing
the vials in a, home-made, water bath-heated block, set at 70°C and passing
Nitrogen at a low pressure. Figure 1 outlines the schematic used to fractio-
nate a total mixture of the standards, and later applied to the liquid fuels,
along with the eluents utilized to provide the optimum conditions for the
separation.

Gas Chromatography-Mass Spectrometry: Experimental Conditions

The GC/MS system used was an HP 5995 B equipped with a library search system.
The mass spectrometer was used in the electron impact (EI) mode with an ioni-
zation potential of 70 eV. Gas Chromatographic conditions appear as a footno-
te in Table 1. Standards were chromatographed individually and in their res-
pective mixtures of acids, bases or neutrals to determine their retention
characteristics and the best resolution conditions.

RESULTS & DISCUSSION

Chromatogram 1 shows the total mixture of acids, bases and neutrals standards
before fractionation, while chromatograms 2, 3 and 4 are for the acidic, ba-
sic and neutral fractions,respectively,after the total mixture has been suc-
cessively separated on cation-exchange and silica modified columns, according
to the developed schematic in Fig. 1. Chromatograms 2 - 4 were generated un-
der identical chromatographic conditions for comparison purposes. These con-
ditions along with peak numbers identification appear in Table 1.

Chromatogram 1, in addition to being complex, shows that co-elution of seve-
ral of the components is inevitable, even with the slow temperature programm
employed. These problems are overcome after the total mixture is fractionated,
as chromatograms 2 - 4 confirm.

Chromatogram 2 shows that the acidic fraction is pure; no overlap of basic or
neutral components has been detected by GC/MS. Chromatogram 3 demonstrates
that the basic fraction is slightly contaminated with some acidic components
(peaks 31, 33, 39 and 41). The contamination levels are low as indicated by
the relative peak areas measurement. The only contamination of the neutral
components, in this same chromatogram, comes from 2-methyl indole (peak 34).
This compound behaves as a week base and can easily be trapped by a strong
cation-exchanger. This phenomenon is further emphasized in chromatogram 4
for the neutral fraction which shows the complete absence of 2-methyl indole.

The strong overlap of 2-sec-butylphenol (peak 24) and 3-t-butylphenol (peak 25) with the neutral fraction in chromatogram 4, could be due to the steric hindrance of the bulky buthyl groups to adsorption of these respective phenols on the basic silica surface.

Chromatogram 5 shows a basic fraction isolated form a typical Brazilian SRC (Mina do Leão) using the developed schematic. Conditions are the same as in Table 1 except that a 5ºC/min temperature programn was used.

A portion of the total ion chromatogram (T.I.C.) for this same fraction is displayed in chromatogram 6. Both the gas chromatogram and the total ion chromatogram indicate that the various basic components have been well resolved which makes their identification (not attempted) quite possible specially knowing that this fraction should contain the basic compounds as the results in chromatogram 3 indicate.

In conclusion, this work suggests that using the developed schematic any mixture containing acidic, basic and neutral components can be effectively separated into its respective chemical classes, with a minimum overlap among these classes. The method can be refined a little more so as to yield even purer fractions. Work along these lines is under study.

REFERENCES

(1) Paudler, W. and M. Cheplen, Fuel 58, 775 (1979).

(2) Hausler, D., J.W. Hellgeth, L.T. Taylor, J. Borst and W.B. Cooley, Fuel 60, 40 (1981).

(3) Bockrath, B.C., C.L.D. Donne, F.K. Schweighardt, Fuel 57 (1) 4 (1978).

(4) Dutta, P.K. and R.J. Halland, Fuel 63, 197 (1984).

(5) Sternberg,H.W., R. Raymond and F.K. Schweighardt,Science 188, 149 (1975).

(6) Francisco, M.A. and J.G. Speight, Am. Chem. Soc. Fuel Chem. Div. Prepr. 29 (1) 26 (1984).

(7) Hertz, H.S., J.M. Brown, S.N. Chesler and S.A. Wise, Anal. Chem. 52, 1650 (1980).

(8) McKay, T.F., M.M. Boduszynski and D.R. Laltham,Liquid Fuels Technology 1 (1) 35 (1983).

(9) Jewell, D.M., J.H. Weber, J.W. Bunger, H. Planchar and D.R. Laltham, Anal. Chem. 44 (8) 1391 (1972).

(10) Burchill, P., A.A. Herod and E. Pritchard, J. Chrom. 246, 271 (1981).

(11) Burchill, P. A.A. Herod and E. Pritchard, Fuel 62, 20 (1983).

(12) Altgelt, K.H. D.M. Jewell, D.R. Laltham and M.L. Selucky, Chromatogr. in Pet. Anal., Marcel Dekker, New York, Ch. 9, pp. 185-214 (1979).

(13) Ibid, Ch. 11, pp. 273-286.

(14) Burchill, P., A.A. Herod, J.P. Mahon and E. Pritchard, J. Chrom. 265, 223 (1983).

(15) Finseth, D.H., Z.T. Przyslski and C.E. Schmidt, Fuel 6, 1174 (1982).

(16) Ramijak, Z., A. Šolc, P. Arpino, J.M. Schmitter and G. Guiochon, Anal. Chem. 49, 1222 (1977).

TABLE 1 – Composition of Standards Utilized for Preparative Acid-Base-Neutral Separation. Numbers Correspond to Peaks in Chromatograms 1-4*

PEAK NUMBER	COMPONENT	PEAK NUMBER	COMPONENT	PEAK NUMBER	COMPONENT
1	Cyclohexyl Acetate	15	8-Methyl-Quinoline	29	3-t-Butyl Phenol
2	Phenetole	16	Phenol	30	2-Amino Teralin
3	5-Ethyl, 2-Methyl Pyridine	17	0-Cresol	31	P-Methoxy Phenol
4	Benzyl-Ethyl-Ether	18	Diphenyl Ether	32	Indole
5	N, N-Dimethyl Aniline	19	1,2,3,4-Tetrahydro-Quinoline	33	m-Methoxy Phenol
6	2,3-Dihydro,2-methyl-Benzofuran	20	2,6-Dimethyl-Quinoline	34	2-Methyl Indole
7	2,3-Dihydro-Benzofuran	21	P-Cresol	35	2,3-Dimethyl Indole
8	N-Methyl Aniline	22	1-Indanol	36	Dibenzothiophene
9	Aniline	23	4-Ethyl Phenol	37	7,8-Benzoquinoline
10	2,4-Dimethyl Aniline	24	2-Sec-Butyl Phenol	38	Acridine
11	0-Ethyl Aniline	25	2-Phenyl-Pyridine	39	2-Naphthol
12	Benzyl Alcohol	26	3-Phenyl-Pyridine	40	1,2,3,4-Tetrahydro-Carbazole
13	2-Amino Pyridine	27	Dibenzofuran	41	Resorcinol
14	Quinoline	28	Capric Acid	42	Carbazole

* CHROMATOGRAPHIC CONDITIONS: 50 m x 0.2 mm I.D. Fused Silica Carbowax 20 M Capillary; Column Temperature: 60°C Isothermal for 5 min, then 2°C/min temperature program to 240°. Flame Ionization Detector 280°C; Injector 250°C. Carrier Gas Helium at 1 ml/min. Split Ratio 1:15.
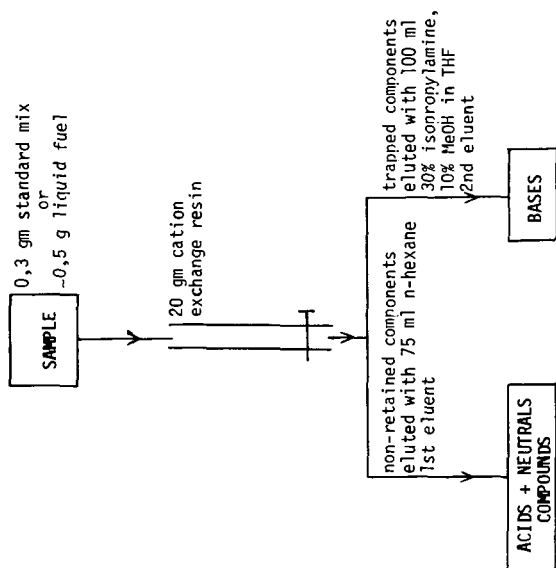
276

SAMPLE | 0,3 gm standard mix
or
~0,5 g liquid fuel

20 gm cation exchange resin

non-retained components eluted with 75 ml n-hexane 1st eluent

trapped components eluted with 100 ml 30% isopropylamine, 10% MeOH in THF 2nd eluent → BASES

ACIDS + NEUTRALS COMPOUNDS

20 gm silica "modified with KOH" column

non-retained components eluted with 75 ml $CHCl_3$ 1st eluent → NEUTRALS

trapped components eluted with 75 ml 20% Formic Acid in THF 2nd eluent → ACIDS

FIGURE 1- Separation Scheme Developped for Fractionating Liquid Fuels into Acids, Bases and Neutrals Components.
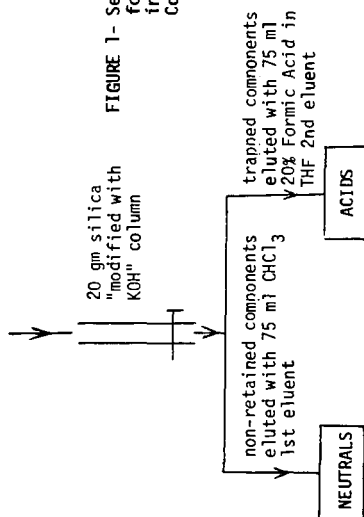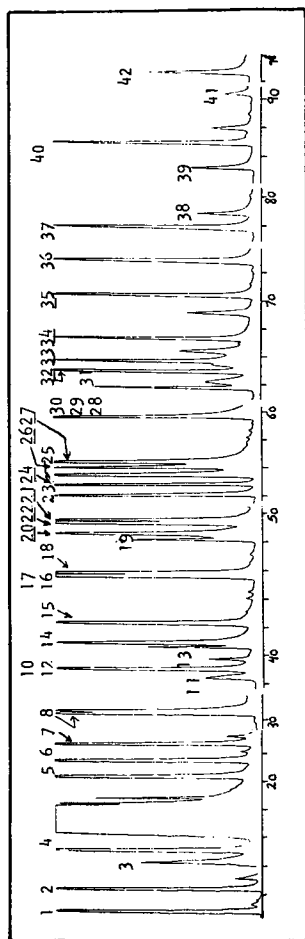
Figure 1. TOTAL MIXTURE OF ACIDS, BASES AND NEUTRALS STANDARDS BEFORE FRACTIONATION. CONDITIONS SAME AS TABLE 1.
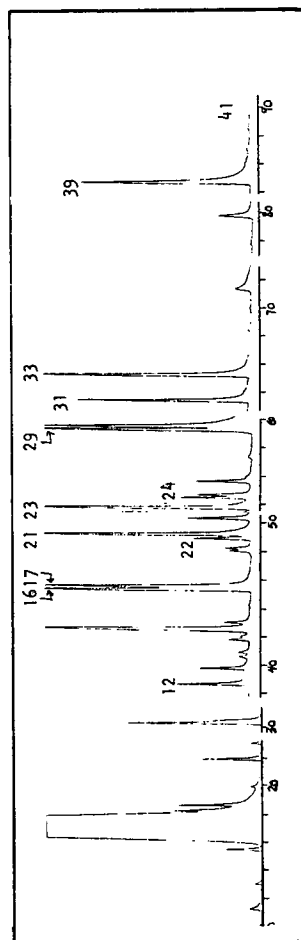

Figure 2. ACID FRACTION OBTAINED AFTER FRACTIONATION. CONDITIONS SAME AS TABLE 1.
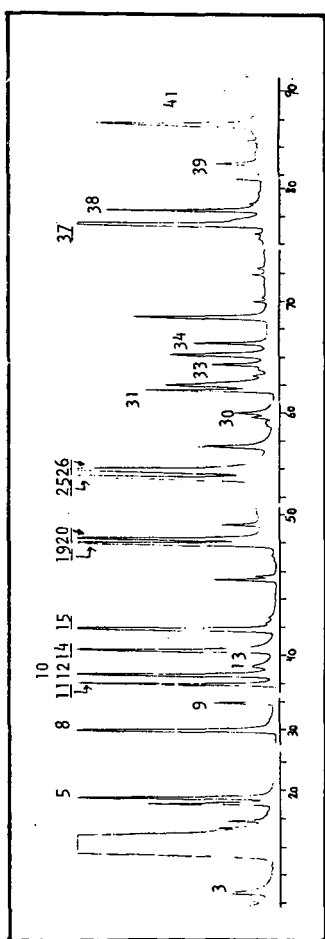
Figure 3. BASIC FRACTION OBTAINED AFTER FRACTIONATION. CONDITIONS SAME AS IN TABLE 1.
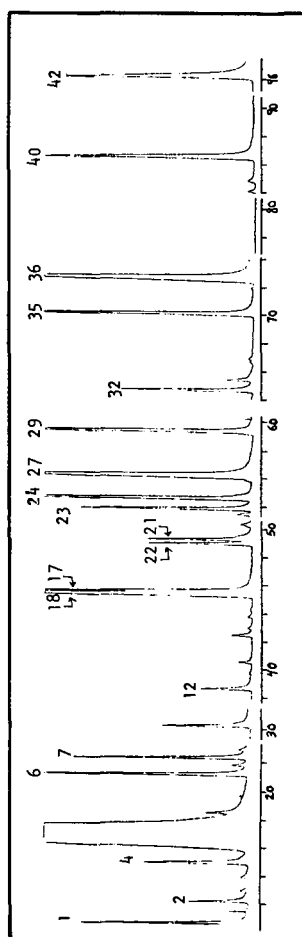

Figure 4. NEUTRAL FRACTION OBTAINED AFTER FRACTIONATION. CONDITIONS SAME AS IN TABLE 1.
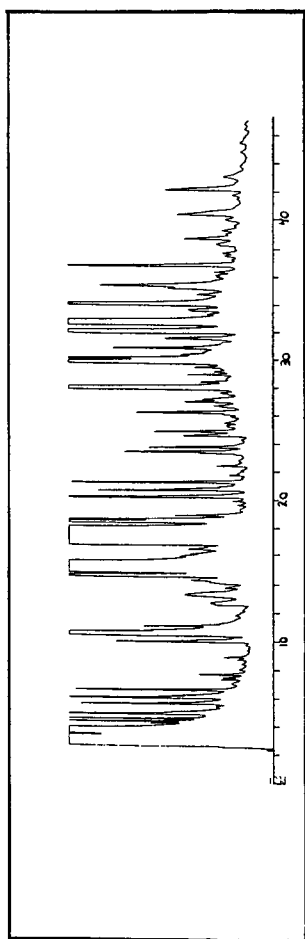
Figure 5.   BASIC FRACTION ISOLATED FROM BRAZILIAN SRC (Mina do Leão).
            CONDITIONS SAME AS IN TABLE 1, EXCEPT TEMPERATURE PROGRAMN 5°C/MIN.
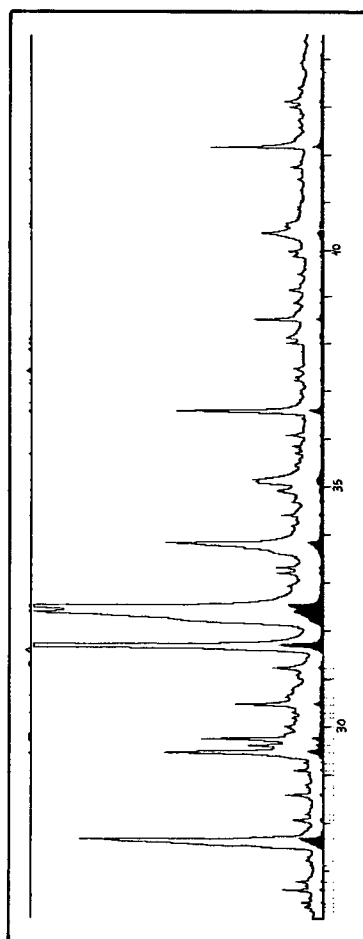
Figure 6.   A PORTION OF THE TOTAL ION CHROMATOGRAM(T.I.C.) FOR BASIC FRACTION ISOLATED FROM
            Mina do Leão SRC. CONDITIONS SAME AS IN FIGURE 5.

CHEMICAL AND BIOLOGICAL EVALUATION OF OILS AND TARS PRODUCED UNDER VARYING COAL DEVOLATILIZATION CONDITIONS

Vassilis C. Stamoudis

Geochemistry Section
Energy and Environmental Systems Division
Argonne National Laboratory
Argonne, IL 60439

INTRODUCTION

Oils and tars are among the major coal-gasification by-products having potentially adverse health and environmental consequences. The production of oils and tars during gasification, pyrolysis, and hydropyrolysis is related to the initial coal devolatilization reactions. The yield has been shown to vary with temperature, pressure, residence time, gas/solid contact, gaseous environment, and presence of catalytic surfaces. Further, coal-gasification oils and tars have been shown to contain toxic chemicals, including polynuclear aromatic amines and hydrocarbons [1-4]. A comprehensive report of an extensive study relating process conditions to chemical and toxicological characteristics of coal-gasification oils and tars has been published [5]. A summary of some of the results and important findings is presented here.

EXPERIMENTAL

Experiments were conducted in a 2-lb/hr entrained-flow reactor operated by the Mellon Institute, in close cooperation with Environmental Research and Technology, Inc. The samples were analyzed by Argonne National Laboratory. Forty-nine successful runs of the reactor covered the following conditions: (a) reactor temperatures = $600°C$, $800°C$, and $1000°C$; (b) gas-phase residence times = 0.2 s and 1.3 s; (c) reactor pressures = 3 atm and 10 atm; (d) reactant gases = He, H_2, CO_2, and steam; and (e) coal types = lignite and subbituminous coal. The organic by-products were trapped by means of three successive traps, and the trapped condensates were combined in proportion to the amounts produced. The combined oil/tar samples were then analyzed for organic compounds using computer-controlled, fused-silica, capillary-column gas chromatography (GC) (Hewlett-Packard 5880A). The aromatic relative retention index (RRI) [5,6] and the concentration of each peak were calculated and printed using custom software. GC/mass spectrometry (GC/MS) was used as necessary to confirm that the correct name was assigned to each RRI.

The Ames mutagenicity of the heavy tar trap samples was measured using the Ames assay (Salmonella TA98 strain with S-9 activation) [5]. All process conditions and chemical and toxicological data were entered into a mainframe computer, where the data were analyzed with great ease and flexibility by applying statistical analysis routines (CMS/SAS).

RESULTS AND DISCUSSION

The chemical composition of the combined oil/tar samples (Fig. 1), varied considerably, but the samples consisted mainly of aromatic compounds of one to four rings (Fig. 2). Therefore, the combined oil/tar samples were monitored routinely by RRI-GC for 62 chemicals, mainly one- to four-ring aromatic hydrocarbons (ranging from benzene to chrysene), and certain phenols and naphthols, acetophenone, indole, benzothiophene, benzofurans, and dibenzofuran.

In general, the most important of the process variables affecting chemical composition and mutagenicity was temperature. As seen in Fig. 1, the 1000°C-run samples were simpler mixtures in which phenols were absent and the level of alkylation was much reduced (Fig. 3). The amount of chromatographable material in these samples was very high. The mutagenicity of the heavy tar trap samples from the 1000°C runs was moderate (Fig. 4). Because the 600°C-run mixtures were much more complex, an additional 44 chemicals were monitored for several of these samples. The amount of phenols was high, and more polar and higher molecular weight materials were present, making the amount of nonchromatographable material higher. However, the muta-genicity associated with the 600°C-run heavy tar trap samples was very low. The 800°C-run combined oil/tar samples had both of the above characteristics -- a clearly higher degree of alkylation, intermediate chromatographability, and high mutagenicity (Fig. 4).

CONCLUSIONS

The results of this study suggest that changes in coal devolatilization conditions can significantly alter the chemical composition and toxicological properties of by-product oils and tars. The results also emphasize the importance of computer-assisted chromatographic analysis and data handling. Further, information of this kind is very useful in helping managers and engineers to design and build energy efficient and environmentally acceptable coal-conversion facilities.

ACKNOWLEDGMENTS

REFERENCES

[1]   Stamoudis, V.C., S. Bourne, D.A. Haugen, M.J. Peak, C.A. Reilly Jr., J.R. Stetter, and K. Wilzbach, *Chemical and Biological Characterization of High-Btu Gasification (The HYGAS Process), I: Chemical Characterization of Mutagenic Fractions,* in Coal Conversion and the Environment: Chemical, Biological, and Ecological Considerations, D.D. Mahlum, R.H. Gray, and W.D. Felix, eds., U.S. Department of Energy, CONF-80-1039, pp. 67-95 (1981).

[2]   Stamoudis, V.C., D.A. Haugen, M.J. Peak, and K.E. Wilzbach, *Bio-Directed Chemical Characterization of Condensates from Synfuel Processes*, in Advanced Techniques in Synthetic Fuel Analysis, C.W. Wright, W.C. Weimer, and W.D. Felix, eds., U.S. Department of Energy, CONF-81-1160 (PNL-SA-11552), pp. 201-214 (1983).

[3]   Haugen, D.A., M.J. Peak, K.M. Suhrbier, and V.C. Stamoudis, *Isolation of Mutagenic Aromatic Amines from a Coal-Conversion Oil by Cation-Exchange Chromatography*, Analytical Chemistry, 54:32-37 (1982).

[4]   Haugen, D.A., V.C. Stamoudis, M.J. Peak, and A.S. Boparai, *Isolation of Mutagenic Polycyclic Aromatic Hydrocarbons from Tar Produced during Coal Gasification*, in Polynuclear Aromatic Hydrocarbons: Formation, Metabolism, and Measurement, M. Cook and A.J. Dennis, eds., Battelle Press, Columbus, Ohio, pp. 607-620 (1983).

[5]   Fillo, J.P., V.C. Stamoudis, J.R. Stetter, and S.W. Vance, *Influence of Coal Devolatilization Conditions on the Yield, Chemistry, and Toxicology of By-Product Oils and Tars*, U.S. Department of Energy, DOE/ET-14746-11 (ANL/SER-2), 243 pp. (1983).

[6]   Stamoudis, V.C., *A Gas Chromatographic Scheme, Based on Relative Retention Indices, for Rapid Quantitative and Qualitative Analysis*, Pittsburgh Conf. on Analytical Chemistry and Applied Spectroscopy, Atlantic City, N.J., Paper No. 72, (March 1982).
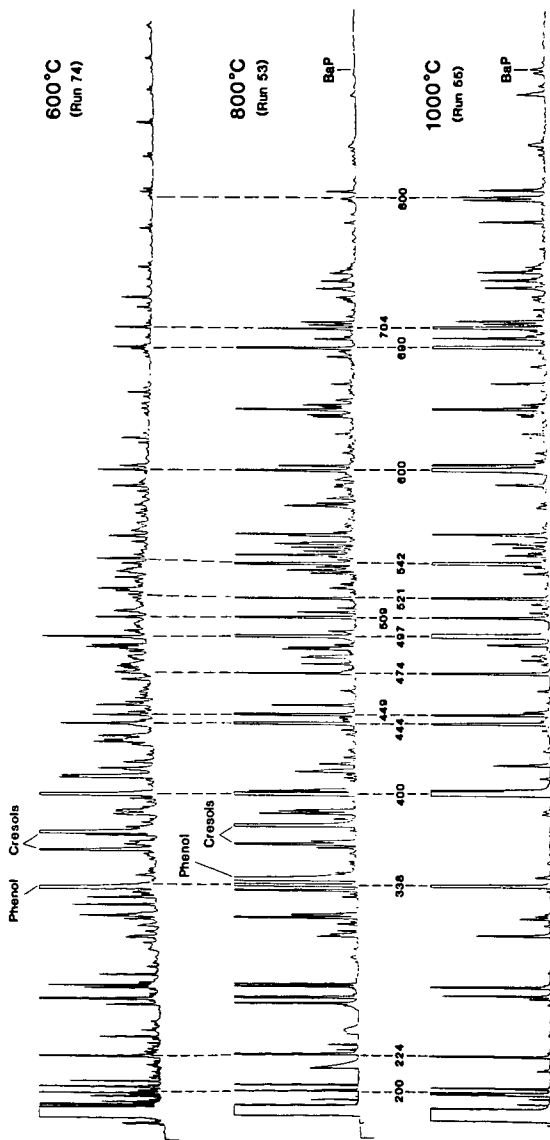
FIGURE 1 Typical GC Chromatograms for Combined Oil/Tar Samples Produced at 600°C, 800°C, and 1000°C (Peaks are labeled with the RRI: 200, benzene; 224, toluene; 338, indene; 400, naphthalene; 444, 2-methylnaphthalene; 449, 1-methylnaphthalene; 474, biphenyl; 497, acenaphthylene; 509, acenaphthene; 521, dibenzofuran; 542, fluorene; 600, phenanthrene; 690, fluoranthene; 704, pyrene; 800, chrysene; BaP, benz[a]pyrene. GC conditions: 50 m x 0.23 mm OV-101 fused-silica capillary column from Hewlett-Packard; initial oven temperature (20°C for 2 min) raised to 270°C at 2°C/min and held at 270°C for 20 min; splitless injection; He carrier gas)

FIGURE 2 Analysis of Total Chromatographable Organics in Combined Oil/Tar Samples Versus Ring Structure for Reactor Runs 74 (600°C), 72 (800°C), and 73 (1000°C) (In the three-digit ring index, first digit = total number of rings, second digit = number of aromatic rings, and third digit = number of alicyclic rings)
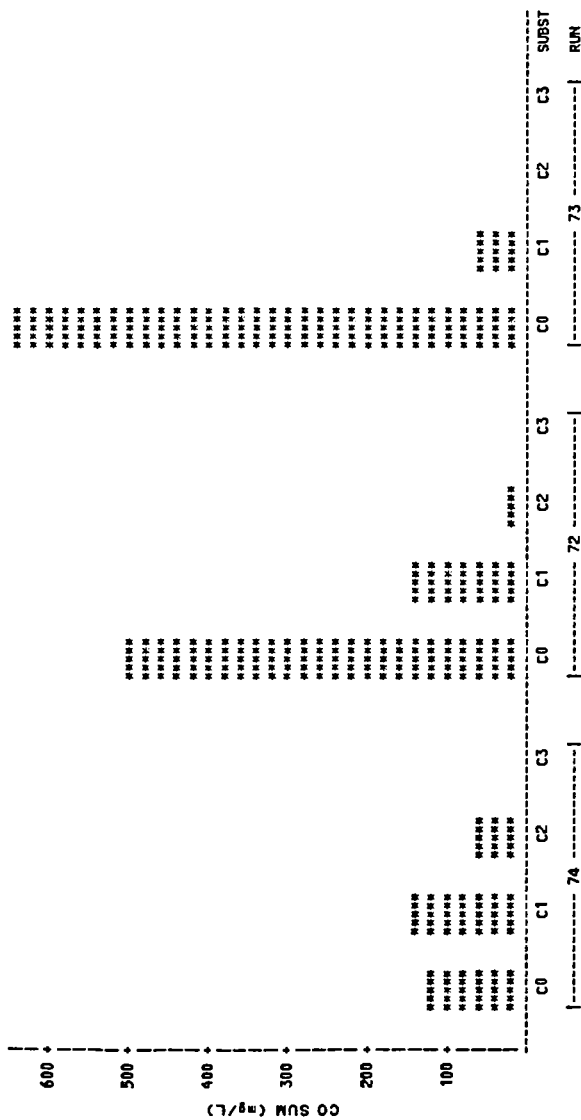
FIGURE 3 Analysis of Total Chromatographable Organics in Combined Oil/Tar Samples Versus Alkyl Substitution for Reactor Runs 74 (600°C), 72 (800°C), and 73 (1000°C)
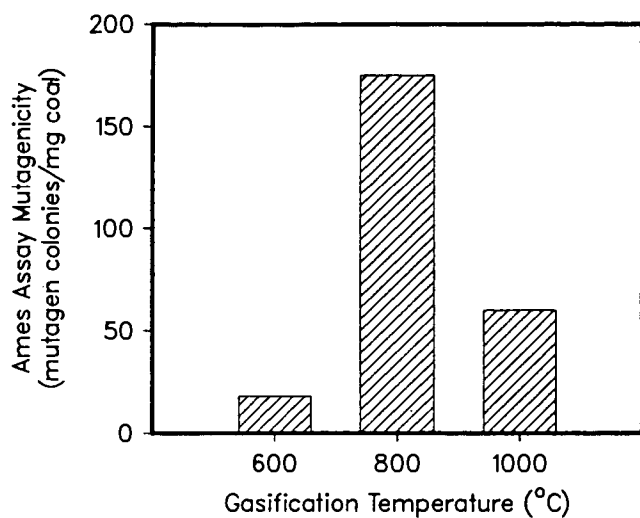
FIGURE 4 Mutagen Formation in Coal Devolatilization (calculated from dose response mutagenicity measurements)

THE FORMATION OF HYDANTOINS IN GASIFIER CONDENSATE WATER

E.S. Olson, J.J. Worman, and J.W. Diehl

University of North Dakota Energy Research Center
Box 8213, University Station
Grand Forks, North Dakota 58202

A number of 5,5-diakyl and 5-alkylhydantoins have been detected in the condensate water from the gasification of Indian Head (ND) lignite in the UNDERC slagging fixed bed gasifier (1, 2). These compounds were characterized by extensive GCMS studies (3) and quantitatively analyzed in samples of process water resulting from various stages in a pilot scale gasifier water treatment plant at UNDERC (4, 5). 5,5-Dimethylhydantoin and 5-ethyl-5-methylhydantoin constitute the major portion of the organic compounds remaining in the condensate water after extraction with diisopropyl ether and steam stripping (5). Because of their biological activity, they represent a potential health hazard in the effluents from a commercial gasifier. Although hydantoins can be adsorbed on activated carbon (3) and degraded by a bacterial nitrification system (6), the expense of removal from the water justifies an effort to gain a better understanding of the formation of hydantoins in the condensate water with the goal of predicting the extent to which the reaction will occur under various conditions.

The hydantoins do not form directly in the gasifier. They were shown to be either absent or present in low concentrations in water samples which were collected from a side stream sampler on the UNDERC gasifier and quickly frozen. When this side stream condensed water was heated in a constant temperature bath at 40°C, hydantoin concentrations increased in an approximately second-order manner. The formation is believed to proceed by the Bucherer-Berg reaction, the same reaction used in commercial hydantoin synthesis, from ammonia, carbonate, hydrogen cyanide and various ketones and aldehydes at a pH of 8.5.

A kinetic study was undertaken to obtain useful rate data for this reaction (7). Reliable and reproducible concentration data for acetone and cyanide were impossible to obtain for the raw gasifier condensate water because of the presence of reversible addition products of cyanide such as acetone cyanohydrin and 2-amino-2-methylpropanonitrile as well as large amounts of sulfide. Thus a model system was investigated where acetone cyanohydrin was reacted with excess ammonium carbonate at concentrations approaching those obtained in the condensate water, 0.020M and 0.25M, respectively. The reaction was studied at 50°, 70°, and 90°C using a capillary GC (OV351 phase) for the analysis of 5,5-dimethylhydantoin (DMH) using 4-methoxyphenol as the internal standard (4).

Linear second order plots were obtained for this reaction at the three temperatures. Table I gives the calculated pseudo second-order rate constants and linear regression fit.

Table I. Pseudo Second-Order Rate Constants and Least Squares Fit at Various Temperatures.

t(°C)	50	70	90
k_2' ℓ mole^{-1}hr^{-1}	1.86	3.60	4.62
r^2	0.999	0.998	0.997

The initial concentrations of acetone and cyanide were varied in order to determine their effect on the rate of formation of DMH. When the acetone concentration was doubled, keeping the original cyanide, ammonia, and carbonate concentrations constant, the rate of the reaction doubled at 90°C. A decrease in cyanide concentration to one-half of its original value decreased the rate by one-half. Table II gives the values of the initial rates of formation of DMH at 90°C varying acetone and cyanide concentrations.

Table II. Initial Rate of DMH Formation at Varying Acetone and Cyanide Concentrations. Ammonia and Carbonate Concentrations Were Held Constant at 0.50M and 0.25M, Respectively.

Initial Rate (mmoles $\ell^{-1}hr^{-1}$)	Acetone Concentration (M)	Cyanide Concentration (M)
123	0.02	0.02
220	0.04	0.02
60	0.02	0.01

In order to verify that the rate also depends on the concentrations of ammonia and carbonate, which were present in large excess in these experiments, the 90°C experiment was repeated using 0.02M acetone cyanohydrin and changing the concentration of ammonium carbonate to 0.20M. The expected pseudo second order behavior was again exhibited (r^2 = 0.998) and the observed rate constant was 2.8 liters mole^{-1}hr^{-1}. The value expected for 0.8 times the concentration of ammonia and carbonate is 2.9 liters mole^{-1}hr^{-1}.

This established that the rate of formation of DMH was first order in all of the reactants as expressed by the following equation:

$$\text{Rate of formation of DMH} = k\,[\text{Acetone}]\,[\text{HCN}]\,[\text{NH}_3]\,[\text{CO}_2]$$

This kinetic data is valuable in predicting the rate of formation of DMH in coal gasification condensate water, provided the model is applicable. The pH of the model solution and the condensate water remained constant at around 8.4, but the effects of small changes in pH on the rate are not fully known.

In the earlier experiment with sidestream condensate water, it was noted that the concentration of acetone decreased by one-half at the endpoint when the hydantoin concentration no longer increased. This implies that the limiting species for formation of hydantoins in the UNDER gasifier water is cyanide. The hydrogen cyanide peak in the GC analysis had also disappeared. When condensate water was analyzed from initial runs of the Great Plains Gasification Plant which uses coal of the same Beulah-Zap seam as Indian Head coal, negligible hydantoins and HCN were found.

Similarly when Indian Head lignite was used in the METC gasifier, the condensate water contained negligible hydantoins and HCN. In both cases acetone and 2-butanone concentrations were significant.

Data on actual HCN concentrations in the raw gas and quenched gas are not available for these gasifiers. A thorough study was reported by Anastasia on the HYGAS gasifier using Illinois No. 6 coal (8). Although 10% of the nitrogen in the coal was converted to HCN, only 1% of the total HCN entered the condensate water. Most of the HCN (80%) remained in the gas phase (quenched gas) and the

rest dissolved in the oil-tar phase. We expect that significant amounts of HCN are also produced in the gasification of lignite and the factors which determine how much of the HCN ends up in the condensate water are of importance.

One major factor for determining the cyanide concentration in the condensate water is how long the aqueous phase is in contact with the gas phase and oil-tar phase. Diffusion of the HCN at the interface of the aqueous phase with the gas and oil phases and subsequent reaction with acetone and acetone imine over a long period of time will build up the concentration of cyanide addition products which reversibly interconvert and eventually proceed to hydantoin. The residence times for water in the UNDERC spray washer (quench water system) and tar-oil-water separator are several hours which can allow for considerable diffusion buildup of the cyanide conjugates which form significant amounts of hydantoin.

Literature Cited

1. Mohr, D.H., Jr. and King, C.J. Report LBL-13584, Lawrence Berkeley Lab., November 1981, in "Processing Needs and Methodology of Contaminated Water Streams from Synfuel Processes," DOE Symposium, Germantown, Maryland, June 1981.

2. Olson, E.S.; Diehl, J.W.; and Miller, D.J. ASMS 30th Annual Conference on Mass Spectrometry and Allied Topics, Honolulu, Hawaii (1982); Abstracts, p. 818.

3. Olson, E.S.; Diehl, J.W.; and Miller, D.J. Anal. Chem., 1983 55, 1111.

4. Olson, E.S. and Diehl, J.W. 186th ACS National Meeting, Washington, D.C. (1983); Abstracts, ANYL 63.

5. Willson, W.G.; Hendrikson, J.G.; Mann, M.D.; Mayer, G.G.; and Olson, E.S. In report DOE/METC/84-13 (Feb. 1984) Twelfth Biennial Lignite Symposium: Technology and Utilization of Low-Rank Coals Proceedings, Vol. I, ed. by Kube, W.R.; Sondreal, E.A.; and Rao, C.D., p. 265-299.

6. Personal communication, G.G. Mayer and J. Gallagher (UNDERC).

7. Diehl, J.W.; Olson; E.S., and Worman, J.J., Fuel, accepted for publication.

8. L.J. Anastasia in Advanced Techniques in Synthetic Fuels Analysis, ed. by Wright, C.W.; Wiemer, W.C.; and Felix, W.D., Tech. Inform. Ctr., USDOE (1983), p. 105.

A STUDY OF THE REDUCTION, ALKYLATION, AND REDUCTIVE ALKYLATION
OF A VOLATILE BITUMINOUS COAL

Narayani Mallya and Leon M. Stock

Department of Chemistry, University of Chicago, Chicago, IL 60637

INTRODUCTION

Reduction, alkylation, and reductive alkylation have been investigated by several different research groups to increase the solubility of coals for structural studies and to develop a greater understanding of the chemical factors essential for the conversion of the intractable coal molecules into soluble or liquid products (1,2). Several lines of evidence suggest that the higher ranking bituminous coals with 88 to 89% C(daf) are more readily converted to products that are soluble in common organic solvents than the lower ranking bituminous or subbituminous coals. The structural factors responsible for the facile reduction reactions of the higher ranking coals have not, as yet, been established. Accordingly, we have undertaken astudy of the relative effectiveness of reduction, alkylation, reductive alkylation and other reactions for the conversion of a vitrinite-rich, low volatile bituminous coal from the lower Kittanning seam in Pennsylvania--PSOC 1197--to soluble products and compared the results obtained in this work with the results obtained in previous studies of lower ranking coals.

EXPERIMENTAL PART

The coal sample was obtained from the Pennsylvania State University Sample Bank. The sample was ground to -325 mesh and then dried in vacuum at 60°C to constant weight.

Reduction.--The coal was reduced in three different ways: A) the coal (1 g) was suspended in liquid ammonia (200 ml) with 64 mmoles of potassium; B) the coal (1 g) was suspended in liquid ammonia (200 ml) with 110 mmoles of potassium; C) the coal (1 g) was suspended in liquid ammonia (200 ml) with 68 mmoles of potassium and 68 mmoles of 2-methyl-2-butanol. All the reactions were carried out at -78°C for 6 hours. Ammonium chloride was added to the reaction mixture to destroy any residual potassium and, thereby, interrupt the reaction. The ammonia was then evaporated and dilute aqueous hydrochloric acid was added to the residue. The mixture was filtered and the solid coal product was collected and dried in a vacuum oven at 60°C.

Alkylation.--The sample of PSOC-1197 was also alkylated in three different ways. Reductive butylation was carried out as described in a previous publication from this laboratory (3). About 60 mmoles of potassium and 80 mmoles of butyl iodide were used in the reaction. Non-reductive butylation was conducted using sodium amide in ammonia at -78°C as described by Ignasiak and coworkers (4). In this reaction, the coal (1 g) was treated with sodium amide (15 mmoles) for 6 hours. 1-Butyl iodide (15 mmoles) in benzene (50 ml) was then added to the reaction mixture which was stirred for 48 hours. The reaction was terminated by the addition of dilute, aqueous hydrochloric acid. The acidified coal product was collected and dried in vacuum at 60°C. The conventional alkylation reaction was carried out as described by Liotta and his coworkers (5). The coal (1 g) was stirred with 22% tetrabutylammonium hydroxide (30 ml) for 3 hours. 1-Butyl iodide (15 mmoles) in tetrahydrofuran (50 ml) was added and the suspension was

stirred for 2 days. The reaction mixture was acidified by the addition of dilute hydrochloric acid. The product was then collected by filtration, washed with water, and dried in vacuum at 60°C.

Measurements.--The solubilities of the coals and the freshly prepared reaction products in pyridine and tetrahydrofuran were determined by Soxhlet extraction. Elemental analyses were obtained by the Huffmann Laboratories and by the Illinois State Geological Survey. The solid state carbon NMR spectra (CP/MAS) were measured at the National Science Foundation Regional Center at Colorado State University using a JEOL FX 60Q system. The acidities of the coals and the reaction products were determined using the procedures described by Schafer (6) and Mallya and Zingaro (7).
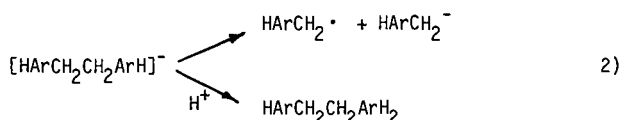
RESULTS AND DISCUSSION

The results obtained in this investigation of the reduction, alkylation, and reductive alkylation of a low volatile, bituminous coal with 88% C(daf) are summarized in Tables 1, 2, and 3. The original coal is only modestly soluble in tetrahydrofuran and in pyridine. However, the reduction reactions of this coal with potassium in liquid ammonia, reactions 1 and 2 in the Tables, proceed readily to yield substances that are much more soluble in the organic solvents than the original coal. The facility with which this coal is reduced is remarkable, but not unexpected in view of the results obtained by Given, Wender, and their associates in studies of the reduction of similar high ranking coals under more vigorous conditions, for example with lithium in ethylene diamine (2). In contrast, Illinois No. 6 coal is neither reduced nor rendered soluble to a significant degree by reduction in liquid ammonia (1,3).

The reduction of the Lower Kittanning coal with 110 mmoles potassium/g coal provides a much more soluble product than the reaction with 64 mmoles potassium/g coal. The reducing agent was not consumed in these reactions. The microanalytical data suggest that about 10 hydrogen atoms/100C are added to the coal in the reaction with 64 mmoles potassium/g coal and that about 12 hydrogen atoms/100C are added in the reaction with 110 mmoles potassium/g. While it is well known that the microanalytical determinations of the hydrogen content of coals and coal products are subject to relatively large errors, we have no reason to doubt the reliability of the data presented in Table 2. Thus, it seems quite pertinent that the difference in the degree of reduction of the two samples is very modest compared to the change in solubility from 25 to 78% in tetrahydrofuran and from 39 to 92% in pyridine. These two reaction products also have virtually identical acid contents, Table 3. Thus, ether cleavage reactions do not appear to be responsible for the much greater solubility of the reaction product obtained with the greater concentration of the reducing agent. The observations are compatible with the idea that additional carbon-carbon bond cleavage reactions occur when the concentration of the reducing agent is increased. Metals in ammonia both reduce and fragment hydrocarbons such as the tetraarylalkanes as illustrated in equation 1) (1,8). Accordingly, we postulate that the higher concentration of reductant leads to a greater steady state concentration of aromatic anions with the result that a somewhat greater fraction of these reactive intermediates undergo carbon-carbon bond cleavage reactions during the reaction interval to produce more soluble, lower molecular weight products. Only a few additional cleavage reactions are required to account for the observations.

$$Ar_2CHCHAr_2 \rightarrow [Ar_2CHCHAr_2]^{\underline{\cdot}} \rightarrow Ar_2CH^- + Ar_2CH\cdot \qquad\qquad 1)$$
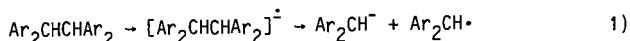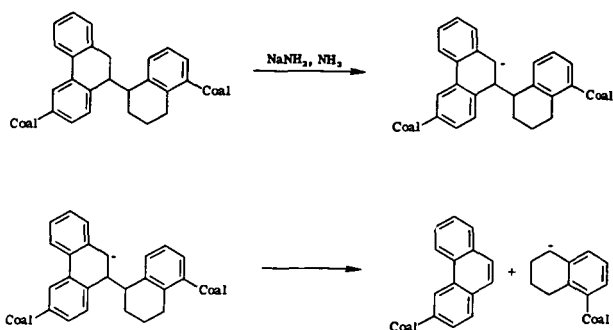
The reduction of the Lower Kittanning coal with potassium and 2-methyl-2-butanol in liquid ammonia at low temperature provides an even more soluble product, Table 1, reaction 3. As in the previous case, this reaction is ineffective for the reduction or solubilization of Illinois No. 6 coal (1). The microanalytical data imply that about 14 hydrogen atoms/100C have been incorporated into the structure of the low volatile bituminous coal. The f(A) values determined at the National Science Foundation Center at Colorado State University, for the reduction product, f(A) ≈ 0.69, and the coal, f(A) ≈ 0.82, imply that 21 hydrogen atoms/100C have been added to the coal. The large change in aromaticity strongly suggests that the aromatic anions and carbanions formed in the initial reduction reactions of this coal are efficiently trapped by the proton donor and converted to alkylaromatic compounds, dihydroaromatic compounds, and similar kinds of materials. The fact that a much more soluble product is formed in this reaction in which the aromatic anions of unstable compounds are rapidly protonated by the alcohol implies that reduction is as important as carbon-carbon bond cleavage in the solubilization of this coal as illustrated in equation 2)

$$[HArCH_2CH_2ArH]^- \quad \begin{array}{c} \nearrow \quad HArCH_2\cdot \ + HArCH_2^- \\[2ex] \underset{H^+}{\searrow} \quad HArCH_2CH_2ArH_2 \end{array} \qquad\qquad 2)$$

The lower Kittanning coal contains 3.3 oxygen atoms/100C. Consequently, we also investigated the role of ether cleavage reactions in its reduction reactions. The original coal contains about 0.5 meq/g of acidic hydroxyl groups; hence there is 0.6 reactive hydroxyl group per 100 carbon atoms. Within the limits of the experimental error, the acidic hydroxyl group content of the reduction products is the same as that of the original coal. To examine this issue in another way, we alkylated the product of the reduction reaction with carbon-13 labeled methyl iodide and recorded the NMR spectrum of the products. No resonance signals were observed for O-methylation derivatives between 50 and 63 ppm. Thus, there are few acidic hydroxy groups in the coal product and ether cleavage reactions do not contribute in an important way to the solubilization of this high rank coal during reduction reactions in liquid ammonia. These results are compatible with the idea that the coal contains heterocyclic ethers such as dibenzofuran. Compounds of this type are reported to undergo reduction rather than carbon-oxygen bond cleavage when treated with metals in liquid ammonia (9).

The lower Kittanning coal was alkylated in two ways. First, the reaction was carried out with a relatively mild base, tetrabutylammonium hydroxide, and 1-butyl iodide in aqueous tetrahydrofuran as described by Liotta and his coworkers (5). This reaction was ineffective for the solubilization of the coal which has less than one acidic hydroxyl group per 100 carbon atoms. In a second attempt to alkylate this coal, the reaction was carried out with sodium amide in liquid ammonia using 1-butyl iodide using a modification of the procedure developed by Ignasiak and his coworkers (4). This method provided a product that was 69% soluble in tetrahydrofuran and 83% soluble in pyridine. The result contrasts sharply with the findings obtained previously for the Illinois No. 6

coal which was not solubilized by this technique (1). The microanalytical data
and the carbon NMR spectrum of the product obtained in a non-reductive alkylation
with carbon-13 enriched methyl iodide are incompatible with a high degree of
alkylation of the coal. These observations, therefore, imply that base-catalyzed
carbon-carbon bond cleavage reactions, equation 3) are more important for the so-
lubilization of this coal than the alkylation reactions of the carbanions formed
during the reaction.

3)

, Reductive alkylation of lower Kittanning coal with potassium and 1-butyl
iodide provides virtually complete conversion of the material into soluble
products. The exact weight gain could not be measured because it was not
possible to remove the organic contaminants, for example residual 1-butyl
iodide, without also dissolving the reductively butylated coal. The micro-
analytical data imply that more than six butyl groups/100C have been in-
corporated into the structure. The degree of solubilization of this coal is
significantly greater than the degree of solubilization of the Illinois No. 6
coal realized in the same reaction. The carbon-13 NMR spectrum of the reduc-
tive methylation product obtained in the reaction with carbon-13 enriched
methyl iodide exhibits an intense band in the C-methyl region from 15 to 40
ppm, but only very weak, almost imperceptible resonances in the O-methyl re-
gion between 55 and 65 ppm. Thus, as in the other reduction reactions of this
coal, O-alkylation is an insignificant process. The resonances of the C-
methyl groups added to the coal appear in three distinct regions near 22, 28,
and 35 ppm, respectively. Unfortunately, the resonances are quite broad and
it will be necessary to examine other C-alkylation products to assign these
resonance signals with confidence.

CONCLUSION

Generally, coals are regarded as insoluble, intractable substances because of
their macromolecular character, significant hydrogen bonding interactions, and the
intermolecular interaction between unbonded aromatic molecules in different frag-
ments of the structure. Solubilization can be realized when these interactions
are disrupted or when the molecular weight is reduced.

Inasmuch as there are few acidic hydroxyl groups in the lower Kittanning coal, hydrogen bonding interactions do not play an important role in determining its behavior in solubilization. Thus, O-butylation of the original coal results in only a very modest increase in solubility. Moreover, no O-alkyl groups are introduced into this coal during reductive alkylation.

The carbon-oxygen and carbon-carbon bond cleavage reactions can reduce the molecular weight of coal molecules. Several lines of evidence indicate that ether cleavage reactions play an insignificant role in the reactions of the lower Kittanning coal. First, there is no increase in the content of acidic hydroxy groups after reduction. Second, there are only traces of O-alkylation products in the reduced coals. Thus, carbon-carbon bond cleavage reactions are much more probable under the conditions of these experiments. The fragmentation reactions of anion radicals such as the simple reaction illustrated in equation 1) occur during reduction and reductive alkylation. Base-catalyzed carbon-carbon bond cleavage reactions of hydrocarbons, as illustrated in equation 3) may occur in the presence of the strongly basic reagents during the non-reductive alkylation reactions. The available results indicate that reduction alone leads to significant increase in solubility and that reductive butylation using the same quantity of reducing agent yields an even more soluble product. Also, previous studies by Wachowska and her associates (10) indicate that the introduction of the large butyl and octyl groups has a large impact on the solubility of the higher rank coals. All these observations are in accord with the suggestion originally made by Wender and his associates that the introduction of hydrogen atoms into coals with significant aromatic character resulted in a disruption of the structure and a reduction of the attractive forces between non-bonded aromatic structures. The impact of the addition of hydrogen atoms is augmented, of course, by the introduction of large alkyl groups. Hence, reduction and alkylation when accompanied by the facile carbon-carbon cleavage in the highly aromatic coal structures provide quite soluble products.

ACKNOWLEDGEMENT

REFERENCES

1) L.M. Stock, "Coal Science", 1 161 (1982)

2) I. Wender, L.A. Heredy, M.B. Neuworth and I.G.C. Dryden in "Chemistry of Coal Utilization" ed. M.A. Elliott, John Wiley and Sons, NY, (1981) pp. 437

3) C.I. Handy and L.M. Stock, Fuel, 61, 699 (1982)

4) B. Ignasiak, D. Carson and M. Gawlak, Fuel, 58, 883 (1979)

5) R. Liotta, Fuel, 58, 724 (1979)

6) H.N.S. Schafer, Fuel, 49, 197 (1970); ibid. 49, 271 (1970)

7) N. Mallya and R.A. Zingaro, in "The Chemistry of Low-Rank Coals" ed. H.H. Schobert, American Chemical Society, Washington, D.C. (1984) pp. 133

8) H. Smith in "Organic Reactions in Liquid Ammonia" John Wiley and Sons, NY (1963) pp. 156

9) M. Smith, in "Reduction" ed. R.L. Augustine, M. Dekker, Inc., NY, (1968) pp. 125

10) H.M. Wachowska, Fuel, 58, 99 (1979)

Table 1. A Summary of the Results Obtained in the Reduction, Alkylation, and Reductive Alkylation of a Low Volatile Bituminous Coal from the Lower Kittanning Seam (PSOC 1197).

Sample Origin	Weight Gain (%)	Result — Extractability (%,daf)[a] —	
		Tetrahydrofuran	Pyridine
Original coal	-	4	6
1. Reduction, K(64 mmoles/g), NH$_3$, -78°C, 6 hrs	3	25	39
2. Reduction, K(110 mmoles/g), NH$_3$, -78°C, 6 hrs	2	78	92
3. Reduction, K(68 mmoles/g), t-C$_4$H$_9$OH, NH$_3$, -78°C, 6 hrs	5	94	96
4. Alkylation, N(C$_4$H$_9$)$_4$OH, C$_4$H$_9$I (13 mmoles/g), THF, Ambient T, 48 hrs	1	16	10
5. Alkylation, NaNH$_2$, C$_4$H$_9$I (13 mmoles/g), NH$_3$, -78°C, 6 hrs	2	69	83
6. Reductive alkylation, K(60 mmoles/g), NH$_3$, 6 hrs, -78°C, C$_4$H$_9$I (80 mmoles/g), THF Ambient T, 48 hrs	-	98	93

[a]The precision realized in replicate experiments is about ± 2%.

Table 2. Microanalytical Data for the Lower Kittanning Coal (PSOC 1197) and Its Reaction Products

Sample Origin	Analytical Data (%, daf)			
	C	H	N	Ash[c]
Original coal[a]	87.4	4.8	1.4	11.3
Reduction, reaction 1[a]	84.9	5.2	1.5	10.3
Reduction, reaction 2[a]	82.9	5.1	1.6	10.3
Reduction, reaction 3[b]	86.4	5.5	1.1	10.8
Alkylation, reaction 4[a]	88.1	4.8	1.7	13.7
Alkylation, reaction 5[a]	88.9	4.8	1.8	10.3
Reductive alkylation, reaction 6[a]	82.5	8.0	1.6	5.7

[a] The analysis was performed by Dr. C. Chaven, Illinois Geological Survey.

[b] The analysis was performed by Huffmann Laboratories, Wheatridge, Colorado.

[c] The analysis was performed in this laboratory.

Table 3. Aromaticity and Acid Group Concentration in the Lower Kittanning Coal (PSOC 1197) and Its Reduction Products.

Sample	Acidity (meq/g, daf)		$f(A)$[a]
	Total	Carboxylic Acid	
Original coal	0.40	<0.01	0.82
Reduction, reaction 1	0.36	-[b]	
Reduction, reaction 2	0.54	-[b]	0.76
Reduction, reaction 3	0.50	<0.01	0.69

[a] The fraction of aromatic carbon content, $f(A) = [(C-C(Aliphatic)/C]$ where C = Area of All Carbon Resonance Signals and C(Aliphatic) = Area of the Aliphatic Carbon Resonance Signal, was determined using CP/MAS NMR spectroscopy.

[b] The carboxylic acid content was not determined.

CATALYTIC HYDRODENITROGENATION OF AN SRC-II COAL LIQUID.
EFFECT OF HYDROGEN SULFIDE

Albert S. Hirschon, Robert B. Wilson, and Richard M. Laine*

SRI International
333 Ravenswood Avenue
Menlo Park, CA 94025

The first step in coal liquefaction yields coal liquids which are high in nitrogen, sulfur, and oxygen. These heteroatoms must be removed before these coal liquids can be transformed into synfuels or petrochemical substitutes. However, the catalytic removal of nitrogen (HDN) and oxygen (HDO) consumes excessive amounts of hydrogen. This excess hydrogen is consumed in the hydrogenation of aromatics. If it were possible to remove the nitrogen and oxygen from coal liquids with a minimum of hydrogen and at lower temperatures than currently used, coal could become an economically viable energy source.

Workers have shown that HDN catalysis of model systems undergoes significant rate enhancement in the presence of H_2S (1-5), and some enhancement in the presence of H_2O (6,7). Other workers (8,9) have shown that the acidity of the support is important in the enhancement of HDN activity.

We have recently suggested, based on mechanistic studies of HDN of nitrogen heterocycles that nucleophiles such as H_2S, H_2O, and perhaps NH_3 can enhance catalysis by promoting heterocyclic ring opening via nucleophilic attack on the metal-complexed heterocycle (10). We have also seen in our work that the addition of acids aids in the hydrogenation of nitrogen containing heterocycles (11). Thus it may be possible to increase the rate of hydrogenation of heterocycles while not effecting the rate of hydrogenation of other aromatics.

The objective of this work is to develop an understanding of how nucleophiles such as H_2S, SH^-, and $S^=$, H_2O, NH_3, and added acids effect the HDN process of coal liquids under catalysis conditions. From the results of our work we have found that the addition of H_2S or added acids to an SRC-II coal liquid enhances the removal of nitrogen under standard HDN conditions.

Experimental Procedures and Materials

SRC-II middle distillate was obtained from the Pittsburg and Midway Mining Co. SRC pilot plant at Fort Lewis, Washington. The cobalt-molybdenum catalyst, HT-400 (3 wt% CoO, 15.1 wt% MoO_3, on Al_2O_3) was obtained from Harshaw Chemical Company. Hydrogen sulfide (H_2S) was obtained from Matheson. Hydrogen (H_2), nitrogen (N_2), and an $H_2S(10\%)/H_2$ gas mixture were obtained from Liquid Carbonic.

Apparatus

Hydrogenation reactions were performed in a 300-mL Autoclave Engineers (AE) Magnedrive stirred reactor, heated with a 1000-W electric furnace (AE). The temperature was controlled with a model CP temperature controller (AE). The autoclave was connected through a sample gas vent to a Carle Series S gas chromatograph (GC) adapted by Carle to analyze C_1-C_3, H_2, O_2, N_2, and H_2S.

Analytical Procedures

Nuclear magnetic resonance (NMR) spectra were obtained on a JEOL FX 90Q spectrometer. NMR samples were prepared by mixing one part by weight of coal liquid with two parts of $CDCl_3$. The conditions for obtaining the ^{13}C NMR spectra were as follows. Samples were made 0.025 M in $Cr(AcAc)_3$. The pulse width was 6 μs and pulse delay

15 s. The NNE option (heterodecoupling with no Nuclear Overhauser enhancement) was chosen for quantitative ^{13}C analyses.

The infrared (IR) spectra were obtained on a Perkin-Elmer 281 spectrophoto-meter. Elemental analyses were obtained from Galbraith Laboratories. (Nitrogen was determined by the Kjeldahl method).

Catalyst Preparation

The HT-400 cobalt-molybdenum catalyst was ground and sieved to obtain a 60- to 200- mesh powder. The catalyst was activated at 400°C in a flowing mixture of H_2S (10%) in H_2 for 24 h, then stored in a Vacuum Atmospheres Dri-box under N_2. (Before the catalyst was sulfided, it was heated for 2 h at 400°C under flowing synthetic air, pretreated with H_2S/H_2 mixture for 1 h at room temperature, then slowly heated to 400°C over a 2-h period). Anal.: Mo, 7.8%; S, 7.75%.

Standard Reaction Procedures

The autoclave was filled under N_2 with the desired quantity of activated catalyst and SRC-II liquid. The reactor was then charged with 1200 psi of H_2 (or H_2/H_2S). For those reactions using H_2S only or when NH_3 was added, the following procedure was used: A tared 20-mL minireactor was filled with H_2S or NH_3 to the desired weight. The minireactor was then connected to the 300-mL autoclave and the system was purged with N_2. The 300-mL reactor was cooled with dry ice, and the gas was condensed into the autoclave.

The system was heated to 400°C and maintained at 400°C for 1 h, at which time the heating furnace was removed. When the reactor had cooled to room temperature, GC analyses were performed on the product gases. The liquid products were removed and filtered to remove the catalyst. Duplicate runs were made at either end of the con-centration range (analyzed nitrogen content deviates no more than 0.02% in the duplicate runs).

Results and Discussion

Treatment of SRC-II with Hydrogen Sulfide (without catalyst)

The data from the reactions of H_2S or H_2S/H_2 with the SRC-II liquid are shown in Table 1. When the SRC-II was treated with H_2S alone, we observed some evolution of gases (1.96 mmol gas/g coal liquid) due to H_2, ethane, and propane. The evolution of gases affects the quality of the remaining coal liquids. As determined by NMR, the fraction of aliphatic hydrogen and carbon decreased from 0.66 to 0.60 and 0.32 to 0.30, respectively, and the H/C ratio decreased from 1.20 to 1.15 from the original SRC-II liquid. In contrast, the treatment of the coal liquid with the H_2S/H_2 mixture resulted in essentially no change in hydrogen content from the original. The IR spectra of these reaction products are similar to that of the original liquid and show no absorptions in the region of 2550 to 2600 cm^{-1} where we expected to see SH stretches. Elemental analyses of the products from the H_2S and H_2S/H_2 reactions showed an increase in sulfur content from 0.30% to 0.54 and 0.43% respectively. These results are in accord with what might be expected based on Stenberg's work at higher temperatures (12) (450°C vs 400°C used here).

Treatment of SRC-II with Sulfided Catalyst

In experiments 3 through 9 we treated 50 g of the coal liquid using a 1% concen-tration of sulfided catalyst. As seen from Table 1 the addition of nucleophiles such as H_2S, HS^-, $S^=$, H_2O, or NH_3, or added acids such as trifluoroacetic acid (TFA), do not have a dramatic effect of the hydrogen uptake (by H/C ratio) or on the aliphatic to aromatic ratios (by NMR) nor were there significant difference in the IR spectra of the products from the runs. However, as seen from the elemental analyses of these

products, the nitrogen content of 0.74% (exp 3) in the baseline run with H_2 decreased to 0.56% (exp 4) in the H_2S/H_2 run, and decreased to 0.42% (exp 9) in the TFA/H_2 run. Figure 1 shows that as the H_2S or TFA concentration increases, the nitrogen concentration of the resultant hydrotreated product decreases. The addition of $S^=$ as Na_2S (exp 7) or the addition of H_2O (exp 5) to the standard reaction resulted in no enhancement over that of exp 3. The addition of NH_3 seemed to inhibit the HDN reaction (exp 6), whereas the combination of NH_3 and H_2S resulted in only a slight inhibition of the HDN reaction (exp 8).

Table 1. Reactions with 1% Sulfided Catalyst at 400°C for 1 h
with 1200 psig of H_2 (or H_2S/H_2)

Experiment[a]	Additive (mole wt%)[b]	%N	%S	H/C	%H$_{alip}$	%C$_{aliph}$
SRC-II	--	0.98	0.30	1.20	66	32
1[c,d]	H_2S (0.27)	1.00	0.54	1.16	60	30
2[d]	H_2S (0.084)	0.92	0.43	1.21	67	33
3	--	0.74	0.04	1.23	71	38
4	H_2S (0.084)	0.56	0.12	1.23	72	40
5	H_2O (0.14)	0.75	--	1.27	72	38
6	NH_3 (0.084)	0.99	0.03	1.24	72	37
7	Na_2S (0.084)	0.72	0.18	1.20	73	38
8	NH_4HS (0.084)	0.87	0.15	1.23	73	39
9	TFA (0.054)	0.42	0.15	1.22	70	37

[a]Duplicate runs.
[b]Moles of additive per 50 g of coal liquid.
[c]No hydrogen used.
[d]No catalyst used.

Conclusions

The addition of free H_2S under coal liquid upgrading conditions aids in the HDN process. These results validate the HDN modeling studies of Bhinde et al. (1) and those of Satterfield (2-5) and are in accord with our predictions (10). Furthermore, in contrast to the runs without catalyst, the addition of H_2S with catalyst leads to the product that has a reduced sulfur content. Our results also show that TFA aids in the HDN process. Although the HDN enhancement resulting from the addition of TFA is most likely due to its acidic properties, since it decomposes during the HDN reaction it is difficult to determine at what step in the HDN process the acceleration occurs. However our preliminary results are encouraging and with further experimentation we may be able to make substantial improvement in the HDN process which will result in considerable cost benefit.

Acknowledgement

REFERENCES

1. M.V. Bhinde, S. Shih, R. Zawadski, J.R. Katzer, and H. Kwart, "Chemistry and Uses of Molybdenum," 3rd Int. Conf. (1979) 184-187.

2. C.N. Satterfield and S. Gultekin, Ind. Eng. Chem. Proc. Des. Dev. (1981) 20, 62-68.

3. J.F. Coccheto and C.N. Satterfield, Ind. Eng. Proc. Des. Dev. (1981) 20, 49-53 and 53-61.

4. Yang, S. H. and C. N. Satterfield, Ind. Eng. Chem., Process Des. Dev., 23, 20 (1984).

5. Gultekin, S., S. A. Ali, and C. N. Satterfield, Ind. Eng. Chem., Process Des. Dev., 23, 179 (1984).

6. C. N. Satterfield and D. L. Carter 2nd Eng. Proc. Des. Dev. (1981) 20, 538-540.

7. L. Berg, F. P. McCandless, H. Bhatia, and A. Yeh, Energy Progress (1983) 3 248-251.

8. A. M. Tait and A. L. Hensley, Am. Chem. Soc. Div. Fuel Chem., preprints (1982) 27, 187-200.

9. B. M. Lok, F. P. Gortsema, C. A. Messina, H. Rastelli, and T.P.S. Izod, Am. Chem. Soc. Div. of Pet, Preprints (1982) 27, 470-480.

10. R.M. Laine, Catal. Rev.-Sci., (1983) 25, 459-474.

11. R. M. Laine, SRI International, 1983, private communication.

12. Stenberg, V. I., W. G. Wilson, D. E. Severson, G. G. Baker, C. L. Knudson, T. C. Owens, and J. R. Rindt, "Low Rank Coal Liquefaction Employing H_2S as a Homogeneous Catalyst," in Synfuels' first Science and Technology Symposium: A Selection of Papers, Abstracts, and Data, McGraw-Hill (1982).

FIGURE 1

EFFECT OF ADDITIVE ON HDN*
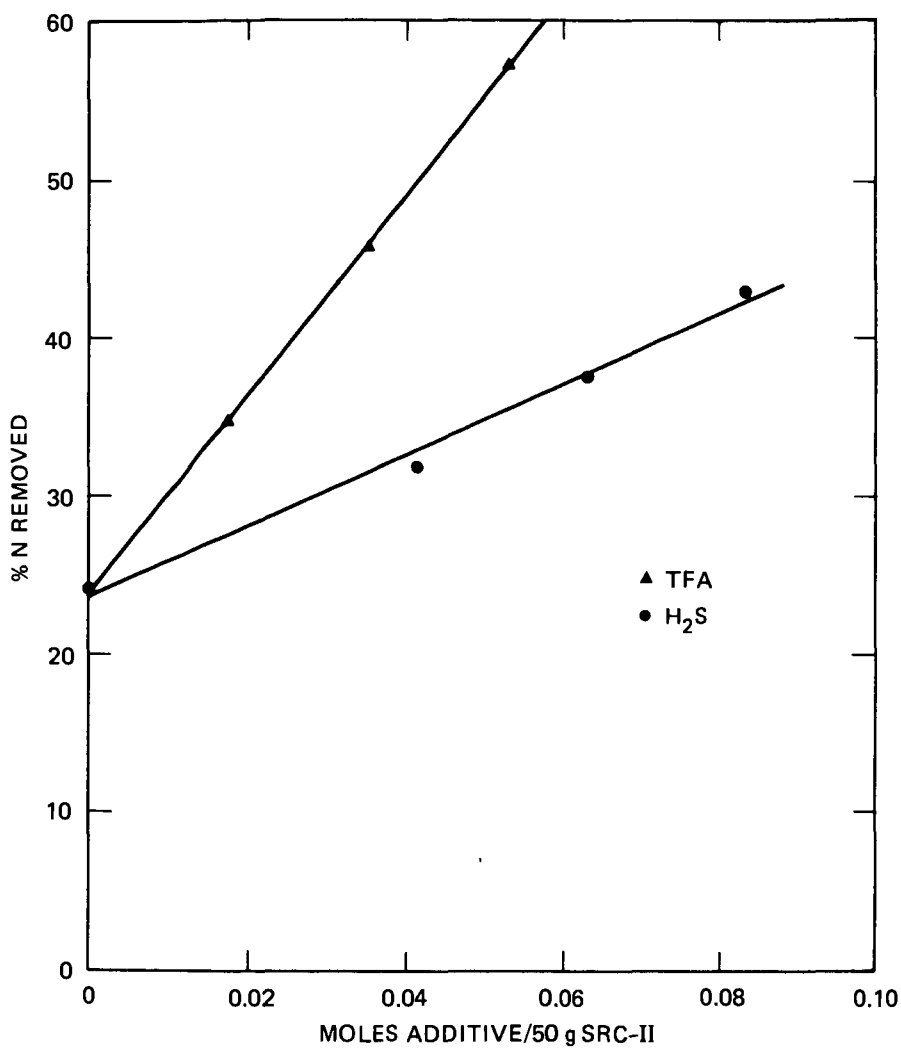
*1 h reaction of SRC-II liquid at 400°C with 1% sulfided CoMo catalyst and 1200 psig H_2

JA-327522-76

INTERACTIVE EFFECTS IN NITROGEN COMPOUND INDUCED STORAGE INSTABILITY IN SHALE DERIVED DIESEL FUEL

John V. Cooney,* Erna J. Beal and Bruce D. Beaver[1]

Combustion and Fuels Branch, Code 6180
Naval Research Laboratory, Washington, D. C.   20375-5000

INTRODUCTION

The autoxidation of middle distillate fuels during periods of storage has been a continuing problem in the utilization of these liquids by the government and commercially. With diesel fuels, instability is commonly defined by the formation of sediments, gums, color bodies and by the accumulation of hydroperoxides. Gravimetric accelerated storage stability tests conducted with model compounds as dopants in otherwise stable distillate fuels have demonstrated that oxidative condensation reactions of polar heterocycles are often deleterious to stability (2-15). In particular, nitrogen containing aromatics (pyrroles, pyridines, indoles, etc.) appear to be very harmful. Correlation of model dopant studies with results obtained with actual unstable fuels has indicated that the autoxidation processes are usually not isolated reactions but are sensitive to the presence of other fuel constituents (11, 13). Certain oxygen and sulfur compounds have been found to markedly alter the extent of model nitrogen compound induced storage instability in both middle distillate and model fuels (3, 4, 6, 16-18). Little is known about the chemical mechanisms of such interactive effects in fuel instability, and possible explanations include acid/base catalysis of oxidation and condensation pathways as well as involvement in radical chain processes. Interactions between different types of nitrogen compounds have also been studied to a limited extent (6, 10), and may similarly be of great importance in actual complex fuels.

As part of an effort to learn more about potential interactive effects, we have examined the autoxidation of two model nitrogen compounds, 2,5-dimethylpyrrole (DMP) and 3-methylindole (3-MI), in a shale diesel fuel in the presence of a second model dopant (t-butylhydroperoxide, an organic acid, or an organic base). The decision to examine DMP and 3-MI as nitrogen compound dopants was based upon a body of earlier work which analyzed the autoxidation behavior of these compounds (in the absence of other externally added active species) in the identical shale base fuel and under identical storage stability test conditions (10-12, 14, 15).

EXPERIMENTAL

Storage Test Techniques

The accelerated storage stability test method used has been described in detail (10-12). Hydroperoxide values were determined in stressed fuel samples following filtration through glass fiber filter paper by iodometric titration (ASTM D-1583-60).

Instrumental Methods

Infrared spectra were obtained as KBr pellets on a Perkin-Elmer Model 681 instrument with a Model 3600 data station (PECDS software). Solution proton nmr spectra were obtained in d_5-pyridine or deuterated chloroform with a Varian EM-390 90 MHz instrument. Elemental analyses were accomplished with a Carlo Erba Model 1106 elemental analyzer. Routine GC separations were made on either a Varian Model 3700 or a Perkin-Elmer Model 3920B gas chromatograph equipped with fused silica capillary columns (OV-101, 50 m x 0.3 mm) and FID detection.

Reagents

The base fuel for the present study was diesel fuel refined from Paraho crude shale oil by SOHIO. This fuel was produced in the U.S. Navy's Shale-II demonstration and is well-characterized (10). A quantity of this fuel was available which contained 24 mg/l of 2,4-dimethyl-6-t-butylphenol (AO-30) as the only additive (designated at NRL as fuel sample "D-11"). The D-11 fuel contained 15 ppm N (w/v) and exhibited good storage stability (10). All compounds used as dopants were pure by nmr, capillary GC, and/or mp. Fresh DMP was stored frozen under a nitrogen atmosphere to prevent autoxidation and it remained colorless under this storage. The concentration matrices for the interactive experiments were prepared so that effects of concentration (of both the DMP or 3-MI and the co-dopant) and of venting of test flasks could be assessed. In instances where the co-dopant was appreciably soluble in the D-11, two concentration levels were used (9.64×10^{-3}M and 3.21×10^{-2}M), which correspond to equivalent nitrogen compound (DMP or 3-MI) concentration levels of 135 and 450 ppm N (w/v). The construction of a 2 x 2 test matrix with both dopants then involved duplicate test flasks at each possible pairing, with additional flasks providing baseline "blank" values for D-11 doped with just the nitrogen compound, just the co-dopant, and the undoped D-11 fuel. In cases where the co-dopant exhibited only limited solubility in the D-11 fuel, a saturated solution was employed.

RESULTS AND DISCUSSION

Autoxidation of DMP and 3-MI in the Presence of t-Butylhydroperoxide (TBHP)

Previous storage stability tests employing DMP and 3-MI as dopants in a stable shale diesel fuel base indicated that while both compounds deteriorated the quality of the fuel, the nature of their instability processes differed substantially (11, 14). The results obtained with DMP and 3-MI are compared below:

Table 1
Comparison of DMP and 3-MI Induced Storage Instability

Property	3-MI	DMP
Induction Period:	yes	not observed
Peroxide Level After Stress (Relative to Fuels Blanks):	slightly less (80°C) slightly more (43°C)	much less (80°C) much less (43°C)
Effect of Venting:	large	minimal
Effect of AO-30:	large	minimal
Reaction Order in Dopant:	?	1.0
Formula of Dopant:	C_9H_9N	C_6H_9N
Empirical Formula of Sediment:	$C_{15.8}H_{15.2}NO_{2.6}$	$C_{6.3}H_{6.7}NO_{1.6}$

Since the storage stability characteristics of these dopants had been examined in detail, it was considered of interest to compare both of these compounds in the context of interactive experiments. The initial study involved the addition of a model nitrogen compound to fuel D-11 together with a hydroperoxide as co-dopant. The hydroperoxide selected was t-butylhydroperoxide since it is available commercially in high purity. The goal of the experiments was to survey the importance of the accumulation of hydroperoxides in a complex fuel in influencing the formation of insolubles during stress when a particular class of nitrogen heterocycles is present.

Accelerated storage stability tests employing DMP and TBHP as co-dopants in fuel D-11 were run at both 80°C (7 and 14 days) and 43°C (49 and 92 days). The gravimetric results, summarized in Table 2, indicated that a definite positive (synergistic) interaction existed between the DMP and TBHP under all conditions examined. The concentration matrix which was studied used DMP at two levels: Lo DMP

= 135 ppm N w/v, equivalent to 9.64×10^{-3} M; and Hi DMP = 450 ppm N (3.21×10^{-2}M). The levels of TBHP used corresponded to the same molar concentration values. Thus, the relative concentration matrix which was used was therefore (expressed as moles of TBHP added/moles of DMP added): Lo TBHP/Lo DMP = 1.0, Lo TBHP/Hi DMP = 0.3, Hi TBHP/Lo DMP = 3.3, Hi TBHP/Hi DMP = 1.0. The results of hydroperoxide analyses also appear in Table 2, and are given as peroxide numbers (ASTM D-1583-60).

Table 2
Storage Stability Test Results for the DMP/TBHP Interaction

| Sample* | Total Insolubles, mg/100 ml (Peroxide Number, meq ROOH/kg fuel) | | | |
	80°C/7d	80°C/14d	43°C/49d	43°C/92d
Fuel Blanks	0.5(0.9)	0.0(3.0)	0.0(0.3)	0.0(1.0)
Lo TBHP Blanks	0.4(39.5)	0.9(34.2)	0.0(58.9)	0.0(17.2)
Hi TBHP Blanks	0.5(80.8)	0.7(84.6)	0.0(100.5)	0.0(60.9)
Lo DMP Blanks	30.2(0.2)	47.4(0.4)	25.4(0.0)	42.6(0.0)
Hi DMP Blanks	89.6(0.0)	171.4(0.2)	97.3(0.0)	153.7(0.0)
Lo TBHP/Lo DMP	37.9(18.8)	80.0(47.1)	33.2(70.6)	59.1(12.6)
Lo TBHP/Lo DMP/v	37.0(16.0)	81.3(70.4)	32.2(63.2)	60.5(10.2)
Lo TBHP/Hi DMP	101.3(7.5)	183.9(12.4)	113.8(22.4)	200.6(5.8)
Lo TBHP/Hi DMP/v	101.3(6.0)	193.9(7.3)	134.5(0.8)	215.2(4.2)
Hi TBHP/Lo DMP	62.7(63.3)	92.0(80.8)	79.4(33.4)	93.7(61.2)
Hi TBHP/Lo DMP/v	66.1(64.0)	95.7(93.8)	72.8(39.2)	95.5(116.5)
Hi TBHP/Hi DMP	160.4(25.0)	257.0(28.0)	233.2(57.3)	277.8(11.2)
Hi TBHP/Hi DMP/v	171.8(15.2)	267.5(20.7)	249.9(106.0)	325.3(47.8)

*The vented test flask trials are those denoted by "v".

In all instances, the presence of TBHP significantly increased the yield of insolubles produced when DMP was also present. Furthermore, the presence of Hi TBHP levels was always associated with more sediment than the corresponding Lo TBHP trials. In examining the peroxide number data, it will be noted that the correlation between the ultimate hydroperoxide levels and the yields of sediment are not good, which is an expected result (10, 11). The peroxide number of unstressed, doped D-11 fuel containing Lo TBHP was 20.7, and 68.9 for Hi TBHP. When DMP was not present, the TBHP dopant did not exert a significant destabilizing effect upon the fuel as measured by sediment generation. The effects of venting of test flasks were seen to be small and variable. Curiously, high levels of hydroperoxide were often observed in some Hi DMP trials after stress when TBHP had been present. Earlier work from our laboratory had indicated that DMP, in the absence of externally added hydroperoxide, was associated with very low peroxide numbers after stress.

A similar experimental matrix was used in the study of the potential interaction between 3-MI and TBHP. Interest in examining this interaction originated with our earlier studies of 3-MI induced fuel instability (11, 14), which showed that 3-MI is able to promote the formation of sediment and gum, but only in the absence of a hindered phenol antioxidant (AO-30). This result, coupled with the existence of a long induction period in the autoxidation of 3-MI in our shale diesel fuels, suggested that a classical free radical mechanism may be involved, which should, in turn, be sensitive to the presence of hydroperoxide present in the fuels.

Storage stability test results for the 3-MI/TBHP interaction are given in Table 3. These results indicate that a synergistic effect is present. Comparison of the 7 and 14 day results at 80°C suggest that an induction period was present. It will be noted that in the absence of externally added TBHP, 3-MI does not effectively promote sediment formation in the D-11 fuel, which contains AO-30. There is little doubt that the addition of TBHP rapidly overwhelmed the antioxidant, present at a level which was somewhat less than 24 mg/1, thereby allowing the autoxidation of 3-MI to proceed. The highest amounts of total insolubles were formed in the 43°C tests.

Venting of the test flasks generally led to a marked increase in the amount of sediment which formed. In these respects, the TBHP induced oxidation of 3-MI in fuel D-11 appears to be very similar to the simple autoxidation of this model nitrogen compound in fuel D-1 (a fuel which is identical in all respects to fuel D-11 except that it does not contain antioxidant) (11). Table 3 also shows peroxide analysis data for one of the stress sets (43°C/91d), which clearly indicates that high levels of hydroperoxide were present in all of the experimental flasks.

Table 3
Storage Stability Test Results for the 3-MI/TBHP Interaction

| Sample* | Total Insolubles, mg/100 ml (Peroxide Number, meq ROOH/kg fuel) | | | |
	80°C/7d	80°C/14d	43°C/49d	43°C/91d
Fuel Blanks	0.0	0.1	0.2	0.0(0.8)
Lo TBHP Blanks	0.0	0.4	0.0	0.0(16.2)
Hi TBHP Blanks	0.6	0.7	0.0	0.0(60.5)
Hi 3-MI Blanks	0.2	0.8	---	---
Lo TBHP/Lo 3-MI	0.7	1.1	0.3	0.0(50.2)
Lo TBHP/Lo 3-MI/v	0.4	3.9	0.5	0.0(76.6)
Lo TBHP/Hi 3-MI	1.5	11.7	2.2	53.6(46.3)
Lo TBHP/Hi 3-MI/v	2.3	12.5	70.7	129.0(36.6)
Hi TBHP/Lo 3-MI	0.7	3.8	2.5	3.7(112.5)
Hi TBHP/Lo 3-MI/v	0.6	4.1	1.5	9.3(159.9)
Hi TBHP/Hi 3-MI	1.7	8.7	33.0	0.7(64.2)
Hi TBHP/Hi 3-MI/v	1.9	17.2	81.2	149.5(56.3)

*The vented test flask trials are those denoted by "v".

Analyses of the sediments obtained with both DMP and 3-MI in the course of these TBHP interactive experiments have indicated that they are very similar, both in elemental composition and spectroscopic character, to sediments obtained in the absence of TBHP. For DMP, a typical sediment obtained in the presence of TBHP is 10.7% N, 60.1% C and 5.5% H; for 3-MI, a typical analysis is 5.5% N, 71.3% C and 5.6% H (these compare favorably with the empirical formulas in Table 1). Thus, it would appear that the TBHP functions as a catalyst or radical initiator rather than as a reactant in sediment formation.

Autoxidation of DMP and 3-MI in the Presence of Organic Acids and Bases

In an extension of our study of interactive effects in the autoxidation of DMP and 3-MI, ten organic acids and bases were examined as co-dopants in fuel D-11. This work was intended to determine whether the autoxidation of the nitrogen compounds is subject to acid or base catalysis, or if condensation products could form in lieu of true catalysis. Ten co-dopants were selected for study: acetic acid (HOAc), hexanoic acid (HA), decanoic acid (DA), p-toluenesulfonic acid (p-TsOH), dodecylbenzene sulfonic acid (DBSA), nicotinic acid (NA), 3-pyridinesulfonic acid (3-PSA), tri-n-butylamine (TBA), N,N-dimethylaniline (DMA) and 4-dimethylaminopyridine (4-DMAP). Most of the co-dopants were examined at two concentration levels ("Hi" and "Lo", as with TBHP); however, some of the compounds were only slightly soluble in D-11, so that a saturated solution was used for these (p-TsOH, NA, 3-PSA). Accelerated storage stability was assessed at 80°C (14d).

With DMP, the carboxylic acids (HOAc, HA and DA) all interacted in a synergistic fashion to increase the amount of sediment generated. A typical set of data is given in Table 4 for the DMP/DA experimental set. The results with the sulfonic acids were more difficult to interpret. Thus, DBSA exhibited a very strong positive interaction with DMP when present at levels of 0.3 or 1.0 equivalent. Yet when all four test flasks (vented and unvented) of the Hi DBSA/Lo DMP interaction were examined (these contain 3.33 equiv. of DBSA relative to DMP) a strong negative

306

interactive effect was seen. The interactive effects for p-TsOH were seen to be
small in magnitude and variable. A very potent base catalyst, 4-DMAP, was observed
to interact with DMP in a positive fashion whenever it was present. By contrast,
interaction with other base catalysts (TBA, DMA) or low-solubility zwitterionic
species (NA, present at ca. 0.3 ppm N w/v, and 3-PSA, present at less than 0.2 ppm N
w/v) did not lead to significant synergism under these test conditions.

<div align="center">

Table 4
Storage Stability Test Results for the DMP/DA Interaction
Fuel D-11 - 80°C/14 days - mg/100 ml

</div>

Sample*	Filtered Sediment	Adherent Gum	Total Insolubles
Fuel Blanks	0.1	0.0	0.1
Lo DA Blanks	0.1	0.1	0.2
Hi DA Blanks	0.1	0.1	0.2
Lo DMP Blanks	45.0	2.4	47.4
Hi DMP Blanks	165.2	6.2	171.4
Lo DA/Lo DMP	82.7	3.0	85.7
Lo DA/Lo DMP/v	84.2	2.6	86.8
Lo DA/Hi DMP	247.7	5.8	253.5
Lo DA/Hi DMP/v	238.8	5.3	244.1
Hi DA/Lo DMP	78.4	2.3	80.7
Hi DA/Lo DMP/v	96.2	2.6	98.8
Hi DA/Hi DMP	264.0	5.0	269.0
Hi DA/Hi DMP/v	279.2	5.3	284.5

*The vented test flask trials are denoted by "v".

Elemental and spectroscopic analyses were applied to the samples of DMP induced
sediment from these interactive experiments. It was not possible to obtain an
elemental analysis from the sediment formed in the DMP/DBSA trials, as their
tarry/waxy nature precluded proper sampling technique. However, the incorporation of
molecules of DBSA into the sediment is implied by: (a) the fact that such a large
amount of sediment (up to 1300 mg/100 ml) was generated that the DMP alone is unable
to account for the mass, and (b) a number of complex absorption peaks appear in the
S=O/S-O region of the infrared. Thus, the DBSA may serve as a reactant in addition
to or instead of serving as a catalyst. The incorporation of sulfur into DMP-derived
sediments has been observed by other workers when thiophenol was used as a co-dopant
(16-18); it has been considered possible that in situ oxidation of thiols to sulfonic
acids may be a viable pathway (4, 6). The DMP-derived sediments produced in all nine
other interactive experiments proved to be remarkably similar to the insoluble
material generated by DMP without co-dopant. Thus, it would appear that the
carboxylic acids and 4-DMAP are serving as true catalysts.
In a similar manner, the interaction of 3-MI with the ten acid/base co-dopants
was examined in D-11 fuel using 80°C-14d storage stability tests. With the three
carboxylic acids (HOAc, HA and DA), synergism was noted, with the highest levels of
insoluble material present in Hi 3-MI flasks (ca. 6-60 mg/100 ml of sediment was
generated, as compared with 0.8 mg/100 ml in the flasks which contained only 3-MI).
Venting of test flasks seemed to be associated with higher levels of sediment. As
was the case for DMP, the interactive effects of 3-MI with the sulfonic acids were
difficult to interpret. With p-TsOH, the interactive effect was uniformly small and
indeterminant. With DBSA, it was possible to generate small quantities of sediment
under most conditions, but only one set of conditions (Hi DBSA/Hi 3-MI/unvented) led
to the formation of large amounts of solids (ca. 70 mg/100 ml). With 4-DMAP, base
catalysis of 3-MI autoxidation was not evident. In light of the superior catalytic
nature of 4-DMAP, this result was somewhat unexpected, especially in light of a
recent suggestion that base-catalyzed oxidation of 3-MI could be significant (19).
Nicotinic acid (NA) was found to be catalytic in its interaction with 3-MI, with a
maximum of ca. 30 mg/100 ml of sediment formed in the Hi 3-MI/vented trials (a

saturated solution of NA was used, 0.3 ppm N w/v). Despite the apparent failure of
4-DMAP, dimethylaniline (DMA) exhibited synergism with 3-MI, but the effect was
largest when DMA was present at a "Lo" level. Tri-n-butylamine (TBA) actually
appeared to inhibit the autoxidation of 3-MI slightly. The final co-dopant,
3-pyridinesulfonic acid (3-PSA) showed a very slight positive interactive effect,
forming ca. 6 mg/100 ml of solids in the Hi 3-MI flasks.

    Analysis of the sediments generated in the 3-MI interaction experiments was
limited by the small amounts of materials isolated on the glass fiber filter pads.
Elemental analyses could only be conducted on the sediments from the carboxylic acid
interactions; these all contained ca. 5.7% N, 72.5% C and 5.8% H, and so are almost
identical in elemental composition to 3-MI induced sediment which formed in the
absence of the co-dopants. Spectroscopic examination of the sediments confirm that
the heterogeneous material generated is also similar. Table 5 is a qualitative
summary of the results obtained with DMP and 3-MI where an organic acid or base was
present as a co-dopant.

Table 5
Summary of Relative Interactive Effects with Organic Acids and Bases

| Co-Dopant** | Interactive Effect* | |
	DMP as Dopant	3-MI as Dopant
HOAc	++	++v
HA	++	++v
DA	++	++
p-TsOH	i	i
DBSA	++	++v
NA	i	++v
3-PSA	i	+
TBA	+v	-
DMA	i	+
4-DMAP	+	i

*Key to symbols: ++ = strong synergism, + = weak synergism
                 - = weak inhibition, i = indeterminate effect
                 v = sensitive to venting of test flasks
**Refer to the text for the identity of the abbreviations.

CONCLUSIONS

    Hydroperoxide dissolved in a shale derived diesel fuel can interact in a strong
synergistic fashion with polar nitrogen heterocyles to lead to the formation of
significant amounts of sediment and gum. Carboxylic and sulfonic acids similarly
assist in the degradation of fuel quality by interacting with alkylpyrroles and
indoles. Interactions with organic bases appear to be of a smaller magnitude.

ACKNOWLEDGMENT

REFERENCES

1.   NRC/NRL Cooperative Research Associate Postdoctoral Fellow, 1984-1986.
2.   J. W. Goetzinger, C. J. Thompson and D. W. Brinkman, DOE Report No.
     DOE/BETC/IC-83/3, October 1983.

3. J. W. Frankenfeld, W. F. Taylor and D. W. Brinkman, DOE Report No. DOE/BC/10045-12, February 1981.
4. J. W. Frankenfeld, W. F. Taylor and D. W. Brinkman, DOE Report No. DOE/BC/10045-23, March 1982.
5. J. W. Frankenfeld, W. F. Taylor and D. W. Brinkman, Ind. Eng. Chem. Prod. Res. Dev., 22: 608 (1983).
6. J. W. Frankenfeld, W. F. Taylor and D. W. Brinkman, Ind. Eng. Chem. Prod. Res. Dev., 22: 615 (1983).
7. K. E. Dahlin, S. R. Daniel and J. H. Worstell, Fuel, 60: 477 (1981).
8. J. H. Worstell and S. R. Daniel, Fuel, 60: 481 (1981).
9. J. H. Worstell, S. R. Daniel and G. Frauenhoff, Fuel, 60: 485 (1981).
10. R. N. Hazlett, J. V. Cooney and E. J. Beal, DOE Report No. DOE/BC/10525-4, June 1983.
11. J. V. Cooney, R. N. Hazlett and E. J. Beal, DOE Report No. DOE/BC/10525-8, June 1984.
12. J. V. Cooney, E. J. Beal and R. N. Hazlett, Preprints, Div. of Petro. Chem., ACS, 28(5): 1139 (1983).
13. J. V. Cooney, E. J. Beal and R. N. Hazlett, Preprint, Div. of Petro. Chem., ACS, 29(1): 247 (1984).
14. J. V. Cooney, E. J. Beal, M. A. Wechter, G. M. Mushrush and R. N. Hazlett, Preprints, Div. of Petro. Chem., ACS, 29(4): 1003 (1984).
15. J. V. Cooney, E. J. Beal and R. N. Hazlett, Liq. Fuels Tech., 2(4): 395 (1984).
16. N. F. Yaggi, S. H. Lee, J. Ge and N. C. Li, Preprints, Div. of Fuel Chem., ACS, 29(1): 178 (1984).
17. S. H. Lee, J. H. S. Ge and N. C. Li, Preprints, Div. of Petro. Chem., ACS, 29(4): 996 (1984).
18. L. Jones, R. N. Hazlett, N. C. Li and J. Ge, Fuel, 63: 1152 (1984).
19. Z. Yoshida, Heterocycles, 21: 331 (1984).

THE EFFECT OF ACTIVATION AND PROMOTION ON A FISCHER-TROPSCH CATALYST

H.W. Pennline, J.M. Stencel, M.F. Zarochak, S.S. Pollack, and R.R. Anderson

U.S. Department of Energy
Pittsburgh Energy Technology Center
P.O. Box 10940
Pittsburgh, Pennsylvania 15236

INTRODUCTION

Since the late 1970's, an interest in the production of gasoline and other transportation fuels from synthesis gas has been renewed. A conceptual scheme for the production of gasoline from low-ratio synthesis gas is the two-stage method developed by Mobil [1]. In this process, mixtures of hydrogen and carbon monoxide are reacted in a slurry bubble column containing a conventional Fischer-Tropsch catalyst in the first stage. The product from this step is then sent to the second-stage reactor that contains the shape-selective zeolitic catalyst ZSM-5. One of the goals of the indirect liquefaction research program at the Pittsburgh Energy Technology Center is to investigate catalyst systems in the slurry phase that are potential candidates for the first-stage process. These catalyst systems should process low ratios (0.5/1 to 1/1 of H_2/CO) of synthesis gas to produce a high yield of light olefins and gasoline-range hydrocarbons.

Certain results in the literature indicate that synthesis gas conversions with iron-manganese oxide catalysts yield a suppressed C_1-fraction and a large C_2-C_4 light-hydrocarbon fraction that deviates from that predicted by Schulz-Flory kinetics [2,3]. A recent three-phase study with iron-manganese catalysts of various compositions found that hydrogenation of olefins occurred along with olefin isomerization reactions [4]. The C_2-C_4 content of the hydrocarbon distribution followed Schulz-Flory kinetics and did not exceed the 56 weight percent maximum predicted by Schulz-Flory. Since these results with iron-manganese catalyst were not as good as those reported in the patent literature, two areas of interest -- catalyst activation and promotion -- were investigated with the intent of improving olefin selectivity and catalyst activity and stability.

In this study, the activation and promotion of a 21Fe/79Mn catalyst were investigated in a slurry reactor. The effects of the process parameters of temperature, pressure, and reducing gas composition on the activation step and on the subsequent catalyst activity and product selectivity were studied. Also, the alkali promotion of the iron-manganese catalyst with potassium carbonate was investigated. Slurry samples were taken at various times on stream, and the catalyst was analyzed by surface techniques so that the catalyst properties could be correlated with process results.

EXPERIMENTAL

The catalyst was prepared in a continuous, stirred precipitation reactor similar to a unit used by Kölbel and Ralek [5]. Nitrates of iron and manganese were reacted with ammonium hydroxide. Batches of the washed

and vacuum-dried coprecipitate were crushed, sieved through a 100-mesh screen, and homogenized by rolling. A portion of the total batch was further crushed and sieved through 325 mesh (44 μm). Catalyst for all the tests in this study was obtained from this portion. The fresh catalyst was about 14 weight percent iron and 52 weight percent manganese.

The slurry studies were conducted in a one-liter stainless steel stirred reactor as described elsewhere [6]. Typically, fifty-one grams of iron-manganese catalyst that were sieved through 325 mesh (44 μm) were placed in the reactor with the molten medium wax to make a 13.5 weight percent suspension based on unreduced catalyst weight. The high-boiling paraffinic wax (P-22 from Fisher Scientific Company) had an average carbon number of 28. The reactor system was sealed, cooled, leak-tested, and purged with helium. At the desired activation pressure, the temperature was increased to the desired activation temperature under a flow of helium. Isothermal conditions within the reactor were established by means of a sliding thermocouple in a thermowell in the reactor. The impeller was stopped and gas flow was decreased to a small amount, at which time the unexpanded slurry level was lowered to 0.5 liter by using the reactor pressure to force the excess wax through a dipleg and filter and into a heated wax trap. The impeller was then restarted, and once isothermal and isobaric conditions were reestablished, the inert flow was stopped and the activation gas was introduced. Unless specified, activation usually lasted for twenty-four hours. At the end of this activation, the liquid level was again readjusted, and the system pressure and temperature were adjusted to 200 psig and 275°C, respectively. Synthesis feed gas was introduced in increments over the next hour until a weight hourly space velocity (WHSV) of 1.21 hr^{-1} was reached. (WHSV is defined as grams of gas per hour per gram of charged catalyst.) Trap drainings, flows, and gas analyses were measured on a twenty-four hour basis for material balance determinations. Unless otherwise stated, tests in this study used a 1H$_2$:1CO feed gas.

The gaseous and liquid products were characterized by various analytical techniques. Gas exiting the reactor system was analyzed for hydrogen, carbon monoxide, carbon dioxide, nitrogen, and hydrocarbons up to C$_8$ by gas chromatography. The liquid condensate in the trapping system was collected and physically separated into an aqueous fraction and an oil fraction. The aqueous phase was analyzed by mass spectrometry to detect oxygenates, and the water content was determined by the Karl Fischer reagent technique. The liquid hydrocarbon samples were characterized by fluorescent indicator adsorption (FIA) ASTM D-1319 to determine the functionality of the liquid oil, and by bromine number ASTM D-1159 to check the olefin content. Infrared studies were also performed on the oil fractions. Relative amounts of terminal, trans-internal, and beta-branched-terminal olefins were deter- mined by infrared spectral analysis. The wax fraction, which was dependent on the trapping system, and selected liquid oil samples for a particular period of time were also analyzed by gas chromatography with a capillary column.

Slurry samples were withdrawn from the reactor at various times on stream. The wax-encapsulated iron-manganese catalysts were characterized by X-ray photoelectron spectroscopy (XPS) and X-ray diffraction (XRD). A mild washing of the slurry-catalyst samples by sonication in toluene was performed before the XPS analysis. These washed samples still contained

slurry wax, but it was at a level that permitted XPS data acquisition while simultaneously preventing oxidation of the catalyst surface. The samples were then either spread onto holders or pressed into thin wafers for subsequent XPS data acquisition. Preliminary XPS data were also obtained from activation of an iron-manganese catalyst treated in situ with hydrogen in the XPS. These data were acquired from wafered samples after gaseous treatment at pressures near 1.5 atm and temperatures between $275^\circ C$ and $450^\circ C$. Preliminary results of various activations with iron-manganese catalyst in a thermogravimetric analyzer (TGA) were also obtained.

RESULTS AND DISCUSSION

In a previous study with various iron-manganese catalysts [4], a standard activation with carbon monoxide was used. With the 21Fe/79Mn catalyst used in this study, the catalyst was activated with carbon monoxide as the base-line case at 2.25 WHSV, $275^\circ C$, and 200 psig for 24 hours. All activations were conducted in situ. Activation parameters investigated were temperature ($275^\circ C$ versus $300^\circ C$), pressure (0 psig versus 200 psig), and gas composition (CO, CO followed by H_2 -- Kölbel-type [3], synthesis gas, and hydrogen). Slurry reactor results for selected periods during a test are shown in Table 1. Synthesis process conditions for all the tests were 1.21 WHSV of $1H_2/1CO$ feed gas, $275^\circ C$, and 200 psig unless otherwise indicated. In the tests where carbon monoxide was used to reduce the catalyst, the carbon dioxide was monitored in the exit gas by an infrared detector. In all cases, after the beginning of the carbon monoxide reduction, the carbon dioxide concentration reached a maximum during the first two hours and thereafter asymptotically approached a zero concentration.

As in past work with iron-manganese catalysts, the functionality of the product in the base-line test SL-54 changed with time on stream. As seen in Table 1, the light olefin content decreased with synthesis time due to olefin hydrogenation. This is paralleled by FIA results on the liquid oil, which reveal that with time on stream, the oil becomes more paraffinic and less olefinic. Also with catalyst aging, the olefinic products exhibit more double-bond isomerization. If the 2-butene/1-butene ratio is used as an index for olefin isomerization, this ratio -- thus, isomerization -- increased in the C_4 fraction with time. Similarly, by infrared analysis of the liquid oils, the ratio of internal to terminal olefins also increased with time.

The catalyst in test SL-57 was activated identically to the base-line test except at $300^\circ C$. This higher temperature of activation increased the initial activity of the catalyst but also increased the deactivation rate of the catalyst. A lower pressure (0 psig) of activation was used in test SL-60, and this increased the initial activity over the base-line test. A Kölbel-type of activation in test SL-58 (CO treatment for 24 hours at $275^\circ C$ and 200 psig, followed by H_2 treatment at $275^\circ C$ and 200 psig) had activity results similar to those of the base-line test SL-54.

The trends in the product selectivity were the same for all the tests (see Table 1). With time on stream, the hydrocarbon selectivity shifted to a lighter fraction; the olefin content decreased; and a larger percentage of olefin isomers occurred. A minor exception is noted in the Kölbel-type

activation test, where the internal-to-terminal olefin ratios in both the gas and oil phases went through a minimum during the first part of the test.

The major differences in the activation studies occurred when the catalyst was activated at 275°C and 200 psig with hydrogen or synthesis gas ($1H_2/1CO$) as compared to carbon monoxide. No catalyst activity occurred with hydrogen activation, and only slight conversion (<2%) occurred with a synthesis gas activation. Investigating a higher iron-to-manganese ratio catalyst, Maiti et al. [7] claimed that a $MnFe_2O_4$ spinel and MnO were the major phases at hydrogen reduction temperatures below 300°C. The XPS information in the latter section will clarify this point.

The addition of a structural promoter to the 21Fe/79Mn catalyst was attempted to stabilize the activity and maintain a high light-gas olefin content. Schulz and Gokcebay [8] claimed that potassium addition to their iron-manganese catalysts reduced secondary olefin hydrogenation and isomerization reactions. Based on this, several batches of 21Fe/79Mn catalyst were impregnated with various amounts of potassium. Three different potassium levels were investigated: 0.1, 0.4, and 1.3 weight percent. Results are listed in Table 1. An activation with carbon monoxide at 2.25 WHSV, 275°C, and 0 psig for 24 hours was done in situ for each test.

As compared to test SL-60 that had an unpromoted catalyst, the activity of the 0.1% potassium catalyst was about the same except after 119 hours on stream, where the potassium-promoted catalyst had deactivated significantly. The 0.4 and 1.3 weight percent potassium-promoted catalysts had very high initial activities [50 mole percent (H_2 + CO)-conversion] but decreased after 200 hours on stream to values comparable to the unpromoted catalyst.

The hydrocarbon distribution for the unpromoted iron-manganese shifts to a lighter fraction with time and to a lower olefin content with a larger fraction of olefin isomers. The lowest loading of 0.1 weight percent potassium did not seem to change these trends. However, for the catalyst with the 0.4 weight percent potassium loading, the product distribution shifts to a higher carbon number with time. The percent olefinic product actually increases with time, and the internal/terminal olefin ratio decreases -- indicating less olefin isomerization. At the highest potassium loading in test SL-62, the hydrocarbon distribution is relatively constant and is shifted to higher molecular weights. The olefin content is high (85 weight percent), and the internal/terminal olefin ratio is about an order of magnitude less than with the unpromoted iron-manganese catalyst. With this iron-manganese catalyst, a high loading of potassium is evidently needed to prevent olefin hydrogenation and isomerization reactions. However, the product distribution is shifted so that only about 30 weight percent of the hydrocarbon product is C_2-C_4 rather than the 40 weight percent obtained with the unpromoted catalyst.

The XPS analysis of the wax-encapsulated iron-manganese catalysts determined the surface atomic ratios Fe/Mn and C/Mn (see Table 2). These results can be correlated with the activity of a catalyst during three-phase testing. For example, the (H_2+CO) conversion in SL-61 was negligible throughout the slurry run. Such inactivity is mirrored in the C/Mn ratios that are constant throughout the test and are lower than C/Mn for other slurry tests. In relation to test SL-61, XRD and in situ XPS results with

an unpromoted iron-manganese catalyst under hydrogen with temperatures ranging from 275°C to 450°C revealed that metallic iron was not produced. Instead, a solid solution of FeO-MnO and/or a Fe-Mn spinel is formed. Hence, the constant and low C/Mn ratio in SL-61 suggests that iron is not available for iron carbide formation during synthesis gas exposure, and thus, no conversion/activity is observed during the test.

The variations in the atomic ratios for slurry tests SL-54 through SL-60 are related to differences in the activation gas sequence and the activation parameters for the unpromoted iron-manganese catalyst. In general, the trend in these tests is for the Fe/Mn values to decrease with time on stream. Correspondingly, the C/Mn values increase with time on stream and can be related to carbon deposition as a function of time on stream and/or as a difference in the amount of slurry wax retained by the catalysts after toluene sonication. In all cases, the catalyst deactivated to some extent over the first 200 hours on stream. More specifically, an increased carbon content was found on the catalyst activated under carbon monoxide at 300°C (SL-57) compared to the catalyst activated under carbon monoxide at 275°C (SL-54) with synthesis time. This increased C/Mn ratio, as independently confirmed by TGA results, is probably related to an enhanced amount of iron carbide and/or carbon formation during the activation and usage stages of SL-57. Such enhancement paralleled the faster deactivation rate for SL-57. The corresponding C/Mn ratios for SL-58 show that H_2 reduction after CO exposure (Kölbel-type activation) decreases the carbon content on the catalyst to levels below SL-57. Such a decrease may be related to greater formation of metallic Fe after the hydrogen reduction, as indicated by the high Fe/Mn ratio after 48 hours on stream.

Table 2 also reports XPS results from the potassium-promoted tests SL-62 through SL-64. In general, for these tests, the Fe/Mn ratio increases with time on stream, unlike results with the unpromoted catalysts. Also, the C/Mn ratio increases with time on stream. In all cases with the promoted catalyst, the potassium appears to enhance the surface iron concentration during a test. The potassium also appears to increase surface carbon deposition during a test. The catalyst in test SL-64 deactivated significantly during the experiment, and this could be related to the rapidly increasing C/Mn ratio during the test.

SUMMARY

The effects of various activations of an iron-manganese catalyst on synthesis gas conversion were investigated in a slurry reactor. Although the activation temperature and pressure did affect catalyst activity, olefin hydrogenation and isomerization reactions still appear to be significant in all cases. The activating gas composition had the most dramatic effect, with the catalyst exhibiting no activity after a hydrogen activation. Potassium promotion of the iron-manganese catalyst succeeded in increasing the activity and increasing the percentage of olefins in the light gas fraction. However, the hydrocarbon distribution was shifted to a higher average molecular weight. The XPS results of catalyst slurry samples at various process times were correlated with the catalytic process results to explain the particular catalyst performance.

314

DISCLAIMER

Reference in this report to any specific commercial product, process, or service is to facilitate understanding and does not necessarily imply its endorsement or favoring by the United States Department of Energy.

ACKNOWLEDGMENT

REFERENCES

[1] Mobil Final Report, U.S. DOE Contract No. DE-AC22-80PC30022, June 1983.

[2] Bussemeier, B.; Frohning, C.D.; Horn, G.; Kluy, W. German Patent 2 518 964, 1976.

[3] Kölbel, H.; Tillmetz, K.D. U.S. Patent 4,177,203, 1979.

[4] Pennline, H.W.; Zarochak, M.F.; Tischer, R.F.; Schehl, R.R. Paper No. 14c, presented at the AIChE Summer National Meeting, Philadelphia, Pa., August 1984.

[5] Kölbel, H.; Ralek, M. Catal. Rev. Eng. 1980, 21, 225.

[6] Zarochak, M.F.; Pennline, H.W.; Schehl, R.R. DOE/PETC/TR-84/5, U.S. Department of Energy, 1984.

[7] Maiti, G.C.; Malessa, R.; Baerns, M. Applied Catal. 1983, 5, 151.

[8] Schulz, H.; Gokcebay, H. Proc. Organic React. Conf., Charleston, S.C., April 1982.

Table 1: Results of Activation and Promotion Studies.

Test	SL-54				SL-57			SL-58			SL-60		
Synthesis Time on Stream, hr*	47	118	142	191	47	119	167	43	115	187	48	120	204
CO-Conversion, mole percent	27.4	26.9	27.3	20.6	36.3	25.9	16.2	25.2	26.5	16.3	35.7	32.4	29.1
(H₂+CO)-Conversion, mole percent	29.8	27.5	29.0	24.1	38.3	29.2	15.8	25.0	25.5	19.7	35.6	33.1	30.1
Hydrocarbon Distribution, wt%													
CH₄	8.0	8.8	8.4	9.2	6.8	9.1	14.0	8.9	9.4	10.7	6.9	7.2	7.8
C₂-C₄	41.7	43.0	42.4	44.2	37.2	37.1	45.8	43.9	43.5	40.3	38.3	39.1	40.7
C₅₊	50.2	48.2	49.2	46.6	56.0	53.8	40.2	47.2	47.1	49.1	54.8	53.7	51.5
Olefin Content C₂-C₄ Fraction, wt%	76.5	70.8	70.7	69.4	74.2	62.2	50.5	73.5	71.9	63.9	76.8	72.3	68.8
Internal/Terminal-Olefin Ratio	1.1	1.5	1.7	1.9	0.94	2.3	--	2.1	1.6	1.9	0.67	1.1	1.8
2-Butene/1-Butene Ratio	0.30	0.45	0.53	0.56	0.29	0.69	1.0	0.35	0.30	0.55	0.21	0.30	0.44

Test	SL-63		SL-64			SL-62		
Potassium Loading, wt%	0.1		0.4			1.3		
Synthesis Time on Stream, hr*	48	119	46	118	187	47	119	191
CO-Conversion, mole percent	32.9	14.6	56.3	32.9	18.0	59.5	40.5	30.4
(H₂+CO)-Conversion, mole percent	32.8	15.2	50.2	29.5	18.6	50.0	33.9	25.9
Hydrocarbon Distribution, wt%								
CH₄	7.0	16.6	9.4	9.5	6.6	3.7	3.6	3.8
C₂-C₄	32.3	48.8	37.6	37.1	29.3	21.0	23.4	25.1
C₅₊	60.7	34.6	53.0	53.4	64.1	75.3	73.0	71.1
Olefin Content C₂-C₄ Fraction, wt%	65.4	45.4	65.2	67.4	69.3	83.8	84.8	85.9
Internal/Terminal-Olefin Ratio	1.4	3.0	1.5	1.2	0.63	0.14	0.16	0.23
2-Butene/1-Butene Ratio	0.50	0.25	0.45	0.33	0.11	0.03	0.04	0.05

*Slurry Synthesis Conditions: 1.21 WHSV of 1H₂/1CO, 275°C, 200 psig.

316

Table 2: Fe/Mn and C/Mn Atomic Ratios from XPS Analysis of Iron-Manganese Slurry Catalysts Sampled From the Slurry Reactor After Specified Activation Step(s) and After Specified Times on Stream.

Slurry Test	SL-54	SL-57	SL-58	SL-61	SL-60	SL-63	SL-64	SL-62
Fe/Mn								
CO-Activation	0.23	0.30	0.34		0.16	0.18	0.29	
H_2-Activation								
~48 hours	0.22	0.20	0.32	0.29	0.16	0.20	0.53	0.16
~100 hours			0.43	0.29		0.28		
~200 hours	0.16	0.14	0.19	0.29	0.15		0.50	0.24
C/Mn								
CO-Activation	4	6	10		10	7	8	
H_2-Activation								
~48 hours	6	12	6	6	19	13	23	16
~100 hours			10	4		15		
~200 hours	7	28	16	4	52		59	34

317

CATALYTIC SYNTHESIS OF METHANOL FROM HYDROGEN AND CARBON MONOXIDE ON A COPPER-ZINC OXIDE SUPPORTED CATALYST

Rajesh M. Agny and Christos G. Takoudis

School of Chemical Engineering
Purdue University
W. Lafayette, IN 47907

INTRODUCTION

Most kinetic studies of methanol synthesis over Cu/ZnO catalysts have been carried out using mixtures of carbon monoxide and hydrogen. But in some cases (1) the synthesis gas has also contained carbon dioxide (2). Power rate laws as well as complicated rate expressions have been proposed over the years. The detailed kinetics of the surface processes is virtually unknown. With the exception, perhaps, of the near-atmospheric work by Saida and Ozaki (3), investigations of the kinetics of methanol synthesis over Cu/ZnO catalysts have been done at pressures on the order of 75 atm (1,4-8). A major drawback of several such kinetic studies is the use of integral reactors.

In this study, we investigate the kinetics of methanol synthesis over a commercial $Cu/ZnO/Al_2O_3$ catalyst in a differential reactor at pressures in the range from 3 to 15 atm and temperatures between 250 and 290° C (9).

EXPERIMENTAL METHOD

A high pressure unit is used for the kinetic experiments (9). The reactor system consists of a U-tube made of stainless steel 304, 0.95 cm OD and 0.09 cm thick. The U-tube is suspended vertically in a Techne fluidized sand bath SBS-4. In the direction of flow, the U-tube contains a length of glass wool, a preheating section of Potters silica glass spheres P-047, a second length of glass wool to isolate the catalyst bed from the glass spheres and a final glass wool plug above the catalyst bed to prevent carry-over of the catalyst (9). Omega iron-constantan thermocouple probes TT-J-30 are used for temperature measurements. Our data reveal that the fixed bed we use is isothermal (9). The reactor system is pressurized by a Grove back pressure regulator 91W. The reactor effluent is led to a Carle sampling valve 7707. During analysis, the effluent sample is carried by the carrier gas (hydrogen) to a Varian Aerograph Gas Chromatograph 202-B. A Chromosorb 102 column permits separation of CO, CO_2, and methanol. The gas chromatograph is coupled with a Houston Instrument chart recorder A521X-14K to enable qualitative and quantitative analysis of the effluent. Based on gas chromatographic analysis of CO bubbled through methanol at different temperatures, it is concluded that the weight percent of the components in the reactor effluent can be estimated by using Dietz's thermal conductivity weight factors (10).

A 5 g $Cu/ZnO/Al_2O_3$ catalyst sample (C79-2-01 of United Catalysts, Inc., Kentucky.) of average size equal to 0.077 cm is reduced with hydrogen at 1 atm and 290° C for 15 hours (9). No further pretreatment is done during the rest of the experimental span. A reaction interval of one hour is found to be sufficient to produce reproducible steady-state product distributions. Steady state reaction data are collected at temperatures between 250 and 290° C, pressures in the range of 3 to 15 atm, $H_2/CO = 2.1 - 2.4$

and total flow rates between 70 and 120 cc/min (STP). The catalyst composition measured with a Dispersive Analyzer is on an oxygen free basis: 40.6 wt.% Cu, 50.3 wt.% Zn and 9.1 wt % Al. The specific surface area of this catalyst, determined by BET with N_2, is 37.8 m^2/G.

RESULTS

The $Cu/ZnO/Al_2O_3$ catalyst is tested at three temperatures, 250, 270 and 290°C. Typical measured steady state conversions are summarized in Table 1 along with the conditions used. No deactivation of the catalyst is observed at the experimental conditions studied, based on periodic tests conducted at "standard conditions" which were chosen to be 11.2 atm, 250°C and H_2/CO ratio equal to 2.3. As a consequence of a rigorous design of our differential reactor, heat and mass transfer effects are negligible (9).

Methanol is the main product at the conditions studied. Carbon dioxide and water (in trace amounts) are formed as side products. No other by-products are observed at the conditions used. It is observed that the reaction rate increases as the temperature increases in the temperature range 250 to 290°C. Also, the reaction rate increases as the total pressure increases at constant temperature and H_2/CO ratio (Table 1). Note that at 250 and 270 °C the methanol synthesis reaction in our system is far from equilibrium whereas at 290 °C the reverse reaction becomes important.

Starting with power rate laws, several rate expressions were tried to fit our data. Emphasis was laid, on rate expressions containing a small number of parameters. The reaction rate was found to be approximately proportional to the total pressure. This enabled us to eliminate several rate expressions if the observed dependence of rate on total pressure was not followed (9).

Since evidence for the formyl (CHO-) and the methoxy (CH_3O-) species has been reported for Cu/ZnO catalysts during methanol synthesis (1,2,11), two parameter and three parameter kinetic models which can be derived from Langmuir-Hinshelwood type rate expressions were tried. These contained rate determining steps involving a bimolecular surface reaction between an absorbed hydrogen atom and either a methoxy or a formyl adsorbed species. The form of such rate expressions examined is

$$r = k \left\{ P_{CO} P_{H_2}^2 - \frac{P_{MeOH}}{K_{eq}} \right\} P_{CO}^l \cdot P_{H_2}^m \qquad 1)$$

It is found that the best possible fit is obtained with the rate expression (9)

$$r = k \left\{ P_{CO} P_{H_2}^2 - \frac{P_{MeOH}}{K_{eq}} \right\} (P_{CO} P_{H_2}^{0.5})^n \qquad 2)$$

where $k = k_o \exp \left(\frac{-E}{RT} \right)$ and $n = -1.30 \pm 0.03$. The Arrhenius plot of the temperature dependence of k is presented in Figure 1. With a single pre-exponential factor and a single overall activation energy obtained from linear regression of the rate constant data, large deviations (30-40%) are observed between predicted and measured reaction rates. Therefore, it is proposed that there is a decrease in the overall activation energy with temperature (Fig. 1). The overall activation energies and the corresponding pre-exponential factors computed at each temperature from Figure 1, are presented in Table 2. The error

accompanying the estimation of the activation energy is about $\pm$ 1000 cal/gmol based on the error involved in calculating the activation energy from the Arrhenius plot and the 15% maximum relative error in observed reaction rates. Equation 2 fits all our data with a maximum relative error of less than 15% (Fig. 2).

DISCUSSION

From the structure of rate Equation 2 we note that (i) the kinetics of the reverse reaction is accounted for; (ii) this rate expression contains only two parameters, the rate constant and an empirical constant, n (1,3,6,9); (iii) the reaction rate depends on a positive power of partial pressure of hydrogen and on a negative power of the partial pressure of carbon monoxide (1,9); and (iv) the measured overall activation energy decreases with increasing temperature (Table 2).

The term $P_{CO}P_{H_2}^{0.5}$ (Eq. 2) represents a formyl species, CHO-, formed by a reactive collision between CO and an adsorbed hydrogen atom. Mechanisms proposed by Herman *et al.*, (4) and Kung (11) involve the formyl species as one of the surface intermediates. Assuming the formyl species to be the most abundant surface intermediate and the last reaction step of both mechanisms to be rate determining, a rate expression similar to Equation 2 can be derived (9,12).

In the mechanism reported in (4), the intermediates are proposed to be bonded to the surface cation via the carbon atom. Such a proposal is feasible for noble-metal catalysts because relatively strong metal carbon bonds can be formed, and there is ample evidence that CO adsorbs molecularly on these metals with the carbon end pointing towards the metal (11). However, it is proposed that the large dipole moments and the relatively uneven electron density distribution on oxide surfaces favor bonding of the surface to the oxygen atom of the intermediate (11). Thus a methoxy type derivative should be more likely.

In the mechanism proposed in (11), the formation of the methoxy intermediate from the formyl species involves rupture of two bonds and formation of three bonds. An elementary step is expected not to involve multiple bond ruptures and formations. This proposed elementary step of such a mechanism must therefore be looked upon cautiously in the absence of independent evidence that supports such a step.

The indication of the formyl species from the kinetics observed and the examination of the shortcomings of the mechanisms proposed in (4,11) allow us to suggest the mechanism (9)
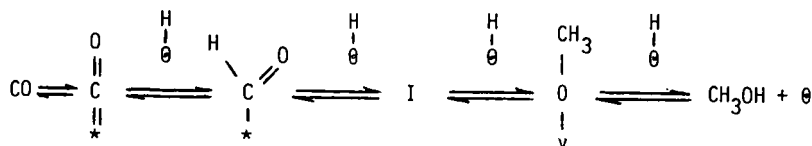
for the supported Cu/ZnO catalyst we used. Here the symbols *, θ and v represent a metal cation, a zinc or an oxygen site, and an oxygen vacancy respectively. "I" represents a likely intermediate between the formyl and methoxy species (9). Its possible structure needs to be investigated.

Rate equation 2 can be derived from this mechanism by assuming that the formyl species is the most abundant surface intermediate and that the surface reaction between the methoxy species and an

adsorbed hydrogen atom is the rate determining step (Agny, 1984). The main difference between this mechanism and the mechanism reported in (11) is the addition of an intermediate I between the formyl and methoxy intermediates.

Recently, coadsorption of CO and H_2 on ZnO and Cu/ZnO catalysts has been investigated at 270 K and subatmospheric pressures by Saussey *et al.*, (13). The infrared spectrum of a mixture of CO and H_2 adsorbed on ZnO or Cu/ZnO reveals a pair of weak bands which have been assigned to vibrations of a surface formyl species. This is to our knowledge, the first report presenting direct evidence for a formyl species resulting from CO and H_2 interaction on Cu/ZnO catalysts. Deluzarche et al. (14) claim to have identified, by reactive scavenging, the formyl species on nickel. Kung (11) presents certain organometallic chemistry analogs to substantiate the formyl and methoxy species as intermediates in the mechanism he has proposed for methanol synthesis on ZnO and Cu/ZnO catalysts. These findings support our suggestion that adsorbed formyl species can be the most abundant surface intermediate (9), although further studies are necessary for such a proposal.

Formaldehyde has never been observed as an intermediate in methanol synthesis over ZnO or Cu/ZnO catalysts. A plausible explanation, perhaps, is that formaldehyde being a highly reactive intermediate undergoes rapid conversion in some species like the methoxy. Saida and Ozaki (3), who have studied the kinetics of methanol synthesis over a $Cu/ZnO/Cr_2O_3$ catalyst at near atmospheric pressures, conclude that quantitative interpretation of their data is possible only by assuming a reaction sequence involving formaldehyde. In a very recent work, Tawarah and Hansen (15) have investigated the kinetics of methanol decomposition over ZnO in the temperature range 563 to 613 K. Based on their observations, they confirmed the presence of formaldehyde in the reactor effluent with a mass spectrometer and with chemical methods. Invoking the principle of microscopic reversibility, it may be concluded that some of those intermediates (15) participate in the methanol synthesis reaction.

Ample evidence exists for the methoxy species on ZnO and ZnO/Cr_2O_3 catalyst (16-19). Since the active forms appear to be the metal cations for both ZnO and Cu/ZnO catalysts, it seems reasonble to assume the formation of methoxy species on the Cu/ZnO catalysts. Recently, the methoxy species has also been observed on a Cu/ZnO catalyst during methanol synthesis (20). For Cu/ZnO catalysts it is proposed that the intermediates, in the course of their progress towards the product methanol, orient themselves to form the more favorable oxygen-surface bond (11). These arguments lend support to the inclusion of a methoxy intermediate in the mechanism proposed for methanol synthesis over a $Cu/ZnO/Al_2O_3$ catalyst.

There can be considered to be three possible ways of CO_2 formation (i) the Boudouard reaction, (ii) the water gas shift reaction, and (iii) oxidation-reduction of the catalyst. In our reaction system, the carbon and oxygen balances based on CO in the feed and CO, CO_2 and CH_3OH in the reactor effluent are always closed. This enables us to suggest that the Boudouard reaction can be eliminated as a source of CO_2 (9).

Van Herwijnen and Dejong (21) have investigated the kinetics and mechanism of the water gas shift reaction on a Cu/ZnO catalyst in the range of 172 to 230°C and pressures ranging from 1 to 6 atm. With a feed mixture containing CO, N_2 and small amounts of H_2O, they find their Cu/ZnO catalyst to be active in the forward direction of this reaction. This finding allows us to suggest that at our experimental conditions (250–290°C, 3–15 atm), such a reaction is likely.

321

Herman *et al.*, (4) have tested a $Cu/ZnO/Al_2O_3$ catalyst for a H_2/CO (76/24) mixture without CO_2. Although this catalyst is found to be selective to methanol, it is rapidly and irreversibly deactivated. Their examination of the catalyst by optical spectroscopy reveals only the pink color that is characteristic of copper. They attribute this to oxidation-reduction of the catalyst.

In view of these arguments and lack of any spectroscopical analysis of our catalyst, both the water gas shift reaction and oxidation-reduction of the catalyst are probably responsible for the formation of CO_2 at the conditions of our experiments.

SUMMARY

The kinetics of methanol synthesis from carbon monoxide and hydrogen over a commercial $Cu/ZnO/Al_2O_3$ catalyst has been investigated at temperatures between 250 and 290 °C and pressures between 3 and 15 atm. The highest catalytic activity is observed at 290 °C. A two parameter kinetic model that quantitatively describes the observed patterns is presented. It is also proposed that the formyl species, CHO-, appears to be the most abundant surface intermediate, and the rate determining step seems to be the surface reaction between the methoxy intermediate and an adsorbed hydrogen atom. Based on this study and current knowledge of supported Cu/ZnO catalysts, a mechanism for the methanol synthesis is proposed. The main feature of this mechanism is the shift from a carbon-surface bond to an oxygen-surface bond during the course of reaction.

NOMENCLATURE

E = Activation energy, cal/gmol

k = Rate constant, gmol/g·cat/sec/atm

k_o = Pre-exponential factor, gmol/g·cat/sec/atm

K_{eq} = Equilibrium constant of the methanol synthesis reaction

n = Empirical constant

r = Reaction rate, gmol/g·cat/sec

R = Universal gas constant, cal/gmol/K

T = Temperature of reaction, K

REFERENCES

1. Klier, K., Chatikavanij, V., Herman, R.G., and Simmons, G.W., *J. Catal. 74*, 343, 1982.

2. Henrici-Olive, G., and Olive, S., "Catalyzed Hydrogenation of Carbon Monoxide", Springer-Verlag, New York, 1984.

3. Saida, T.,and Ozaki, A., *Bull. Chem. Soc. Jpn. 37*, 1817, 1964.

4. Herman, R.G., Klier, K., Simmons, G.W., Finn, B.P., and Bulko, J.B., *J. Catal. 56,* 407, 1979.

5. Shimomura, K., Ogawa, K., Oba, M., and Kotera, Y., *J. Catal. 52,* 191, 1978.

6. Leonov, V.E., Karabaev, M.M., Tsybina, E.N., and Petrishcheva, G.S., *Kinet. Katal. 14,* 970, 1973.

7. Rozovskii, A.Y., Kagan, Y.B., Lin, G.I., Slivinskii, E.V., Loktev, S.M., Liberov, L.G., and Bashkirov, A.N., *Kinet. Katal. 16,* 810, 1975.

8. Kagan, Y.B., Rozovskii, A.Y., Liberov, L.W., Slivinskii, E.V., Lin, G.I., Loktev, S.M., and Bashkirov, A.N., *Dokl. Akad. Naukk SSSR 224,* 1081, 1975.

9. Agny, R.M., "Catalytic Synthesis of Methanol from Carbon Monoxide and Hydrogen over a Commercial Cu/ZnO/Al$_2$O$_3$ Catalyst", M.S. Thesis, Purdue University, 1984.

10. Dietz, W.A., *J. Gas Chromat. 5,* 68, 1967.

11. Kung, H.H., *Catal. Rev. Sci. Eng. 22,* 235, 1980.

12. Vannice, M.A., *J. Catal. 37,* 462, 1975.

13. Saussey, J., Lavalley, J., Lamotte, J., and Rais, T., *J. Chem. Soc. Chem. Commun.,* 278, 1982.

14. Deluzarche, A., Hinderman, J.P., and Kieffer, R., *Tegrahedron Lett.,* 2787, 1978.

15. Tawarah, K.M., and Hansen, R.S., *J. Catal. 87,* 305, 1984.

16. Deluzarche, A., Kieffer, R., and Muth, A., *Tetrahedron Lett.,* 3357, 1977.

17. Nagarjunan, T.S., Sastri, M.V.C., and Kuriacose, J.C., *J. Catal. 2,* 223, 1963.

18. Borowitz, J.L., *J. Catal. 13,* 106, 1969.

19. Ueno, A., Onishi, T., and Tamaru, K., *Trans. Faraday Soc. 67,* 3585, 1971.

20. Griffin, G.L., and Roberts, D.L., "Multi-component Adsorbate Interactions of Cu/ZnO Methanol Synthesis Catalysts", paper presented in the 75th Annual Meeting AIChE, November 14-18, 1982, in Los Angeles, California.

21. Herwijnen, T.V., and Dejong, W.A., *J. Catal 63,* 83, 1980.

ACKNOWLEDGEMENTS

TABLE 1.

Steady State Data of Methanol Synthesis of Cu/ZnO/Al$_2$O$_3$ Catalyst C79-2-01 of United Catalysts, Inc.

Run #	Reactor Temperature (°C)	Reactor Pressure (atm)	$\frac{H_2}{CO}$ F	Flow Rate at STP (cc/min)	Conversion of CO to Methanol (%)	Reactor Effluent Composition (%)				
						CO	H$_2$	CH$_3$OH	CO$_2$	H$_2$O
1	250	14.3	2.4	102	0.27	29.4	70.5	0.08	a	a
2	250	12.6	2.4	100	0.24	28.9	70.9	0.07	a	a
3	250	11.2	2.2	77	0.22	31.1	68.8	0.07	a	a
4	250	9.4	2.2	79	0.19	31.6	68.3	0.06	a	a
5	250	7.7	2.1	83	0.15	32.5	67.4	0.05	a	a
6	250	6.2	2.2	79	0.13	31.6	68.3	0.04	a	a
7	270	14.2	2.3	104	0.91	29.4	70.0	0.26	0.27	a
8	270	11.0	2.2	112	0.61	30.9	68.8	0.18	0.09	a
9	270	9.5	2.4	101	0.54	29.5	70.2	0.16	0.07	a
10	270	7.8	2.2	100	0.42	30.9	68.9	0.13	0.07	a
11	270	6.2	2.2	103	0.32	30.9	68.9	0.11	0.06	a
12	270	3.4	2.1	106	0.16	32.0	67.9	0.05	a	a
13	290	14.3	2.4	101	1.35	29.0	70.0	0.40	0.51	a
14	290	11.2	2.3	116	0.96	29.8	69.6	0.30	0.26	a
15	290	9.5	2.2	100	0.81	30.6	68.8	0.27	0.27	a
16	290	7.7	2.1	103	0.63	31.4	68.1	0.20	0.24	a
17	290	6.2	2.2	97	0.48	30.7	69.0	0.15	0.14	a
18	290	3.5	2.2	99	0.22	31.3	68.6	0.07	a	a

a Trace amounts.

TABLE 2.

Pre-exponential Factors and Overall Activation Energies for Methanol Synthesis over Cu/ZnO/Al$_2$O$_3$ Catalyst C79-2-01 of United Catalysts, Inc.

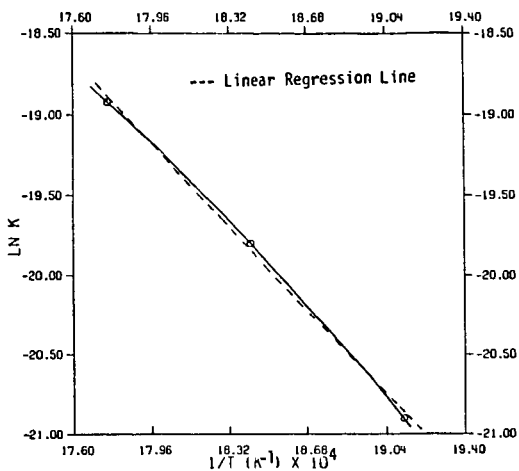| Temperature (°C)	Pre-exponential Factor (gmol/g·cat/sec/atm)	Overall Activation Energy (cal/gmol)
250	13,600	34,000 ± 1,000
270	1,890	29,500 ± 1,000
290	48	25,000 ± 1,000

Figure 1. Arrhenious Plot for the Methanol Synthesis Reaction in our System (Eq. 2).
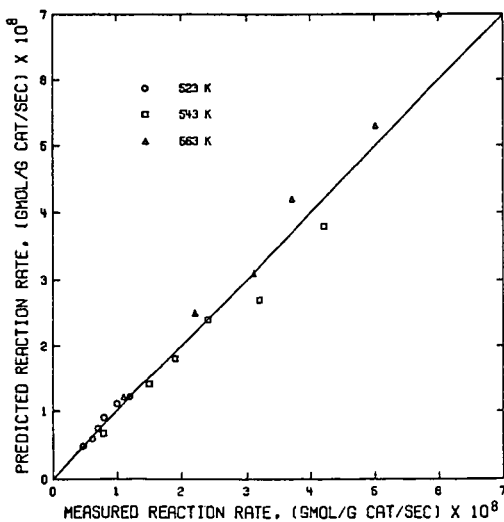

Figure 2. Comparison Between Measured Reactions Rates and Predicted Reaction Rates (Eq. 2).

STEAM PYROLYSIS OF SHALE AND PETROLEUM
GAS OIL MIXTURES
by
Harry P. Leftin and David S. Newsome

The M. W. Kellogg Company
Research & Development Center
16200 Park Row
Houston, Texas 77084

ABSTRACT

Light gas oil and heavy gas oil from Paraho shale oil and their mixtures with a petroleum light gas oil were pyrolyzed in the presence of steam at 880-900°C and contact times between 60 and 90 milliseconds in a nonisothermal bench scale pyrolysis reactor. Blending of petroleum LGO into the shale oil feeds provided product yields that were the weighted linear combination of the yields of the individual components of the blends. Partial denitrogenation and a pronounced decrease in the rate of coke deposition on the reactor walls was observed when petroleum gas oil was blended with the shale gas oils.

INTRODUCTION

Steam pyrolysis of hydrocarbons in tubular reactors is the key process for production of gaseous olefins that serve as major raw materials for the petrochemical industry. While the recent concern regarding cost, supply and availability of petroleum derived feedstocks for petrochemicals production has subsided, at least temporarily, the long term outlook remains sufficiently clouded that the present breathing spell affords an opportunity to examine potential alternative feed sources. These concerns have lead to several investigations[11,12,13] of shale oil as feed for olefins production. Indeed, the M. W. Kellogg Company have recently completed a study[4] to evaluate shale oil fractions and hydrotreated shale oil fractions as feed for olefins production in conventional pyrolysis. The authors concluded from this study that shale oil distillates produce ethylene, propylene and benzene yields similar to those from petroleum, however coking rates were unacceptably high for all except the lightest fraction. Mild hydrotreating improved the tube wall fouling rate of the shale oil naphtha and light gas oil fractions to the range typical of petroleum light gas oil (LGOP); that for the heavy gas oil (HGOS) was improved but still unacceptable. In another study[5], more extensive prerefining by hydrotreating reduced the heteroatom concentration and provided yields of olefins comparable with or exceeding those from petroleum fractions. Substantially lower ethylene yield was obtained from severely hydrotreated TOSCO II distillate due to steam reforming during pyrolysis. Coking rates and liquid products yields were not reported.[5]

While it is clear that shale oil has the potential to eventually be a major source of hydrocarbon for both fuel and chemical production, the near term prospects call for limited production from subsidized programs. Since dedicated refineries and petrochemical plants cannot be justified to utilize this material, it will be necessary either to upgrade the shale oil to its petroleum equivalent or to improve its processability by blending it with conventional petroleum. Indeed, even when shale oil production begins to expand as petroleum declines, the blending of these to produce feedstocks will presage the smooth evolution of shale oil specific processing technology.

The literature on steam pyrolysis of shale oil distillates is limited but adequate to indicate its potential as feedstock, particularly after some prerefining. The literature on steam pyrolysis of petroleum distillates is extensive. However, no literature exists in the cocracking of shale and petroleum distillates. Cocracking of petroleum derived feedstocks has been shown to provide expected product yields, that is, yields which are the linear combination of yields of the individual components of the blend. However, coking behavior of such feedstock mixtures showed[7] remarkable effects where the coking rate of a suitably blended feedstock mimicked the rate of the less coking feed component.

The present study was undertaken to determine the cracking and coking behavior of shale oil distillates under conditions of millisecond pyrolysis and the effects of admixture of petroleum LGO on these properties. Particular interest was paid to liquid products.

EXPERIMENTAL:

Apparatus:

The bench scale pyrolysis furnace and flow system have been described previously in detail.[8,9,10]

The experimental arrangement for pyrolysis comprised a feed system, vaporizer preheater, an electrically heated furnace and product recovery system. Liquid feedstocks were fed from Ruska metering pumps into the vaporizer where they were mixed with superheated steam before passing through the preheater and into the reactor. The reaction zone was an annulus between a reactor tube and a coaxial thermowell, both of 310 stainless steel. Temperature profiles were measured with a calibrated chrome-alumel thermocouple manually driven along the length of the reactor. On leaving the reaction zone, the process stream was rapidly cooled by admixture with a recycled stream of cooled product gas.[6] The quenched products were further cooled against chilled water in an indirect heat exchanger and water condensate plus liquid products were separated by means of a small cyclone separator which was an integral part of the product gas recycle quench system.

To avoid formation of carbon oxides due to steam reforming reactions, as was observed in other studies with hydrotreated shale oil distillate,[5] the walls of the stainless steel reactor were maintained in a catalytically inactive form by sulfiding and the pyrolysis experiments were performed in the presence of 50 ppm sulfur which was introduced to the system as ethyl mercaptan contained in the process feed water.

At the completion of a pyrolysis run the amount of coke deposited on the reactor tube wall during the run was determined by burning out with a steam-air mixture.[10] To accomplish this, the pyrolysis system is modified by replacement of the quenching system with a CO_2 collection system. Air and water rates are controlled by rotameters and needle valves. Contaminant CO_2 is removed from both the water and bottled air used in the burn-off. After the combustion gases leave the reactor, the bulk of the unreacted water is removed with a room temperature trap, and residual water vapor is removed with a drying agent. The dry gases then enter a CuO bed maintained at high temperature to convert any CO to CO_2 and is then passed through another drying agent prior

to being absorbed in a preweighed ascarite/magnesium perchlorate tube. Total carbon deposited in the reactor is calculated from the weight of CO_2 collected. A gas chromatograph in the system periodically measures the CO_2 level in the combustion gas stream to determine when a burnout is completed.

After a pyrolysis run/burnout cycle is completed, the reactor tube is conditioned for the next run by reducing and sulfiding the reactor walls with a flow of hydrogen and hydrogen sulfide.

Product Analysis:

Two gas samples, for duplicate analysis by mass spectrometry, were taken in the first third and final third of the run period. Results of duplicate mass spectrometric determinations fell within the established limits for this analytical method, and the averaged values were then used.

Liquid product, after separation from process steam condensate, is assayed into gasoline (36-218°C), light fuel oil (218-343°C) and heavy fuel oil ($343°C^+$) by gas chromatographic simulated distillation (GCSD) as defined in ASTM method D-2887. Yields of individual C_6-C_8 aromatics (BTX) were obtained by G.C.

Total organic nitrogen present in the C_5^+ liquid products from selected runs was determined by the Kjeldahl method. Boiling range distribution of nitrogen was determined using a gas chromatographic simulated distillation method modified by use of a detector specific for organic nitrogen. The method involves injecting a sample into a chromatographic column equipped with effluent splitter leading to a Thermionic Specific Detector (TSD) for nitrogen and a Flame Ionization Detector (FID) for carbon. The area from the TSD for each time interval is recorded on magnetic tape while the area from the FID over the entire chromatogram is recorded separately. From these data and previously determined calibration factors, nitrogen concentration and boiling range distributions may be determined using the conventional GCSD temperature vs time plot. A Varian 3700 G.C. equipped with TSD and FID was employed for this work.

Feedstocks

Shale light gas oil (LGOS) and heavy gas oil (HGOS), prepared by distillation from Paraho shale oil, were samples of the same materials used in an earlier steam pyrolysis study (4). An Arabian light gas oil comprised the petroleum derived light gas oil (LGOP) used in this study. Blends of shale gas oils and the petroleum gas oil were prepared to contain 20, 40, 60 and 80 wt% petroleum gas oils. Thus a total of ten feedstocks were examined. Inspection data for these feedstocks and blends are summarized in Table I.

DATA AND DISCUSSION

Runs were carried out at maximum temperatures (Tm) of a parabolic temperature profile (9) between 744°C and 899°C with steam dilution corresponding to steam/hydrocarbon weight ratios between 0.5 and 1.0. All runs were isobaric at

a total pressure of 13-15 psig (90-105 kPa). Most of the runs were carried out under millisecond contact times (less than 0.1 seconds); however, one run on each of the neat shale gas oils (LGOS and HGOS) was carried out at conventional contact time (about 0.3 seconds) to determine the effect of this variable on product yields. With the exception of those runs where excessive reactor coking (Runs 11,12 & 13) forced early run termination, material balances fell between 95% and 100%.

Tables II and III summarize the individual run conditions and the observed yields and conversions for all runs with light and heavy shale gas oils (LGOS and HGOS), respectively. Runs No. 1 and 10 were carried out under conventional contact time conditions similar to those used in an earlier study.[4] Results for both the neat LGOS and HGOS are in excellent agreement with the earlier data.[4]

Comparison of runs 1 and 2 show the effect of conventional vs millisecond conditions on pyrolysis of neat LGOS. These data show an enhancement in selectivity to ethylene as described previously[3] for operations at increased temperature and decreased contact time. A similar comparison (Runs 10 & 11) for pyrolysis of heavy shale gas oil (HGOS) was precluded by the rapid coking of the reactor.

Pyrolysis of Shale-Petroleum Gas Oil Blends:

Gaseous Product:

In runs No. 3,4,5,6 and 7, blends of an Arabian light gas oil (LGOP) and shale light gas oil (LGOS) were pyrolyzed under closely identical operating conditions. Conversion and product yields changed monotonically in the mixtures between those for neat LGOS and for neat LGOP. Figure 1 illustrates the changes in conversion and yields of major gaseous products for the LGOS/LGOP feedstock blends. Yields of major products for these blends are the arithmetic weighted average of the yields for the individual feedstocks in the blends. Accordingly, full yield benefits normally attainable from separate steam pyrolysis of shale LGO may be realized by cocracking the shale feed with petroleum gas oil in an existing gas oil pyrolysis furnace. Since the shale oil feed, in this case, is intrinsically poorer in terms of ethylene yield, a proportional penalty in furnace ethylene capacity will obtain. To some extent, this penalty can be compensated by increasing severity or decreasing hydrocarbon partial pressure, e.g. runs no. 2 vs 3.

Due to the higher coking rates attendant to the pyrolysis of the shale heavy gas oil (HGOS), fewer data are available for this feedstock. Figure II summarizes the conversion and yields of major gaseous products for cocracking HGOS/LGOP blends. While these data are limited to blends at the low end of the HGOS content, extrapolation to 100% HGOS provides an estimate yield that might be realized from high severity pyrolysis of neat HGOS. The extrapolated results appear reasonable in view of those obtained from HGOS under milder conditions (Run 10).

Liquid Products:

Gasoline and fuel oil become major products of olefins production processes when liquid hydrocarbon feedstocks are used in steam pyrolysis. These, so-called, co-products comprise from 35-55 wt% of the feed depending on feed properties and pyrolysis conditions. Consequently, these liquid co-products exert a large effect on the economics of naphtha and gas oil pyrolysis for both petroleum or shale oil derived feedstocks.

With the exception of a related study (4) which reports the gasoline and fuel oil yields from pyrolysis of shale oil distillates, no literature exists on the effects of operating conditions on yields or on the quality of these liquid products. In the present work both of these topics were investigated.

Yields of boiling range fractions of the pyrolysis liquids as determined by gas chromatographic simulated distillation (GCSD) (ASTM method D-2887) are summarized in tables II and III. Gasoline yield from LGOS appears to be somewhat greater than that for the petroleum gas oil studied. This result may not be unique, however, since gasoline yield is known to depend on characteristics of various petroleum gas oils. It is of greater interest that the yield of potential motor gasoline appears to change little with either pyrolysis severity or with composition of the blended feedstocks. Since gasoline yields for LGOS are comparable to those of petroleum feedstock, it is of interest to determine the quality of this for use as motor fuel. A special gas chromatographic method was used to provide data needed for calculation of Research Octane Number (RON) of the gasoline fraction in the pyrolysis liquid from Run #9 (60% LGOS/40% LGOP). According to this method, a cutting column is used to separate the gasoline from the higher boiling materials which are discarded in a back flush. The gasoline cut is fed to a capillary column for quantitative analysis and identification of the components in the gasoline. The Research Octane Number calculated from this G.C. analysis using the method of Anderson et al (1) was found to be 99.4.

Light and heavy fuel oil yields are greater for the shale oil feedstocks and these vary linearly with composition for the blended feedstocks.

Nitrogen Distribution:

Shale oil as well as its distillate fractions have a high content of organic nitrogen, typically between 1 and 2 wt percent. Since nitrogen is a catalyst poison for current refinery operations and a detriment to liquid fuel products, most schemes for utilization of shale oil require upgrading by severe hydrotreating. While steam cracking (a non catalytic process) is not inhibited by organic nitrogen, the quality and hence the value of liquid products are adversely affected. Typically in steam pyrolysis of liquid feedstocks approximately one half of the feed is converted to gaseous products which contain no organic nitrogen. It becomes very interesting then to determine to what extent, if any, this gasification involves net denitrogenation of feedstock and also to determine the distribution of remaining nitrogen among the liquid products.

Boiling range distribution of organic nitrogen in the LGOS feedstock and in the pyrolysis liquid products from runs with neat LGOS (Run #8) and with LGOS/LGOP blend (Run #9) were determined by gas chromatography. Results are illustrated in Figure III and summarized in Table IV.

TABLE IV

Nitrogen Distribution in Pyrolysis Liquid Fractions

Run No.	8		9	
	Wt% of Feed	Wt% N	Wt% of Feed	Wt% N
Liquid Fraction				
C_5-218°C (Liquid only)	17.0	2.34	17.9	0.26
C_5-218°C Total gasoline(a)	21.7	1.83	21.6	0.22
218-354°C Fuel Oil	21.1	2.72	20.6	0.71
354°C + Hy Fuel Oil	11.9	4.08	10.7	4.23
Whole Liquid Product	50.0	2.92	49.2	1.39
% Nitrogen Balance(b)	98.6		72.5	
Apparent Denitrogenation %	1.4		27.5	

(a) Includes C_5,C_6 gasoline components contained in the gas samples.

(b) Total Nitrogen in Liquid Products/N in Feed.

In Figure III, the results of gas chromatographic determination of cumulative nitrogen content as a function of boiling point (retention time) is plotted against the analogous data for cumulative carbon (GCSD) in the liquid samples. In this way, the retention time is eliminated from the plot and a distribution curve relating the nitrogen content with the carbon content is obtained in which the slope of the curve at any point is the concentration of nitrogen in the fraction of the sample boiling below that point. Thus a straight line with unit slope (45°) indicates uniform nitrogen concentration in all fractions of the total liquid.

Nitrogen in the LGOS feedstock is fairly uniformly distributed over the entire boiling range (Figure III-a). The liquid produced from pyrolysis of neat LGOS contains almost all of the organic nitrogen from the feed and this nitrogen is also broadly distributed over the boiling range of this product (Figure II-b). In this case, there is a small trend toward increasing nitrogen concentration with increasing boiling range.

A pronounced change in nitrogen distribution (Figure III-c) is found in the liquid product from cracking a blend of LGOS and LGOP. In this case, the nitrogen concentration is strongly shifted into the heavier portion of the pyrolysate and a significant part of the feed nitrogen appears to have been removed. Partial denitrogenation by steam pyrolysis provides a clear economic benefit from cocracking shale oil/petroleum blends. Additional benefits may be derived from the reduced nitrogen content of the gasoline and light fuel oil products which, although they still require upgrading, can be denitrogenated with less severe hydrotreating than would be required for denitrogenation of the entire feedstock or the products from separate cracking of LGOS. Disposition of the heavy fuel is an equivalent problem in either case. In any event, cocracking of shale oil and petroleum feedstocks offers an interesting alternative to severe hydrotreating of shale oil.

Reactor Tube Wall Fouling:

The high fouling rate exhibited by heavier shale oil fractions has been identified (4) as being the major hurdle that must be overcome in its utilization as feedstock for olefins production. Partial hydrotreatment of the pyrolysis feed resulted in reducing the fouling rate (4) but not to an acceptable level, especially for the heavy gas oil (HGOS). Severe hydrotreatment, on the other hand, reduced fouling adequately (5) but at considerable expense due to high hydrogen consumption and the high pressures required (2).

Inhibition of tube wall coking in pyrolysis furnace tubes by cocracking in the presence of a low coking hydrocarbon has recently been described (7). It has now been found that an analogous phenomenon occurs in the cocracking of shale gas oils in admixture with a low coking petroleum gas oil. Figure IV illustrates this effect for both the HGOS/LGOP and LGOS/LGOP feed blends. With the addition of less than 40% LGOP to LGOS, the fouling rate of the feedstock combination is substantially reduced and closely approaches the rate characteristic of the petroleum gas oil itself. Substantially more LGOP must be added to suppress the fouling rate of HGOS. This is in accord with the intrinsically higher coking propensity of the heavier shale feedstock.

While the fouling behaviour of the HGOS and LGOS blends with LGOP is in qualitative agreement with the coke inhibition index (CII) concept,[7] it does not agree quantitatively with the correlation developed for petroleum feedstocks. High organic oxygen and nitrogen contents of the shale liquids exert a positive influence on their coking properties as evidenced by the observed (5) decrease in coking rate upon removal of these heteroatoms.

According to the observed coking behavior of mixtures of shale and petroleum distillates, acceptably low coking rates can be expected from blends containing significant quantities of shale liquid. This provides an interesting alternative to hydrotreating prior to pyrolysis.

CONCLUSIONS:

Shale oil distillates may be a substitute feed for olefins production in high severity pyrolysis. Cocracking in admixture with suitable petroleum derived feedstocks offers a potential alternative to costly hydrotreating by providing partial denitrogenation of the liquid fuel coproducts as well as by largely overcoming the barrier due to the inherent excessive tube wall fouling characteristics of the shale oil liquids.

REFERENCES

1. P. C. Anderson, J. M. Sharkey & R. P. Walsh, J. Inst. Petr. 58 ,84 (1972).

2. R. F. Anderson, et al, D.O.E. Report No. FE-2315-25, (May 1978).

3. B. P. Ennis, H. P. Boyd & R. Orriss, Chem. Technol. 5 ,(11) 693 (1975).

4. H. J. Glidden & C. F. King, Chem. Eng. Prog. 76 ,(12) 47 (1980).

5. C. F. Griswold, A. Ballut, H. R. Kavianian, D. F. Dickson & V. F. Yesavage, Chem. Eng. Prog. 75 ,(9) 78 (1979).

6. J. Happel & L. C. Kramer, Ind. Eng. Chem., 59 ,39 (1967).

7. H. P. Leftin & D. S. Newsome, U.S. 4,176,045, Nov. 27, 1979.

8. H. P. Leftin, D. S. Newsome, T. J. Wolfe & J. C. Yarze, "Industrial and Laboratory Pyrolysis", Am. Chem. Soc. Symposium Series 32 ,373 (1976).

9. H. P. Leftin and A. Cortes, Ind. Eng. Chem. Proc. Des. & Dev. 11 ,613 (1972).

10. D. S. Newsome & H. P. Leftin, Chem. Eng. Prog. 76 ,(5) 76 (1980).

11. C. G. Rudershausen & J. B. Thompson, Prepr. Div. Pet. Chem. Am. Chem. Soc. 23 ,(1) 241 (1978).

12. E. G. Shultz, J. B. Guyer & H. R. Linden, Ind. Eng. Chem. 47 ,2479 (1955).

13. P. D. Smith, P. F. Dickson & U. F. Yesavage, Prepr. Div. of Pet. Chem. Am. Am. Chem. Soc. 23 ,(2) 756 (1978).

TABLE I

FEEDSTOCK INSPECTIONS

TYPE	SHALE	LIGHT GAS OIL BLENDS			PETROLEUM	SHALE	HEAVY GAS OIL BLENDS			
Feed Designation	LGOS	L-1	L-2	L-3	LGOP	HGOS	H-1	H-2	H-3	H-4
Wt% Shale oil	100	80	60	40	0	100	80	60	40	20
Wt% Petroleum LGO	-	20	40	60	100	0	20	40	60	80
ASTM Dist'n (°F)										
IBP	424	-	-	-	335	662	-	-	-	-
10%	458	-	-	-	427	714	-	-	-	-
30%	497	-	-	-	478	756	-	-	-	-
50%	536	-	-	-	512	797	-	-	-	-
70%	572	-	-	-	546	844	-	-	-	-
90%	614	-	-	-	599	889	-	-	-	-
E.P.	637	-	-	-	638	918	-	-	-	-
°API	28.9	31.0	33.1	35.3	39.9	19.7	23.3	27.2	31.2	35.4
Molecular Wt(1)	210	212	213	215	218	371	325	290	261	238
Elemental Analysis (Wt%)										
C	85.16	85.39	85.61	85.84	86.29	85.41	85.59	85.76	85.94	86.15
H	12.36	12.57	12.79	13.00	13.43	11.38	11.79	12.20	12.61	13.02
N	1.49	1.20	0.90	0.60	N.D.	2.14	1.71	1.28	0.86	0.43
S	0.76	0.63	0.49	0.35	0.09	0.64	0.53	0.42	0.31	0.20
O	1.78	1.42	1.07	0.71	N.D.	1.64	1.31	0.98	0.66	0.33
H/C Atom Ratio	1.73	1.75	1.78	1.80	1.85	1.59	1.64	1.69	1.75	1.80

(1) Calculated

TABLE II
STEAM PYROLYSIS OF SHALE LIGHT GAS OIL
AND MIXTURES WITH PETROLEUM LIGHT GAS OIL

Run #	1	2	3	4	5	6	7	8	9
Feed Composition:									
Wt% LGOS	100	100	100	80	60	40	0	100	60
Wt% LGOP	0	0	0	20	40	60	100	0	40
Temp. max (°C)(a)	766	899	899	899	899	899	899	882	879
Log Mean θ (Sec)(a)	0.32	0.073	0.086	0.086	0.088	0.093	0.091	0.090	0.094
H_2O/Oil (g/g)	1.00	1.02	0.50	0.50	0.50	0.50	0.50	0.50	0.50
Outlet Pressure (Psig)	13	13	15	15	15	15	15	15	15
Conversion $(1-C_5+)$	49.8	48.0	46.1	46.4	51.6	53.1	61.6	44.4	46.9
Yields (Wt%)(Basis Output)									
H_2	0.44	0.73	0.72	0.68	0.72	0.73	0.84	0.55	0.59
CH_4	8.70	10.9	10.7	9.87	10.6	10.8	11.5	9.08	8.21
C_2H_2	0.06	0.88	0.82	0.76	0.74	1.05	0.90	0.29	0.32
C_2H_4	15.6	20.4	18.1	18.7	21.9	22.7	27.5	16.3	19.0
C_2H_6	3.63	2.01	2.37	2.32	2.49	2.39	2.59	2.70	2.13
C_3H_4	1.14	0.65	0.64	0.60	0.56	0.63	0.82	0.38	0.31
C_3H_6	11.6	7.56	7.63	7.93	8.79	8.94	10.2	8.90	9.36
C_3H_8	0.60	0.18	0.08	0.11	0.15	0.30	0.12	0.31	0.40
C_4H_6	3.28	3.23	3.26	3.37	3.84	3.59	4.78	3.15	3.05
C_4H_8	4.71	1.49	1.67	1.93	1.93	1.89	2.20	3.24	3.45
C_4H_{10}	0.10	0.01	0.15	0.13	0.02	0.01	0.17	0.06	0.09
C_5+(liq)	49.0	51.3	53.2	52.9	48.1	46.6	38.2	54.7	52.9
Coke	1.24	0.72	0.70	0.66	0.31	0.28	0.21	0.35	0.21
Gasoline (C_5-218°C)	20.6	20.2	21.3	19.3	21.2	21.2	18.7	21.7	21.6
Fuel Oil (218°-343°C)	20.4	19.0	20.0	20.3	17.1	17.3	13.0	21.1	20.6
Fuel Oil (343°-454°C)	6.43	7.49	7.89	8.26	6.27	5.34	4.45	8.48	8.71
Pyrolysis Tar (454°C+)	1.57	4.61	4.01	5.08	3.52	2.76	2.05	3.43	1.98
BTX(b)	4.3	4.4	5.8	6.2	7.4	7.5	7.0		5.1
Tube Wall Fouling:									
Run Length (Min.)	237	89	111	69	120	120	120	131	135
Wt of Coke Product (gm)	1.03	0.85	1.59	0.96	0.79	0.71	0.54	1.41	0.83
Coking Rate (mg/min)	4.53	9.60	14.3	13.8	6.59	5.91	4.51	10.8	6.15
Nitrogen Wt%									
Gasoline	–	–	–	–	–	–	–	1.83	0.22
Fuel Oil	–	–	–	–	–	–	–	2.72	0.71
Fuel Oil + Tar	–	–	–	–	–	–	–	4.08	4.23
Nitrogen Balance Prod/Feed (%)	–	–	–	–	–	–	–	98.6	72.5
RON (C_5-218°C)	–	–	–	–	–	–	–		99.4

(a) Temperatures between 600°C and Tmax.
(b) Benzene, Toluene, O,M & P Xylene, Ethylbenzene and Styrene.

335

TABLE III

STEAM PYROLYSIS OF SHALE HEAVY GAS OIL AND MIXTURES WITH PETROLEUM LIGHT GAS OIL

Run #	10	11	12	13	14	15	16
Feed Composition:							
Wt% HGOS	100	100	80	60	40	20	0
Wt% LGOP	0	0	20	40	60	80	100
Temp. Max (°C)[a]	744	899	899	899	899	899	899
Log Mean θ (Sec)[a]	0.33	0.07	0.07	0.07	0.073	0.071	0.063
H_2O/Oil (g/g)	1.00	0.75	0.74	0.76	0.75	0.77	0.79
Outlet Pressure (Psig)	13	15	15	15	15	15	15
Conversion ($1-C_5^+$)	36.5	[b]	[b]	[b]	52.7	59.4	66.6
Yields (Wt%) Basis (output)							
H_2	0.45	–	–	–	0.67	0.79	0.82
CH_4	9.66	–	–	–	9.74	11.0	11.4
C_2H_2	0.05	–	–	–	0.81	1.10	0.81
C_2H_4	10.6	–	–	–	23.2	26.6	28.1
C_2H_6	3.74	–	–	–	2.17	2.36	2.42
C_3H_4	0.42	–	–	–	0.53	0.74	1.01
C_3H_6	7.51	–	–	–	9.06	10.2	12.6
C_3H_8	0.52	–	–	–	0.20	0.25	0.30
C_4H_6	1.45	–	–	–	3.85	4.34	5.57
C_4H_8	2.00	–	–	–	2.26	2.08	3.40
C_4H_{10}	0.08	–	–	–	0.16	0.03	0.01
C_5^+(liq)	49.2	–	–	–	46.9	40.4	33.3
Coke	14.3	–	–	–	0.40	0.20	0.13
Gasoline (C_5–218°C)	–	–	–	–	23.4	19.4	19.9
Fuel Oil (218°–343°C)	–	–	–	–	12.8	12.0	8.77
Fuel Oil (343°–454°C)	–	–	–	–	6.04	5.40	3.35
Pyrolysis Tar (454°C$^+$)	–	–	–	–	4.66	3.60	1.28
BTX[c]	–	–	–	–	5.5	3.6	7.1
Tube Wall Fouling:							
Run Length (min)	77	12	29	47	100	123	120
Wt of Coke Produced (gas)	4.27	0.56	1.06	0.94	0.80	0.49	0.32
Coking Rate (mg/min)	55.5	46.6	36.5	20.0	9.97	3.98	2.65

(a) Temperatures between 600°C and Tmax.
(b) Run terminated due to reactor pressure drop buildup from rapid coking.
(c) Benzene, Toluene, O,M & P Xylene, Ethylbenzene and Styrene.

FIGURE 2. PYROLYSIS OF SHALE+PETROLEUM GAS OIL BLENDS (LGOS + LGOP). PRODUCT DISTRIBUTION.

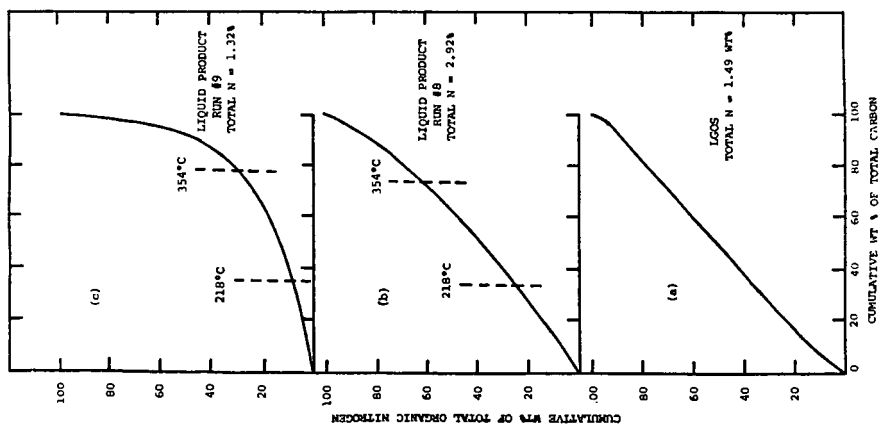FIGURE 1. PYROLYSIS OF SHALE & PETROLEUM GAS OIL BLENDS (LGOS+LGOP). PRODUCT DISTRIBUTIONS.
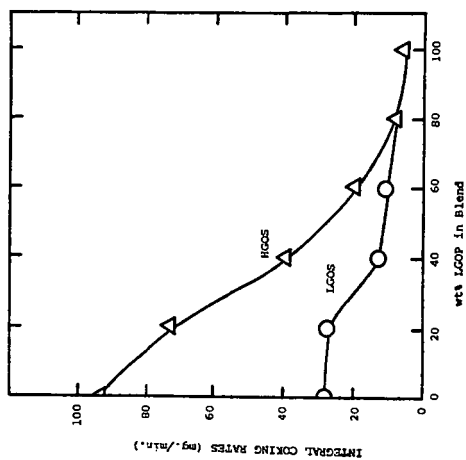
337

FIGURE 4. REACTOR FOULING RATES
SHALE/PETROLEUM GAS OIL BLENDS

FIGURE 3. ORGANIC NITROGEN DISTRIBUTIONS

DETERMINATION OF HYDROGEN DONATING PROPERTIES OF COAL LIQUEFACTION PROCESS SOLVENTS

Douglas W. Later and Donald M. Camaioni

Pacific Northwest Laboratory
Richland, Washington 99352

INTRODUCTION

The hydrogen donating properties of solvents used in direct coal liquefaction processes are of key importance in determining conversion efficiencies and overall product qualities. The reduction of fluorenone to fluorene at 400°C has recently been used in this laboratory to study the hydrogen donating properties of process solvents from different direct liquefaction technologies. Choi and Stock [1,2] have elucidated the mechanism of the reduction of fluorenone by hydrogen donating compounds and have demonstrated the utility of this reduction for evaluating the hydrogen atom transfer properties of coal and coal macerals.

The reduction reaction for fluorenone occurs in three stages [1]. Stage 1 is a radical process which produces 9-hydroxyfluorene as the intermediate product. In stage 2, this intermediate is transformed into bis(9-fluorenyl) ether by a non-radical process. The ether decomposes in stage 3 to produce fluorene and fluorenone via a radical process. In the study by Choi and Stock, it was shown that radical initiators, such as benzyl phenyl thioether or coal, accelerate the reactions of stages 1 and 3. The mechanisms of stages 1 and 3 are formulated in Scheme I. In the absence of initiator, a bimolecular molecule-assisted homolysis reaction [3-5] between fluorenone and donor initiates the reduction reaction:

Reductions conducted in the absence of added initiators measure the ability of the solvent to both initiate the reduction and transfer hydrogen to radicals, whereas reductions carried out in the presence of initiators serve to measure the hydrogen donor ability of the solvent. Thus, the fluorenone reduction reaction provides a simple procedure to assess the relative abilities of process solvents and solvent components to participate in these radical initiating and hydrogen transfer reactions which are important to coal liquefaction.

EXPERIMENTAL

SAMPLES

Fluorenone was prepared by air oxidation [6] of fluorene (Aldrich Chemical) and was recrystallized from methanol to yield material >99% pure as determined by capillary column gas chromatography (GC). Process solvents from two direct coal liquefaction technologies were used in these experiments: (1) a Solvent Refined Coal (SRC)-I process solvent; and (2) a recycle pasting solvent from the Wilsonville, AL integrated two-stage liquefaction (ITSL) process. The physical and chemical properties of these materials are discussed in detail elsewhere [7,8]. Briefly, the SRC-I solvent had a boiling range of 480-850°F and the ITSL pasting solvent was a 650°F+/solid resids material. These liquefaction materials are from

developmental processes and should not necessarily be considered representative of future commercial coal liquefaction products.

The crude solvents were each tested individually for fluorenone conversion efficiency. In addition, chemical class fractions of these materials were obtained by alumina adsorption chromatography. Details of this procedure have been previously reported [9]. Briefly, the crude coal liquefaction materials were separated into four chemical classes: (1) aliphatic hydrocarbons, (2) neutral polycyclic aromatic hydrocarbons (PAH), (3) nitrogen-containing polycyclic aromatic compounds (N-PAC) and (4) hydroxylated PAH (Hydroxy-PAH).

Fluorenone Reduction Reactions

Fluorenone reductions were conducted at 400°C for 1 hr in sealed evacuated quartz tubes. Generally, benzene solutions of reactants were prepared and aliquots were transferred by microliter syringes to 6 mm o.d. quartz tubes (1 mm wall thickness), so as to provide 50 μL total volume containing approximately 5 mg donor and 0.025 mmol fluorenone. Reactions with the ITSL crude process solvent necessitated weighing the material directly into the tubes due to its insolubility in benzene. Loaded reaction tubes were freeze-thaw degassed on a vacuum line prior to flame sealing and thermostating in a Tecam SB-4 fluidized sandbath with TC4D temperature controller.

Quantitative Analyses

Quantitative analyses of the fluorenone reaction products were performed by capillary column GC. A Hewlett-Packard (HP) model 5880A gas chromatograph equipped with a 30 m x 0.25 mm i.d. fused silica DB-5 (J&W Scientific) capillary column was used. The splitless injection technique was used for sample introduction in conjunction with an HP7671A auto sampling device. Each sample was analyzed in triplicate using a flame ionization detector with peak response information stored and manipulated by the HP5880 microprocessor-controlled integrator. 2-Chloroanthracene was added to all reaction products at a concentration of 100 ng/μL and was used as internal standard for all GC quantitative analyses. Calculations for the conversion of fluorenone to fluorene were done on a mole basis with the conversion amounts reported for fluorene as a percentage of the initial fluorenone present in the reaction. This value was then adjusted to reflect a weight-normalized conversion based on a 5 mg quantity of coal liquid used in the fluorenone reduction reaction. Replicate analyses were performed with the mean and standard deviation reported in Table 1. Recovery percentages were also calculated and reported.

RESULTS AND DISCUSSION

The conversion yields for the reduction of fluorenone to fluorene by the crude process solvents and their chemical class fractions are presented in Table 1. For comparison, 9,10-dihydroanthracene was run and was observed to produce a 21±2% conversion of fluorenone; this is in close agreement with the results of Choi and Stock for the same compound [1,2]. Recoveries of fluorenone plus fluorene were greater than 90% for the unfractionated process solvents indicating that little adduction of intermediate fluorene-based radicals with solvent constituents had occurred. The aliphatic hydrocarbon and neutral PAH fractions showed recoveries similar to the crudes; greater than 85%. But, the more polar constituents exhibited lower recoveries (70-80%), which suggests that adduction of fluorenone reduction intermediates with N-PAC (A_3) and hydroxy-PAH (A_4) components occurred under these reaction conditions. Ionic reactions of the 9-hydroxfluorene with these polar fractions likely divert the reduction reaction producing fluorenyl adducts to the

activated aromatic rings. Choi and Stock [1] observed that reductions of benzo-
phenone in the presence of phenol lead to diphenylmethylphenols and other side
products.

The SRC-I solvent showed lower conversion (38%) than the ITSL process solvent
(88%) from the new generation two-stage liquefaction technology. The chemical
composition of the process solvents investigated in these experiments have been
characterized and compared previously [7]. Table 2 provides information regarding
their relative chemical class compositions. The ITSL material contained a wide
range of high boiling, high molecular weight constituents while the SRC-I process
solvent had intermediate boiling point and molecular weight ranges. The ITSL
recycle pasting solvent contained the highest levels of aliphatic hydrocarbons and
had the lowest combined levels of nitrogen and oxygen heteroatomic PAH. Further-
more, from detailed chemical analyses by GC and GCMS [7,8], hydroaromatic compounds
such as dihydropyrene, which are known to be excellent hydrogen-donating compounds,
were major constituents of the ITSL process solvents.

If the relative conversion yields for the different chemical classes are com-
pared for a given coal liquefaction solvent (see Table 1), the chemical class pro-
ducing the lowest conversion was the aliphatic hydrocarbon fraction (A_1), followed
by the neutral PAH isolate (A_2). The N-PAC (A_3) and hydroxy-PAH (A_4) classes pro-
vided the highest yields for the conversion of fluorenone to fluorene. Hence, it is
apparent that the polar constituent of coal liquefaction process solvents partici-
pate well in both the radical initiating and hydrogen donating steps shown in
Scheme I. This observation is consistent with model studies which showed that
1,2,3,4-tetrahydroquinoline produced higher conversions to fluorene than tetralin or
9,10-dihydroanthracene [1,2]. Thus, the reduced levels of N-PAC in the SRC I versus
the ITSL process solvent is one possible reasons for the relatively lower conversion
yields observed for the SRC I material.

Considerable variability in the conversion yields of the neutral PAH fractions
(A_2) of these two process solvents was observed. It was therefore of interest to
compare the chemical/physical properties of these isolates. The neutral PAH iso-
lates of the SRC-I process material displayed only a 7% conversion yield. This
isolate was mostly 2- to 5-ring parent PAH with relatively low levels of alkylated
and hydroaromatic PAH [9]. The neutral PAH isolate (A_2) from the ITSL recycle
pasting solvent had a higher fluorenone conversion yield, 44%, and was
characterized by high levels of alkylated PAH and hydroaromatic compounds. The mean
molecular weight of this isolate was much higher than the SRC I process solvent
[7]. The presence of significant levels of greater than 5-ring PAH in this isolate
was responsible for the shift to higher average molecular weight. Larger aromatic
ring systems provide greater resonance stabilization of radicals derived from PAH
components of this fraction. Greater resonance stabilization energies of radicals
cause lower energies of activation (E_a) for initiation and hydrogen transfer
reactions which equates with increased reaction rates and higher conversions.

SUMMARY

In summary, it is evident from the data presented in this paper using the
fluorenone-fluorene conversion model system that comparative assessments of recycle
solvents with different chemical and physical properties are possible. The polar
constituents of these process materials, the N-PAC and hydroxy-PAH, appeared to be
the most efficient radical initiators and hydrogen donators. The effectiveness of
neutral PAH chemical fractions as reductants was dependent on the amounts of
alkylated and hydroaromatic compounds present, as well as the size distribution of
aromatic ring systems which make up the fraction. The ITSL neutral PAH fraction
showed a better conversion efficiency than the analogous SRC-1 fraction. The addi-
tion of a radical initiating agent, such as coal, is expected to alter the net

fluorenone conversion efficiencies of these crude solvents and solvent fractions, presumably to reflect relative hydrogen donating abilities.

ACKNOWLEDGEMENTS

REFERENCES

1   Choi, C.; Stock, L. M., J. Org. Chem. (in press).
2   Choi, C.; Stock, L. M., "Chemistry and Characterization of Coal Macerals"; Winans, R. E., Ed.; American Chemical Society; Washington D.C., 1984.
3   Franz, J. A.; Camaioni, D. M.; Beishline, R. R.; Dalling, D. K., J. Org. Chem. 1984, 49, 3563.
4   King, H. H.; Stock, L. M., Fuel, 1981, 60, 748.
5   Pryor, W. A., in "Organic Free Radicals"; Pryor, W. A., ed. American Chemical Society; Washington, D.C., 1978; ACS symposium series 69; pp. 33-46.
6   Sprinzak, Y., J. Amer. Chem. Soc., 1958, 80, 5449-5455.
7   Later, D. W. "Two-Stage Coal Liquefaction Process Materials from the Wilsonville Facility Operated in the Non-Integrated and Integrated Modes: Chemical Analysis and Biological Testing"; PNL-5215, NTIS, Springfield, VA, 1984.
8   Mahlum, D. D. "Chemical, Biomedical and Ecological Studies of SRC-I Materials from the Fort Lewis Pilot Plant: A Status Report"; PNL-3474, NTIS, Springfield, VA, 1981.
9   Later, O. W.; Lee, M. L.; Bartle, K. D.; Kong, R. C.; and Vassilaros, D. L.; Anal. Chem. 1981, 53, 1612-1620.
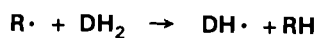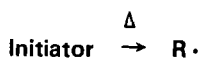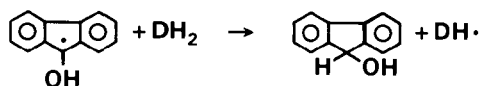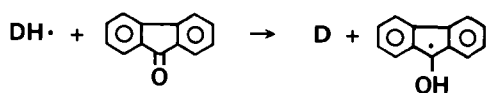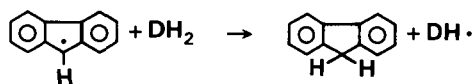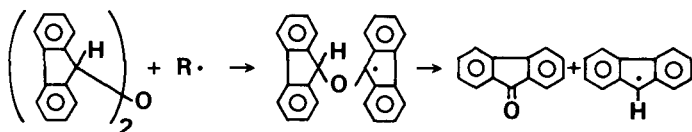
Scheme I. Radical Mechanism for the Reduction of Fluorenone by Hydrogen Donors

TABLE 1. Conversion of Fluorenone to Fluorene by Two Coal Liquids and
Their Chemical Fractions

Sample	Fraction[a]	% Conversion[b]	% Recovery[c]
SRC-I Process Solvent:	Crude	38 ± 2	91
	A_1	1 ± 1	89
	A_2	7 ± 1	95
	A_3	45 ± 4	78
	A_4	43*	81*
ITSL Recycle Pasting Solvent:	Crude	88 ± 1	97
	A_1	9 ± 3	86
	A_2	44 ± 11	91
	A_3	65*	82*
	A_4	57 ± 1	78
Fluorenone Only	---	0	85

(a) Key: A_1 = aliphatic hydrocarbons; A_2 = neutral PAH; A_3 = N-PAC; and
A_4 = hydroxy-PAH.
(b) % conversion is quantity of fluorene in moles versus the initial fluorenone
quantity normalized to 5 mg of sample.
(c) % recovery is the sum of both fluorene and fluorenone as compared with the
initial fluorenone quantity.
* Single point determination.

TABLE 2. Comparative Chemical Class Composition of Process Solvents
from Two Different Direct Coal Liquefaction Technologies

	Aliphatic Hydrocarbons	Neutral PAH/ Hydroaromatic	N-PAC	Hydroxy-PAH
SRC-I Process Solvent	13.9	47.5	13.5	25.1
ITSL Recycle Pasting Solvent	25.9	41.0	21.1	12.0

THE KINETICS OF CATALYTIC HYDROGENATION OF POLYNUCLEAR AROMATIC COMPONENTS IN COAL LIQUEFACTION SOLVENTS*

H. P. Stephens and R. J. Kottenstette

INTRODUCTION

Although the importance of polynuclear aromatic hydrocarbons (PAHs) as hydrogen transfer agents in coal liquefaction has been well established (1,2), there have been few studies of the kinetics of the formation of hydroaromatic donor forms by catalytic hydrogenation. This paper presents the results of hydrogenation experiments performed with single component PAH solutions in an inert solvent and with a complex, multicomponent coal-derived liquid. The rate of hydrogenation of one PAH component found in coal-derived liquids, pyrene, was followed and used to illustrate the impact of reaction conditions on the kinetics and thermodynamics of catalytic hydrogenation of PAHs in liquefaction solvents. The results show that the catalytic hydrogenation behavior of PAHs in complex coal-derived liquids is analogous to that of a single component system. In addition, this study clearly demonstrates PAHs in coal-derived liquids can be quantitatively hydrogenated to donor-solvent products at temperatures as low as 100°C.

EXPERIMENTAL

To establish the thermodynamic behavior of the hydrogenation of pyrene to 4,5-dihydropyrene, reactions were performed over a wide range of conditions: temperatures from 275 to 400°C and pressures from 500 to 2000 psig. Subsequent kinetic experiments with pyrene and the coal-derived liquefaction solvent were performed at 100 and 300°C and hydrogen pressures of 100 and 500 psig.

Materials

Pyrene and n-hexadecane, an inert solvent for the pyrene experiments, were used as received from Aldrich Chemical Company. The coal-derived liquid studied was a hydrogenated Koppers creosote oil used as a start-up solvent in pilot two-stage coal liquefaction experiments (3). Prior to use, it was catalytically dehydrogenated under nitrogen at 425°C. This converted all but approximately 10% of the hydropyrenes to pyrene. Two catalysts were employed for these experiments. Shell 324 M, a Ni-Mo/Alumina catalyst currently used in the second stage of integrated two-stage pilot plant operations (4), was added in its presulfided form to experiments at 275°C and above. Because Shell 324 has a low activity at temperatures below 250°C, reactions performed at 100°C were

catalyzed with a novel catalyst under development, palladium
hydrous titanate (5,6). Both catalysts were added to the
reactors as -200 mesh powders. High purity hydrogen was used
in all experiments.

Apparatus and Procedure

Batch reactions were performed in stainless steel microreactors
(7), equipped with thermocouples and pressure transducers.
Four reactors could be operated simultaneously. After the
reactors were charged with the reactants and catalyst, they
were pressurized with hydrogen and heated to temperature
(heat-up time $\approx$ 1 min) in a fluidized sand bath while being
horizontally shaken at 160 cycles/min. Temperatures and
pressures were recorded with a digital data acquisition system
during the course of the experiments. Following the heating
period, the reactor vessels were quenched (time of quench $\approx$ 10
sec), and the products were removed for analysis.

A separate set of experiments was used to establish that
catalyst particle size and reactor agitation rate were
sufficient to prevent reaction rate retardation due to mass
transfer limitations. It was estimated from reactor heat-up
and quench rates that time at temperature could be determined
to within 0.5 min. Temperatures and pressures were maintained
at the nominal values to within $\pm$ 2°C and $\pm$ 20 psig
respectively.

Product Analyses

The products were washed from the reactor with toluene,
filtered to remove catalyst and transferred to a volumetric
flask. Following the addition of internal standards,
2-methylnaphthalene for the hydrogenation of pyrene in
n-hexadecane and n-tridecane for the creosote oil experiments,
the product solutions were brought to a known volume and
analyzed by gas chromatography.

Packed column chromatography [Hewlett-Packard 5840A with flame
ionization detection (FID)] was sufficient for analysis of the
products from the pyrene reactions. Column and chromatographic
conditions were: 1/8 in x 10 ft. column with Supelco 10%
Sp-2100 on 100/120 Supelcoport, 220°C, 20 cm^3/min nitrogen
carrier gas. However, separation of the product components of
the creosote oil experiments required high-resolution
chromatography (Hewlett Packard 5880A with FID) and a capillary
column: 0.2 mm ID x 30 m long SE 54; 0.56 cm^3/min helium
carrier flow; 100:1 split ratio injection; and a temperature
ramp from 120 to 270°C at 2°C/min.

Gas chromatography/mass spectrometry techniques were used to
identify the order of elution of pyrene and hydrogenated
products. An external standard consisting of a solution of the
internal standard, pyrene, n-hexadecane and 1,2,3,6,7,8-
hexahydropyrene was used to establish FID response factors
relative to the internal standards. The weights (W) of each

component of the product mixture were calculated from the chromatograph area (A), the response of the standard (R_S) and the relative response factor (R_r):

$$W = R_r \cdot R_S \cdot A$$

RESULTS AND DISCUSSION

Thermodynamic Behavior

Qualitative aspects of the hydrogenation of pyrene in n-hexadecane at the higher temperatures of this study can be observed in Figure 1, a plot of the ratio of 4,5-dihydropyrene (H_2Py) to pyrene (Py) concentration as a function of time for experiments performed at 300°C and 500 psig. As can be seen, $[H_2Py]/[Py]$ approaches a constant value which indicates that hydrogenation proceeds by a reversible reaction:

$$H_2 + Py \xrightleftharpoons[k_{-1}]{k_1} H_2Py$$
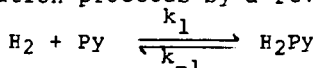
Thus, the maximum (equilibrium) concentration of dihydropyrene $[H_2Py]_e$ which can be formed is limited by the hydrogen pressure P and the value of the equilibrium constant K_p for the reaction:

$$[H_2Py]_e = P \, K_p[Py]_e$$

Results of the experiments at 300°C and 500 psig with creosote oil, Figure 2, have established that the dihydropyrene to pyrene ratio exhibits a similar, though much slower, approach to an equilibrium value.

Results of more than 50 catalytic hydrogenation experiments with pyrene over a wide range of temperatures (275 to 400°C), hydrogen pressures (500 to 2000 psig) and reaction times (5 to 120 minutes) have established the temperature dependence of K_p, as calculated from the pressures and equilibrium concentration ratios of $[H_2Py]_e$ to $[Py]_e$:

$$K_p = \frac{1}{P} \frac{[H_2Py]_e}{[Py]_e}$$

A van't Hoff plot of these values is given in Figure 3. Linear regression of the data yields the temperature (degrees Kelvin) dependence of K_p for the hydrogenation of pyrene to dihydropyrene:

$$\ln K_p = \frac{5330}{T} - 15.86$$

Extrapolation of this equation shows that low temperature hydrogenation greatly favors the formation of dihydropyrene. For example, consider hydrogenation at 500 psig and two temperatures 400°C and 100°C. Although conversion of pyrene to dihydropyrene is limited to 15% at 400°C, equilibrium

conversion at 100°C is greater than 99%. Thus, at high
temperatures pyrene hydrogenation is a reversible process,
while at low temperatures, it is essentially an irreversible
process. In addition, higher values of K_p at low
temperatures permit a substantial reduction in hydrogen
pressure to achieve comparable or better conversions.

Kinetics

For reversible reactions, the approach to equilibrium can be
modeled as a first-order process with an effective rate
constant equal to the sum of the forward and reverse rate
constants (8):

$$\ln \frac{X_e}{X_e - X_t} = (k_1 + k_{-1})t$$

where X_t and X_e are the extents of reaction at time t and
at equilibrium. For pyrene

$$X_t = \frac{[H_2Py]_t}{[Py]_t + [H_2Py]_t}$$

and

$$X_e = \frac{P\ K_p}{1 + P\ K_p}$$

Figure 4 shows a plot of $\ln (X_e/(X_e - X_t))$ vs time at 300°C
and 500 psig for the hydrogenation of pyrene in n-hexadecane
and Figure 5 shows a similar plot for the hydrogenation of
pyrene in creosote oil. As can be seen, although the rate of
hydrogenation of pyrene in the complex solvent may be modeled
by pseudo first-order reversible kinetics, the rate constant on
a catalyst weight basis is two orders of magnitude smaller.
This can be attributed to the presence of many other species in
the creosote oil which compete with pyrene for active sites on
the catalyst.

That catalytic hydrogenation of pyrene proceeds by an
essentially irreversible reaction path at low temperatures is
demonstrated by the results of experiments with pyrene in
n-hexadecane catalyzed with palladium hydrous titanate at 100°C
and 100 psig. Two major products, 4,5-dihydropyrene (H_2Py)
and 4,5,9,10-tetrahydropyrene (H_4Py) are formed under these
conditions. Initial experimentation showed that although the
concentration of H_4Py increased monotonically with reaction
time, the concentration of H_2Py reached a maximum, then
decreased. Because this behavior indicates an irreversible
series reaction path,

$$Py \xrightarrow{k_1} H_2Py \xrightarrow{k_2} H_4Py$$

348
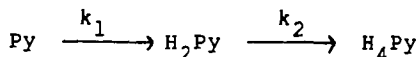
the results of additional experiments (% conversion to H_2Py vs % conversion to H_4Py) were plotted on a series reaction diagram, Figure 6. An excellent fit of the data to a hyperbolic series reaction path expression was obtained:

$$Y + S(X-100) = S(Y+X-100)^{1/S}, \quad S \neq 1$$

where
Y = % conversion to H_2Py
X = % conversion to H_4Py
S = selectivity = k_1/k_2 = 1.5

Therefore, the rate of disappearance of pyrene can be modeled, as shown by Figure 7, by irreversible first-order kinetics:

$$\ln \frac{[Py]_t}{[Py]_o} = k_1 t$$

where $[Py]_o$ is the initial concentration of pyrene.

That pyrene in a complex liquefaction solvent can be hydrogenated irreversibly at low temperatures was demonstrated by hydrogenation of creosote oil at 100°C and 500 psig for 30 minutes with palladium hydrous titanate catalyst. No pyrene could be detected in the hydrogenated creosote oil following the reaction. It was completely converted to hydrogenated products.

CONCLUSION

The ultimate application of this study is to provide guidance for establishing optimum conditions for hydrogenation of coal liquefaction process solvents. The results presented here show that high temperature catalytic hydrogenation of PAH hydrogen donor precursors such as pyrene is reversible and that the maximum conversion to dihydropyrene is thermodynamically limited by a low value for the equilibrium constant K_p. Because a higher value of K_p at low temperatures favors formation of the hydroaromatic product, conversion at low temperatures is kinetically limited. However, advantages of low temperature hydrogenation include quantitative conversion of PAHs to hydroaromatics and a substantial reduction of the hydrogen pressure. Additionally, this study has clearly demonstrated that satisfactory hydrogenation rates at low temperatures may be achieved by using more active catalysts, such as palladium hydrous titanate.

REFERENCES

1. D. D. Whitehurst, T. O. Mitchell and M. Farcasiu, Coal
    Liquefaction, Academic Press, New York (1980).

2. E. Gorin, "Fundamentals of Coal Liquefaction,"
    p. 1845-1918, in Chemistry of Coal Utilization, 2nd
    Supplementary Volume, Martin A. Elliot, Ed.,
    Wiley-Interscience, New York (1981).

3. H. D. Schindler, J. M. Chen, M. Peluso and J. D. Potts,
    "Liquefaction of Eastern Bituminous Coals by the ITSL
    Process," Proceedings of the 7th Annual EPRI Contractors
    Conference on Coal Liquefaction, Palo Alto, CA, May 12,
    1982, Electric Power Research Institute (1982).

4. M. J. Moniz, R. S. Pillai, J. M. Lee and C. W. Lamb,
    "Process Studies of Integrated Two-Stage Liquefaction at
    Wilsonville," Proceedings of the 9th Annual EPRI
    Contractors' Conference on Coal Liquefaction, May 8-10,
    1984, Palo Alto, CA, Electric Power Research Institute.

5. H. P. Stephens, R. G. Dosch and F. V. Stohl, Preprints of
    Papers, American Chemical Society, Fuel Division, Vol. 28,
    No. 1, p. 148 (1983).

6. H. P. Stephens, R. G. Dosch and F. V. Stohl, Ind. Engr.
    Chem., Prod. R&D, in press (1985).

7. R. J. Kottenstette, SAND-82-2495, Sandia National
    Laboratories, Albuquerque, NM, March 1983.

8. J. W. Moore and R. G. Pearson, Kinetics and Mechanisms, 3rd
    Ed., John Wiley & Sons, New York (1981).

FIGURE 1. $[H_2Py]/[Py]$ vs. time for hydrogenation
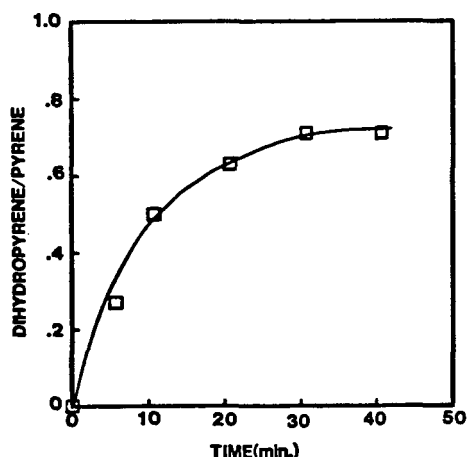of pyrene (100 mg) in n-hexadecane
(1.0 g), 300 C, 500 psig, 15 mg 324M

FIGURE 2. [H$_2$Py]/[Py] vs. time for hydrogenation
of dehydrogenated creosote oil (1.0 g),
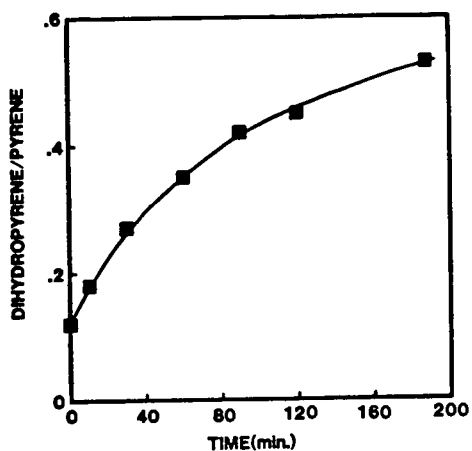300 C, 500 psig, 100 mg 324M

FIGURE 3. von't Hoff plot for hydrogenation of
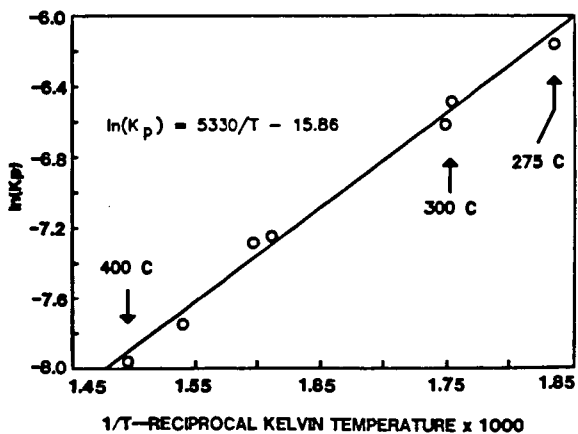pyrene to dihydropyrene, 275 to 400 C

$$\ln(K_p) = 5330/T - 15.86$$

FIGURE 4. Pseudo first-order reversible kinetic plot for hydrogenation of pyrene in n-hexadecane

$k_1 + k_{-1} = 0.13/\text{sec-g}$
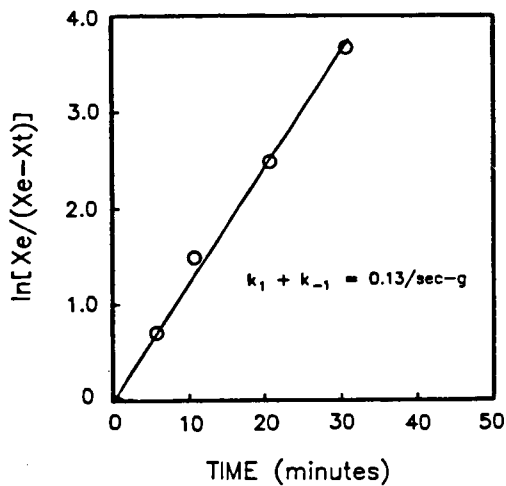
FIGURE 5. Pseudo first-order reversible kinetic plot for hydrogenation of pyrene in dehydrogenated creosote oil
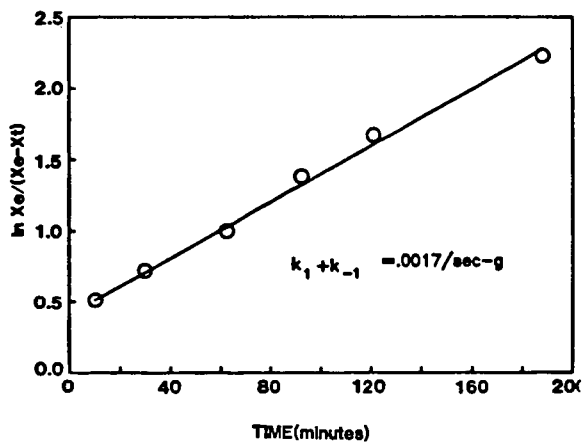
$k_1 + k_{-1} = .0017/\text{sec-g}$

FIGURE 6. Series reaction diagram for hydrogenation of pyrene to di- and tetrahydropyrenes, 100 C, 100 psig
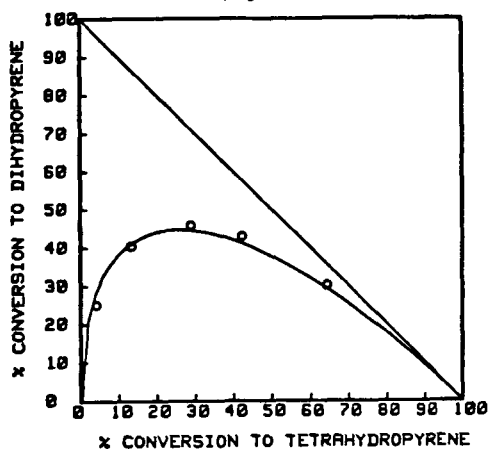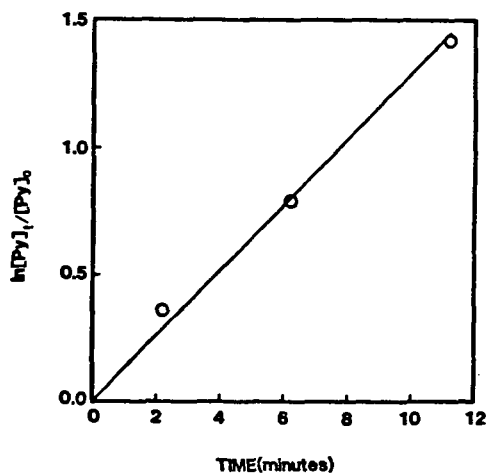

FIGURE 7. Irreversible kinetic plot for hydrogenation of pyrene (100 mg) in n-hexadecane (1g), 100 C, 100 psig, 18 mg Pd titanate

COAL LIQUEFACTION WITH ^{13}C LABELLED CARBON MONOXIDE

S.A. Farnum, A.C. Wolfson, D.J. Miller,
G.E. Gaides, and D.D. Messick

University of North Dakota Energy Research Center
Box 8213, University Station
Grand Forks, North Dakota 58202

Low-rank coals may be successfully liquefied under pressure using CO or mixtures of CO and H_2O or CO and H_2. Following a suggestion in the literature in 1921 (1), Appel and Wender in 1968 reported conversions of both bituminous coal and lignite with CO/H_2O (2). The reaction with lignite was found to be rapid, converting 1:1 lignite/H_2O to benzene-soluble tar plus gases in 87% yield (maf) coal at 2,000 psi initial CO pressure and 380°C. Successful continuous liquefaction of lignite in a Process Development Unit for 28 day runs was demonstrated by Severson and co-workers at the University of North Dakota Chemical Engineering Department's Project Lignite (3, 4). During these runs the wet, as-received coal was processed with 50/50 CO/H_2 (syngas) at about 440°C and 2,500 psig. The heavy product prepared was called "Solvent-Refined Lignite", SRL. Batchelder and Fu evaluated some of the syngas technology in 1979 with respect to process commercialization (5).

The University of North Dakota Energy Research Center has continued to investigate low-rank coal liquefaction using mixtures containing CO. The use of H_2S along with syngas has resulted in much improved processing (6). Recently, low temperature reactions (below 400°C) using CO as the reductant have shown exceptional promise (7).

Several mechanisms for reduction reactions with CO have been proposed. Previous studies at UNDERC have shown that CO apparently reacts more rapidly with coal than does H_2, and that the amount of CO that reacts increases as more as-received lignite is added (8). Whether the CO reacts directly with the coal organic structure or with the water in the coal to produce H_2 in situ, is unknown. The catalytic effect of coal ash on the shift reaction ($CO + \overline{H_2O} = CO_2 + H_2$) may also be a significant factor. Finally, it has been suggested that hydrogen formed from closely bound coal water may be especially active "nascent hydrogen" (2, 9).

We carried out a high temperature study of the reaction of isotopically labelled syngas ($^{13}CO/H_2$) with a Texas lignite at 450°C and 3400-3700 psi in coal-derived solvent (10). This study was designed to determine the amount of CO incorporation into the distilled products and hydrocarbon gases. No incorporation of the ^{13}C was seen, thus eliminating Fischer-Tropsch type reactions, and direct incorporation reactions, such as carbonylation reactions. The only labelled product found was $^{13}CO_2$. At that time we did not examine the insoluble products for ^{13}C incorporation.

The present study was designed to investigate low temperature reactions of three coals of differing rank, Big Brown Texas lignite, Wyodak subbituminous, and Powhatan bituminous coal, with pure CO. The conditions chosen also provide baseline data simulating the first stage in a two-stage liquefaction process. Additional development of analytical methods insured that each part of the product could be examined for ^{13}C incorporation and the gases were more carefully analyzed for $^{13}C/^{12}C$ ratios in each gaseous carbon-containing product by GC/MS.

Experimental

Reactions were carried out in a multiple minireactor assembly designed for simultaneous use of up to twelve 22 mL tubes. The stainless steel tubes each contained a stainless steel stirring bar which mixed slurry and gases when the assembly was agitated in a fluidized sand bath. Five grams of a 40% as-received coal slurry in a coal-derived recycle solvent distillate was charged. Labelled gas, 50/50

[13]CO/CO, or unlabelled CO gas was introduced, via a manifold system, to a pressure of 1,000 psig cold. The assembly was lowered into the bath preheated to the selected temperature, 300°, 340°, or 380°C for 1 hour, rapidly quenched to room temperature, and allowed to equilibrate. Gas weight was obtained by collecting the gas in a preweighed evacuated bomb of known volume relative to the reaction vessel.

The analysis scheme used is outlined in Figure 1. Gas analyses were performed using an automated refinery gas analyzer and $^{13}C/^{12}C$ ratios for the gaseous products were obtained using capillary GC/MS.

A portion of the recovered product was extracted with tetrahydrofuran (THF) and a second portion was microdistilled. A third portion of the recovered product was extracted with CH_2Cl_2 and the solvent was removed with a rotary evaporator at room temperature. A 50 MHz ^{13}C NMR spectrum was obtained for the CH_2Cl_2 soluble fraction using a gated pulse sequence with the decoupler on only during data acquisition. Samples in CD_2Cl_2 with TMS and $Cr(AcAc)_3$ present were pulsed about two hours until the signal to noise ratio was adequate. These spectra were compared with those of samples from reactions performed in the same manner with unlabelled CO. The CH_2Cl_2 insoluble products were examined by 50 MHz Cross Polarization/Magic Angle Spinning (CP/MAS) solid ^{13}C NMR employing total sideband suppression using TOSS dephasing and foldback pulsing before acquisition (11). These spectra were also compared with those of products from reactions run at the same time with unlabelled CO.

Results and Discussion

The weights of product gas, THF insolubles, distillation residue, water, and ash were used to calculate conversions for these reactions. For the purpose of this experiment ^{13}CO and CO were assumed to react at the same rate so that labelled and unlabelled runs could be averaged to obtain yield structures (Table I). The low-rank coals gave better conversion at 300°C but the Powhatan bituminous coal gave better conversions at 340° and 380°C.

Tracer reactions with ^{13}CO are expected to give easily recognizable labelled products because the natural abundance of ^{13}C is only 1.1%. An incorporation of 1% ^{13}C should double the signal. When identical samples for runs with unlabelled CO are compared, an incorporation of only 0.5% should be recognized without difficulty.

The ^{13}C spectra of the soluble and the insoluble products of labelled reactions were carefully compared with those run without labelled CO. No differences were seen for any of the three coal products at 300°, 340°, or 380°C. A comparison of the CH_2Cl_2 insoluble solid spectra from runs using labelled and unlabelled CO are shown in Figure 2.

Gas analyses for selected runs analyzed by capillary GC/MS and GC were used to determine the ratios of ^{13}CO to ^{12}CO and $^{13}CO_2$ to $^{12}CO_2$ and the number of moles of each isotopic compound in the product. The number of moles of CO_2 that was produced from CO was easily calculated since a 50% labelled ^{13}CO was used. The remaining CO_2 produced was assumed to arise from the coal, the only other carbon source present. The number of moles of H_2 found in the product was less than 1/5 the moles of CO_2 formed from CO during the reaction of the two low-rank coals at 300°C. However, during reaction of the bituminous coal, Powhatan (POW1), less CO_2 was formed from the CO added (Figure 3), possibly because the number of moles of water present in the charged coal, POW1, was much smaller, which could limit the shift reactions during the POW1 liquefaction at 300°C. The absence of coal moisture does not, however, limit the conversion of POW1 by CO at higher temperatures, since water may be released by coal thermolysis at 340° and 380°C which could react readily with CO (12).

Table I. Multiple Minireactor Reactions of CO With 40% Coal Slurries for 60 Minutes

No. Runs Averaged	Coal	Temperature, °C	Average Yield (wt % of maf coal)				
			Conversion	Gas	Distillate	Soluble Residuum	Average Closure
5	BB1*	300	20	13.5	3.6	8	92
3	WYO1**	300	24	18	3.7	16	95
3	POW1***	300	16	4.3	6.4	14	96
2	BB1	340	62	24	11.8	27	95
1	WYO1	340	51	30.5	2.0	17.5	94
2	POW1	340	83	29	6.2	46	88
2	BB1	380	77	2	9.3	40	92
2	WYO1	380	72	39	-3.0	35	95
2	POW1	380	87	26	1.9	59	101

Solvent was UNDERC CPU Run 66 D1160 Distillate.

  *BB1 - Big Brown Texas lignite, 8.12% ash, 24.40% water.
 **WYO1 - Wyodak, Wyoming subbituminous coal, 8.37% ash, 24.03% water.
***POW1 - Powhatan, Ohio bituminous coal, 10.78% ash, 2.02% water.

Summary

No ^{13}C incorporation into products other than CO_2 was detected after reactions of Big Brown Texas lignite, Wyodak subbituminous coal, or Powhatan bituminous coal with 50/50 $^{13}CO/CO$ at 300°, 340° or 380°C in recycle solvent for 1 hour. No evidence for a Fischer-Tropsch type mechanism, CO insertion, or carbonylation reactions was found.

These data are consistent with a mechanism involving CO entering into the shift reaction with in situ water. The differing response of the coals can be explained by invoking coal ash liquefaction and shift catalysis and the amount of water intimately connected with each coal (13, 14). The change in response by Powhatan at higher temperatures may be due to a shift mechanism initiated by water released from thermal reactions (12). The success of low temperature CO liquefaction would not be unexpected if a shift reaction mechanism were in operation since the equilibrium constant for the shift reaction favors H_2 and CO_2 at lower temperatures.

Literature Cited

1. Fischer, F. and Schrader, H., 1921, Brennstoff - Chem. 2, 257. (cf. Ref. 2).
2. Appell, H.R. and Wender, I., 1968, Am. Chem. Soc. Div. Fuel Prepr. 12(3), 220.

3. Severson, D.E., Souby, N.M. and Baker, G.G., 1977, <u>Am. Chem. Soc. Div. Fuel Prepr.</u> 22(6), 161.
4. Severson, D.E., Souby, A.M. and Owens, T.C., 1982, "Energy Sources", Vol. 6, No. 3, 173, Crane, Russak and Co., Inc.
5. Batchelder, R.F. and Fu, Y.C., Ind. Eng. Chem. Process Des. Dev., 1979, 18(4), 594.
6. Sondreal, E.A., Willson, W.G. and Stenberg, V.I., 1982, Fuel, 61, 925.
7. Rindt, J.R. and Cisney, S.J., "Low-Temperature Liquefaction of North Dakota Lignite", DOE/FE/60181-21.
8. Knudson, C.L., Willson, W.G., and Baker, G.G. <u>Am. Chem. Soc. Div. Fuel Prepr.</u>, 1981, 26(1), 132.
9. Takemura, Y. and Ouchi, K., 1983, <u>Fuel</u>, 62, 1133.
10. Low-Rank Coal Research Under the UND/DOE Cooperative Agreement, Quarterly Technical Progress Report, April - June 1983, DOE/FE/60181-17, 5-17-5-24.
11. Dixon, W.T., Schaefer, J., Sefik, M.D., Stejskal, E.O. and McKay, R.A., 1982, <u>J. Mag. Reson.</u> 49, 341.
12. Suuberg, E.M., Peters. W.A., and Howard, J.B., in "Thermal Hydrocarbon Chemistry", Advances in Chemistry Series, 183, 1979, Chapter 14, American Chemical Society, Washington, D.C.
13. Lee, J.M., Tarrer, A.R., Guin, J.A., and Prather, J.W., 1977, <u>Am. Chem. Soc. Fuel Div. Prepr. 22(6), 120.</u>
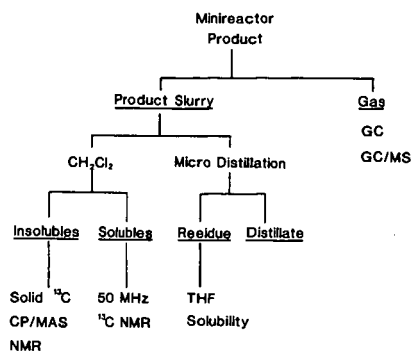14. Given, P.H. Cronauer, D.C., Spackman, W., Lovell, H.L., Davis, A. and Biswas, B., 1975, <u>Fuel</u>, 54, 34.

Figure 1

Minireactor
Product

Product Slurry ──── Gas

CH₂Cl₂   Micro Distillation

Insolubles   Solubles   Residue   Distillate

Solid ¹³C   50 MHz   THF
CP/MAS   ¹³C NMR   Solubility
NMR

Gas
GC
GC/MS

Figure 1. Analysis scheme for minireactor products.

$C_{ar} = 66.3\%$
$C_{aliph} = 33.7\%$

$C_{ar} = 66.0\%$
$C_{aliph} = 34.0\%$
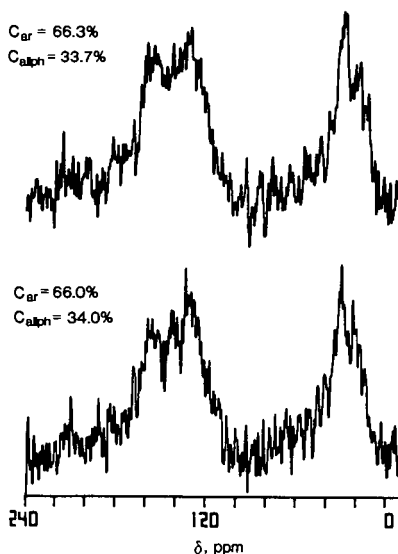
240   120   0

δ, ppm

Figure 2. 50 MHz CP/MAS ^{13}C NMR Spectra of insoluble heavy ends from CO reaction with Big Brown lignite (top) and 50/50 ^{13}CO/CO reaction with Big Brown lignite (bottom).
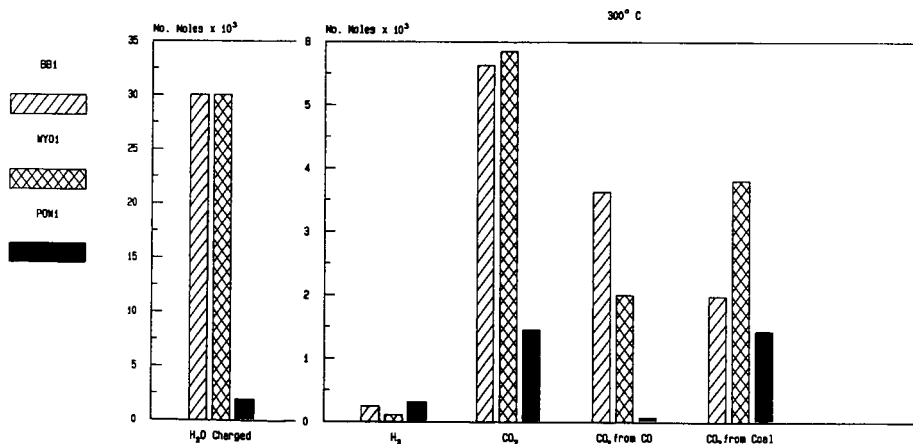
Relative Product Distribution Gases

300° C

BB1

MY01

PO01

No. Moles x 10³

H₂O Charged

No. Moles x 10³

H₂   CO₂   CO₂ from CO   CO₂ from Coal

Figure 3. Gaseous product distribution at 300°C from reactions with 50/50 ^{13}CO/O.

358

WATER-ASSISTED AND NONDONOR-VEHICLE-ASSISTED
COAL LIQUEFACTION

B.D. Blaustein, B.C. Bockrath, H.M. Davis,
S. Friedman, and E.G. Illig

Pittsburgh Energy Technology Center
U.S. Department of Energy
Pittsburgh, PA 15236

and

M.A. Mikita

Department of Chemistry
University of Colorado at Denver
Denver, CO 80202

In continuous coal liquefaction operations, the recycle vehicle has several
functions. First, it serves as the medium in which to slurry the fresh coal feed
and transport it through the preheater into the reactor. Second, it often acts as
a source of hydrogen, i.e., it is a hydrogen donor. Much of the chemistry of coal
liquefaction can be explained by reactions of hydrogen-donor vehicles with coal or
the free radicals generated by thermolysis of coal. In the usual coal lique-
faction process, much of the liquid product serves as recycle vehicle, since the
slurry fed to the reactor is typically two parts recycle vehicle to one part coal.
The throughput of coal for a given reactor might be increased if a lesser quantity
of a readily available material could be substituted for the coal-derived recycle
vehicle. One possible substitute would be water, at least as far as acting as a
slurry medium for fresh coal feed.

Water has been used in the past in the liquefaction or the extraction of coal
for a variety of reasons. When used in combination with carbon monoxide and a
suitable catalyst, water was a source of hydrogen for the reduction of coal [1,2].
In this work, an organic solvent was frequently used in combination with water.
Liquefaction under carbon monoxide has also been carried out with slurries com-
posed of coal and either water or aqueous base without an organic solvent [3,4].
In some cases, water served to carry dissolved metal salts used as homogeneous
catalysts as well as acting as the liquefaction medium [5]. Thus, the elimination
of coal-derived recycle solvents commonly used in liquefaction in favor of water
-- a simple, cheap, and readily available substitute -- has already been
accomplished in the laboratory. In comparison with conventional organic lique-
faction solvents, water has been shown to be quite effective when used in com-
bination with H_2S, in particular under synthesis gas rather than hydrogen [6].
Aqueous liquefaction using impregnated catalysts has also been combined in a
single operation with supercritical water distillation to separate the oil and
asphaltene from the coal char residue [7]. The results clearly show that the
liquids produced by hydrogenation can be extracted by supercritical water and
transported away from insoluble coal residues. It has also been shown that the
simple treatment of coal with supercritical water in the absence of hydrogen or
catalysts renders a substantial portion of the treated coal extractable by tetra-
hydrofuran after the product was cooled and recovered from the autoclave [8]. The
amount of extract obtained depended on the density of the supercritical water.
Higher yields were obtained when coal was injected into supercritical water, thus
providing a rapid heat-up of the coal, than when a coal-water slurry was heated to
operating temperature. From these extraction studies, it is apparent that water
is able to assist the diffusion and dispersal of liquefaction products and
reactants. In addition to these roles, it has also been reported that water may
directly participate as a reactant in the thermolytic chemistry of certain model

compounds. In the presence of water, dibenzyl ether decomposes at 400°C by both pyrolytic and hydrolytic pathways, the latter leading to the formation of benzyl alcohol [9]. The removal of nitrogen from heterocyclic compounds, such as isoquinoline, was also reported to be accelerated in the presence of supercritical water [10].

Taken together, these studies indicate that under various conditions, supercritical water may act as a good liquefaction medium, dissolve or extract coal-derived liquid products, promote the cleavage of certain bonds likely to be found in coal, provide hydrogen through the water-gas shift reaction, and possibly assist the contacting of coal with catalysts or hydrogen. It has also now been made clear by the successful preparation of coal-water mixtures for direct combustion that pumpable slurries can be made at ambient conditions using as little as 30% by weight of water. The present study is intended to evaluate further the role of water, near or above its critical temperature, in the conversion of coal to a liquefaction product. Specifically, we wish to determine whether it is possible, feasible, and, finally, advantageous to use water as a replacement for all or part of the recycle vehicle used for slurrying coal in conventional liquefaction practice. Since water is not a hydrogen donor in the usual sense, the behavior of other nondonors was also examined. It should be pointed out that for coal hydrogenation alone, no vehicle is needed. Much of the previous work on coal hydrogenation was done by simply subjecting dry powdered coal in batch units to a high pressure of gaseous hydrogen, sometimes under the influence of an impregnated catalyst [11].

EXPERIMENTAL

A multireactor consisting of five individual microautoclaves, each of approximately 45-mL capacity and attached to a single yoke, was used to study these reactions [12]. The entire assembly was immersed rapidly into a preheated, fluidized sand bath, allowing heat-up to reaction temperature in 4-6 minutes. Immersion in a second fluidized sand bath held at room temperature provided rapid quenching. The autoclaves were agitated by a rapid horizontal-shaking motion, assuring good mixing of heterogeneous, multiphase mixtures. Individual thermocouples allowed continuous temperature monitoring of each microautoclave. For all experiments reported here, the reactors, once pressurized, were isolated from the gas-handling manifold by a valve and a short length of tubing of negligible volume. This prevented loss of water from the reaction zone due to condensation in the unheated portion of the system. Separate experiments using different reactors, in which it was possible for water to migrate to unheated regions of the system, indicated that such water loss had a profound but erratic effect on measured values for pressure and coal conversion, and generally led to misleading data.

The pressure at reaction temperature was not measured directly in these experiments. Using van der Waal's equation, the partial pressure of water was estimated as 1700 psi at 385°C in those cases where 1.7 g of water was charged. When 3.4 g was charged, the partial pressure was estimated at 2670 psi. At this temperature, the partial pressure due to hydrogen is estimated to be about 2600 psi. Total pressures are thus about 4300 psi or 5300 psi. The density of supercritical water was 0.05 g/mL when 1.7 g was charged and 0.11 g/mL when 3.4 g was charged.

Table 1 gives the analyses of the Illinois No. 6 (River King Mine) bituminous coal and the vehicles used in these experiments.

Most of the conversion values were obtained by the centrifugation method given below. Conversions for run 13 and the three series HD2, HD3, and HD4 were determined by a somewhat different method based on filtration of the insolubles.

TABLE 1. Elemental Analyses of Coal and Vehicles.[a]

Material	C	H	N	O	S
Illinois No. 6 Coal, River King Mine[b]	73.7	5.6	1.5	14.8	4.5
SRC-II Distillate	87.1	8.0	1.4	3.0	0.4
Lummus Vehicle[c]	89.8	6.8	1.0	1.8	0.5

[a] wt.%, daf basis, Huffman Labs, Wheatridge, Colo.

[b] Moisture-free ash content was determined to be 13.6 wt.% for the River King Coal. As used, the coal contained 3 wt.% water.

[c] Obtained from operations of the integrated two-stage Lummus liquefaction plant at Bloomfield, N.J., on Illinois No. 6 coal.

Separate experiments established that similar values were obtained by both methods.

Following gas collection and measurement via water displacement, the reactors were washed out with tetrahydrofuran (THF) together with physical scraping of the reactor walls. The THF was distilled before use to remove the inhibitor. The reactor and contents were sonicated to aid the dissolution and/or dispersion of the products in THF. This was repeated until the THF solution was clear and the reactor tare weights before and after reaction agreed to within +0.01 gram. The total volume of THF so accumulated (~300 mL) was evaporated in a hood to a volume of about 50 mL and transferred to a tared 250 mL centrifuge bottle. Additional THF was added to bring each volume up to ~150 mL, and the bottles were centrifuged at 3500 rpm for 20 minutes. The THF solution was then decanted and an additional 150 mL of THF was added to each residue in the bottle with stirring. This centrifugation/decantation/solvent addition sequence was repeated until the opaque solution became amber and opalescent. Experience indicated that such a process was necessary twice in the higher conversion runs and up to 5 times with lower conversions. The residues (THF-insolubles) were then dried overnight in their bottles in a vacuum oven at 110°C under an aspirator-maintained vacuum. The oven was purged with nitrogen until the temperature was below 60°C, and the bottles with residues were allowed to cool in air and were then weighed. The percent conversion was equal to

$$100 - \frac{\text{wt. THF-insoluble residue - wt. ash}}{\text{wt. moisture, ash-free coal}} \times 100$$

The reproducibility was usually within 1-2%.

The THF solutions obtained from the above procedure were roto-evaporated under an aspirator vacuum in tared, 250-mL round-bottom flasks. When no more solvent was seen to condense, the flasks were dried and the THF-soluble products were thus obtained. In some cases, cyclohexane solubles were isolated using a similar procedure. The THF extracts were transferred to 250-mL centrifuge tubes with 25.0 ± 1 mL of hot THF with the aid of sonication. To these solutions, 125 mL of cyclohexane was added and the centrifugation process employed, followed

by a second extraction with an additional 150 mL of pure cyclohexane. The extracts were recovered by roto-evaporation of the solutions and drying in the vacuum oven at 110° overnight.

For a typical run, the gas analysis showed CO_2 and H_2S were the major gases produced, along with the much lesser amounts of methane, ethane, and propane. The yields for one run were 4.2 wt.% for CO_2, and 0.3 wt.% each for methane, ethane, and propane, on a daf coal basis.

In experiments 6E and 6F of Table 3, where a coal/water/catalyst slurry was used, the procedure was as follows. Catalyst was added to 8.5 mL of solution of 200 ppm Aerosol OT surfactant (American Cyanamid) in water in a round-bottom flask, and the mixture slowly added to 10 g coal with physical mixing, followed by immersion in a sonic bath for 5 minutes, followed by rotation on a roto-evaporator at atmospheric pressure while submerged in a ice bath for 15 minutes. This slurry did not appear to settle with time. The slurry was mixed by hand again just prior to transfer of 7.4 g to the microautoclave. In experiment 6D, an aqueous solution of catalyst was added to the coal in the autoclave; and in 6G, 6H, and 6J, a solution of catalyst containing 200 ppm Aerosol OT was added. In experiment 6K, a slurry made as in 6E and 6F above was dried in a vacuum oven before use. In experiment 6I, such a dried slurry was added to the autoclave with fresh water.

RESULTS AND DISCUSSION

Table 2 shows the results of runs made to measure conversion of Illinois No. 6 (River King Mine) bituminous coal under a variety of conditions selected to uncover effects of water addition. Since this work was directed toward replacing or reducing the amount of organic recycle vehicle normally employed, all of the experiments reported here were conducted with the relatively low vehicle-to-coal ratios of 0.5 or less. Experiments with higher ratios showed no better conversions. As may be seen, without addition of water, conversions for these high coal-content slurries are quite low at the very moderate reaction temperatures employed. The addition of 0.42 parts water based on coal (the amount contained in a 70/30 coal/water slurry) increases conversion significantly. Evidently, reasonable conversions can be obtained using this minimal amount of water provided the loading of recycle vehicle is not too low, that is 1.6 g or above in the case of HD3-1, -2, and -3. We also note that under these mild, non-catalytic conditions the nature of the reducing gas had little effect, since in one experiment (HD4-2), the substitution of carbon monoxide for hydrogen had little effect on the conversion. The use of the more severe conditions of 1200 psi hydrogen (cold) and 427°C produced a small increase in conversion as expected (13 and HD2-3). However, variables other than reaction severity may have more significant effects, since still higher conversions were obtained at 385°C by appropriate choice of the organic vehicle, as discussed later.

A second series of experiments was run under conditions chosen to reveal the effect of the nature of the organic vehicle used in noncatalytic aqueous liquefaction. In a general way, conversions increased moderately as the organic vehicle was changed from one usually considered to be a poor hydrogen donor (1-methylnaphthalene) to vehicles considered to be better hydrogen donors (tetralin and 9,10-dihydroanthracene). Thus, the usual concepts of hydrogen-donor liquefaction chemistry may also be applied usefully to this series of less conventional liquefaction systems.

If good conversion in a noncatalytic system requires a minimal amount of an organic vehicle and also benefits from the addition of some water, it is reasonable to ask if the combination of organic vehicle and water is superior to either used separately. The final set of experiments in Table 2 indicates that this is the case. Conversion was poor without either (HD29-4), much improved with water alone (HD29-3), and still better with SRC-II distillate vehicle alone

(HD19-3,4). A combination of SRC-II distillate and water (HD18-3,4) produced a conversion better than either used separately.

Cyclododecane is a high-boiling hydrocarbon expected to be a poor hydrogen donor. When it was used as a nondonor vehicle, the conversion fell between the value for water and that for SRC-II distillate used in a lesser amount. When used in combination with SRC-II distillate, the conversion was not improved over that of SRC-II distillate alone. This stands in contrast to the result obtained for the combination of SRC-II distillate plus water. This different behavior indicates that addition of the second component to SRC-II distillate is not acting simply to dilute the relatively small amount of the recycle vehicle used in these experiments.

Table 3 contains data for the catalytic liquefaction of coal in the presence of water. When various forms of molybdenum are added to the coal, conversions are substantially increased. Clearly, high temperatures are not required for these molybdenum catalysts to influence liquefaction. More important, with catalyst present, the organic vehicle may be totally replaced by water without loss in conversion. As was seen in Table 2, this result was not obtained in the absence of catalyst. The important function of water is also underscored by the rather low conversion obtained with added catalyst but with no vehicle of any kind, i.e., a dry hydrogenation (6K).

Conversion increases continually with catalyst loading up to at least 1000 ppm molybdenum on coal (6A, HD30-1, -2, -3). Of the several methods used for application of the catalyst, none seemed to give notably superior results insofar as THF conversion values are concerned. However, there are indications now under study that the yield of lighter products may change significantly according to the method of catalyst application.

The surfactant, Aerosol OT, used to assist the preparation of coal/water/catalyst feed slurries had a small beneficial effect on conversion in both the presence of catalyst (HD30-4 vs. HD30-1) and the absence of catalyst (HD29-3 vs. 6A). At this point, it is only possible to speculate that the surfactant enhances the action of the water by improving the wetting of the coal.

In one case (6F), a low-boiling ether, THF, was substituted for water. The conversion was unexpectedly high, albeit the catalyst loading was twice that used with water. Tetrahydrofuran is quite effective in swelling River King coal at room temperature. The connection between this property and the liquefaction result is presently unclear, but investigation of a series of lower molecular weight vehicles may shed more light on the structural requirements for superior performance. These and related experiments are in progress.

Table 4 gives the data for analyses of the THF-solubles isolated from runs HD19-1,2 in which 1000 ppm Mo was used as catalyst in conjunction with surfactant. Except for the higher-than-usual oxygen content, these are typical analyses for a coal liquefaction product. The infrared spectrum of the cyclohexane solubles obtained from a dilute CH_2Cl_2 solution shows that about 2.1 wt.% of oxygen is in phenolic OH and the remaining 5% is presumably in ethers. The carbon aromaticity of the THF solubles was determined by ^{13}C-CP/MAS NMR to be 0.72, which is virtually identical to that of the feed coal. The data for characterization of the products in hand so far are in accord with the rather mild conditions used to bring about the conversions.

The preliminary results obtained so far form a basis for an encouraging outlook on liquefaction with water or other nondonor vehicles. High coal conversions were obtained at modest temperatures with use of little or no organic recycle vehicle. Thus, it is possible and feasible to use water as a substitute liquefaction medium. The advantage in doing so in continuous units is still to be

Elemental Analysis (wt.%)[b]	Cyclohexane Solubles	Tetrahydrofuran Solubles[c]	Tetrahydrofuran Insolubles[c]
C	82.9	81.8	24.5
H	7.3	5.9	1.4
O	7.1	7.3	7.5
N	1.2	1.9	0.5
S	1.8	1.9	6.9
Ash (wt.%), 750°C	---	---	66.2
Molecular Weight, $\bar{M}_n$		1300[d]	

[a] Huffman Laboratories, Wheatridge, Colo.

[b] Average of duplicate microanalyses.

[c] Dried to constant weight @ 30°C under vacuum before analysis.

[d] VPO in pyridine at 90°C.

demonstrated. At the least, a different line of investigation is now open whereby important questions regarding the mechanism of liquefaction may be addressed. Since no organic vehicle need be used, the coal-derived products of liquefaction may be analyzed without interference. At the same time, the presence of a fluid medium provides better heat transfer and better dispersion of the reactants than possible with dry hydrogenations. It is expected that further work will be fruitful by determining how the course of liquefaction is affected by the chemical and physical properties of water or other nondonors and by uncovering the important variables associated with the use of dispersed catalysts at mild liquefaction temperatures.

TABLE 2. Liquefaction of Illinois No. 6 (River King Mine) Bituminous Coal.[a]

Run Number(s)	H_2 Pressure cold, psig	Temp., °C	Time at Temp., min.	Vehicle g.	Vehicle Type	H_2O g.	Conv.[b] %	Notes
HD3-5	800	370	60	1.62	LUM	0	55	Lummus vehicle
HD3-4	800	370	60	2.00	LUM	0	67	
HD3-3	800	370	60	1.29	LUM	1.70	61	
HD3-2	800	370	60	1.60	LUM	1.70	80	
HD3-1	800	370	60	2.00	LUM	1.70	79	
HD4-2	800(CO)	370	60	1.60	LUM	1.72	82	
13,HD2-3,4	1185	427	60	1.98	LUM	1.70	86,87	
HD10-3,4	1200	385	40	1.50	MEN	1.70	77,79	1-Methylnaphthalene
HD10-1,2	1200	385	40	1.50	LUM	1.70	82,84	
HD12-3,4	1200	385	40	1.50	SRC-II	1.70	85,87	SRC distillate
HD12-1,2	1200	385	40	1.50	TET	1.70	88,90	Tetralin
HD15-1,2	1200	385	40	1.50	DHA	1.70	91,93	9,10-Dihydroanthracene
HD29-4	1200	385	30	0	---	0	25	
HD29-3	1200	385	30	0	---	3.4	52	
HD19-3,4	1200	385	30	1.50	SRC-II	0	72,74	
HD18-3,4	1200	385	30	1.50	SRC-II	1.7	86,88	
HD29-2	1200	385	30	3.4	CDOD	---	67	Cyclododecane
HD29-1	1200	385	30	1.50	SRC-II	1.7 CDOD	72	Cyclododecane

[a]Coal charge in each case was 4.0 g.

[b]Based on THF extractions.

365

TABLE 3. Catalytic Experiments and Associated Base Cases in Water-Assisted Liquefaction of Illinois No. 6 Coal.[a]

Ex. #	Vehicle	Water, g.	Catalyst[b]	Precursor/Application[c]	THF Conv.
6C	SRC II	1.7	----		86,88
6D	SRC II	1.7	1000 ppm Mo	aqueous sol. $MoS_4^=$	90,92
6E	SRC II	1.7	1000 ppm Mo	NH_4 molybdate/sol. slurry	89,91
6F	SRC II	1.7, THF	2000 ppm Mo	$Mo_2(OAc)_4$/sol. slurry	90
6A	--	3.4	----	surfactant	67
6G	--	3.4	1000 ppm Mo	$MoS_4^=$/surfact. soln.	86,90
6H	--	3.4	1000 ppm Mo	NH_4 molybdate/surfact. soln.	85,87
6I	--	3.4	1000 ppm Mo	$MoS_4^=$ impreg. coal, then water	91
6J	--	3.4	1000 ppm Mo	$MoS_4^=$/surfact. soln.	89,91
6K	--	---	1000 ppm Mo	NH_4 molybdate impreg. coal	76,78
HD30-1	--	3.4	1000 ppm Mo	NH_4 molybdate/surfact. soln.	87
HD30-2	--	3.4	250 ppm Mo	NH_4 molybdate/surfact. soln.	80
HD30-3	--	3.4	100 ppm Mo	NH_4 molybdate/surfact. soln.	73
HD30-4	--	3.4	1000 ppm Mo	NH_4 molybdate/aqueous soln.	84

[a] Reaction conditions: 4.00 g River King coal; 385°C; 30 minutes at temperature; 1200 psig (cold) hydrogen, using 1.50 g SRC-II distillate where indicated.

[b] ppm metal on coal. See Experimental Section for details.

[c] When the use of a surfactant is indicated, aerosol OT was employed at ≈200 ppm in water.

REFERENCES

[1] H.R. Appell, I. Wender, and R.D. Miller, Chem. Ind., 1703 (1969).

[2] H.R. Appell, Energy, 1, 24 (1976).

[3] D.S. Ross and J.E. Blessing, Fuel, 57, 379 (1978).

[4] D.S. Ross, J.E. Blessing, Q.C. Nguyen, and G.P. Hum, Fuel, 63, 1206 (1984).

[5] D.S. Ross, Q.C. Nguyen, and G.P. Hum, Fuel, 63, 1211 (1984).

[6] V.I. Stenberg, R.D. Hei, P.G. Sweeny, and J. Nowok, Am. Chem. Soc. Div. Fuel Chem. Preprints, 29(5), 63 (1984).

[7] P. Barton, Ind. Eng. Chem., Process Des. Dev., 22, 589 (1983).

[8] G.V. Deshpande, G.D. Holder, A.A. Bishop, J. Gopal, and I. Wender, Fuel, 63, 956 (1984).

[9] M.E. Paulaitis, M.T. Klein, and A.B. Stilles, DOE Quarterly Report, DE-FD22-82PC50799, July-September, (1983).

[10] D.M. Tiffany, T.J. Houser, M.E. McCarville, and M.E. Houghton, Am. Chem. Soc. Div. Fuel Chem. Preprints, 29(5), 56 (1984).

[11] C.O. Hawk and R.W. Hiteshue, "Hydrogenation of Coal in the Batch Autoclave," U.S. Dept. of the Interior, Bureau of Mines, Bulletin 622, (1965).

[12] R.R. Anderson and B.C. Bockrath, Fuel, 63, 329 (1984).

ACKNOWLEDGMENT

DISCLAIMER

Reference to a brand or company name is made to facilitate understanding and does not imply endorsement by the U.S. Department of Energy.

AQUEOUS LIQUEFACTION OF ILLINOIS NO. 6 COAL

Bogdan Slomka, Tetsuo Aida,
and Thomas G. Squires

Ames Laboratory*
Iowa State University
Ames, Iowa   50011

INTRODUCTION

Near its critical point (T_c = 374°C, P_c = 218 atm.), water is a good solvent for organic (1) as well as inorganic materials while, at ambient conditions, most organics are insoluble in water. Water is also thermally stable, even at temperatures above 450°C, and has a large heat capacity. Finally, water is very cheap compared to other solvents.

By virtue of this combination of properties, water has great potential as a solvent for coal liquefaction and has drawn the attention of a number of investigators in recent years (2-6). These researchers have established a number of advantages for water including:

    i.   Ease of separation of solvent and product;

    ii.   Minimal char production (2);

    iii. Use of soluble catalysts (3,4); and

    iv. Relatively high liquefaction yields.

Recently, we developed a unique flow mode reactor (7) which has enabled us to isolate processes contributing to coal liquefaction and to investigate them dynamically. Using this reactor with a variety of solvents, we established 300°C as the threshold temperature for thermal chemical solubilization of Illinois No. 6 Coal; and in the 360-420°C range, we obtained conversions ranging from 15% in hexane to 44% in toluene.

Our recent investigations have focused on two important components of coal conversion: thermal chemical reactions and dissolution of coaly material (including thermolysis products) in the solvent; and we are exploring the effects of temperature and pressure on these processes. Here, we report the initial results of our investigation of these effects in the aqueous liquefaction of coal and compare these results to those obtained with other solvents.

EXPERIMENTAL

General

Illinois No. 6 coal from the Ames Lab Coal Library was used in these studies. This coal has the following ultimate analysis (dmmf basis): 78.82% C; 5.50% H; 1.59% N; 2.29% S_{org}; and 10.05% ash. Prior to use, this coal was ground, sized to 60 x 100 mesh, and dried at 110°C overnight under vacuum. Conversions were measured gravimetrically and are reported as % weight loss on a raw coal basis.

Flow Mode Extraction of Coal

The liquefaction experiments were carried out in the apparatus shown schematically in Figure 1. Typically, the reactor was loaded with 500 mg. of coal (leaving a free volume of 0.70 ml); and the system was filled with solvent and brought to operating pressure (usually 3000 psi). Heating (rate $\sim 150^\circ$C/min) and solvent flow (1.0 ml/min) were initiated simultaneously; and constant temperature and pressure were attained within three minutes. Extraction was continued for one or, in some cases, two hours. In some experiments, conditions were changed at predetermined points during the run. After cooling and flushing with nitrogen, the residue was removed from the reactor, dried at 110°C overnight under vacuum, and weighed.

RESULTS AND DISCUSSIONS

The advantages of the Flow Mode Extractor used in these experiments has been established in a previous report from this laboratory (7). These advantages are analogous to those reported for other rapid heating, continuous product removal techniques (e.g. heated grid vacuum pyrolysis (8)) and include suppression of retrogressive reactions and dynamic observation of changes which occur during the course of the conversion.

Flow Mode Extraction of Coal with Water

Our initial experiments were conducted for the purpose of comparing aqueous extraction yields to those which had been obtained using a series of nominally unreactive organic solvents (9). Figure 2 shows a comparison of the extraction yields for these solvents at 420°C and 3000 psi with that of water at 400°C and 3580 psi. Clearly, water is one of the best "nonreactive" solvents for the thermal liquefaction of coal. This conclusion also holds at 370 and 400°C, the other temperatures included in this investigation.

We can find only one basis for comparing batch and flow mode systems in the aqueous liquefaction of Illinois No. 6 Coal. At 400°C Vasilakos reports batch mode conversions of 34.0% (3580 psi) and 29.5% (3070 psi) (10). Under identical conditions in our reactor, we find extraction yields of 38.2% and 33.6%, respectively.

Temperature and Pressure Effects on Aqueous Liquefaction

Because of the unusually high critical pressure of water ($P_c = 3206$ psi; cf. benzene: $P_c = 716$ psi), interesting temperature/pressure/conversion relationships were expected for aqueous extraction of coal. The effects of temperature and pressure on conversion are reported in Table 1. Trends in this behavior are more apparent in Figure 3 which plots conversion vs. density for a series of isotherms.

At 370°C, conversion begins to decrease quite rapidly as the density approaches 0.15 g/ml, and we believe that there are similar "threshold" densities at the higher temperatures. However, pressures fluctuated wildly during the latter experiments, and we were unable to obtain meaningful data under these conditions. In the low density

Table 1. Effect of Temperature and Pressure on the Aqueous Extraction of Illinois No. 6 Coal

Expt. No.	Temperature ($^{\circ}$C)	Pressure (psi)	Density[a] (g/ml)	Weight Loss (%)
16	370	1925	0.061	14.6
17	370	2950	0.151	31.8
18	370	3207	0.485	34.9
22	380	2950	0.128	34.3
11	380	3220	0.174	35.4
21	380	3750	0.482	35.6
19	400	3070	0.113	33.6
20	400	3580	0.163	38.2

a. For pure water (11).

region, it appears that conversion is limited by solubility since thermal processes should proceed at about the same rate under both high and low density conditions.

Our final series of experiments were designed to determine whether the "extract" remaining in the low density residue after extraction for one hour at 370°C and 1925 psi was recoverable by simply increasing the pressure to 2950 psi. We suspected that, at 370°C, much of this material would be fixed by retrogressive reactions during the period of low density extraction. Surprisingly, in a two stage experiment at 370°C (first stage 1925 psi, extraction time 1 hour; second stage 2950 psi, extraction time 1 hour), we obtained an extraction yield of 31.6% compared to 31.8% conversion for one stage extraction at 2950 psi. We are puzzled by this behavior and plan to continue our investigations by analyzing products at discrete intervals during the course of the conversion.

REFERENCES

1a. Barton, P.; Fenske, M. R. Ind. Eng. Chem. Process Des. Dev. **1970**, 9, 18.

1b. Barton, P.; Hajnik, D. F. In "Adsorption and Ion Exchange with Synthetic Zeolites," ACS Symposium Series 135, Flank, W. F., Ed., American Chemical Society, Washington, D. C., **1980**, Chapter 12.

2. Modell, M.; Reid, C.; Amin, S. I., U. S. Patent 4,113,446, **1978**.

3. Barton, P. Ind. Eng. Chem. Process Des. Dev. **1983**, 22, 589.

4. Ross, D. S.; Nguyen, Q. C.; Hum, G. P. Fuel 1984, 63, 1211.

5. Ross, D. S.; Blessing, J. E.; Nguyen, Q. C.; Hum, G. P. Fuel 1984, 63, 1206.

6. Deshpande, G. V.; Holder, G. D.; Bishop, A. A.; Gopal, J.; Wender, I. Fuel 1984, 63, 956.

7. Squires, T. G.; Aida, T.; Chen, Y. Y.; Smith, B. F. Prepr. Pap.-Am. Chem. Soc., Div. Fuel Chem. 1983, 28(4), 228.

8. Freihaut, J. D.; Zabielski, M. F.; Seery, D. J. Nineteenth Symposium (International) on Combustion, The Combustion Institute, 1982, p. 1159 and references cited therein.

9. Unpublished results from this laboratory.

10. Vasilakos, N. P.; Dobbs, J. M.; Parisi, A. S. Prepr. Pap.-Am. Chem. Soc., Div. Fuel Chem. 1983, 28(4), 212.

11a. Canjar, L. N.; Manning, F. S. "Thermodynamic Properties and Reduced Correlations for Gases," Gulf Publishing Company, Houston, Texas.

11b. Keenan, J. M.; Keyes, F. H. "Thermodynamic Properties of Steam," John Wiley & Sons, Inc., 1951.

FIGURE 1. Rapid Heating Flow Mode Reactor
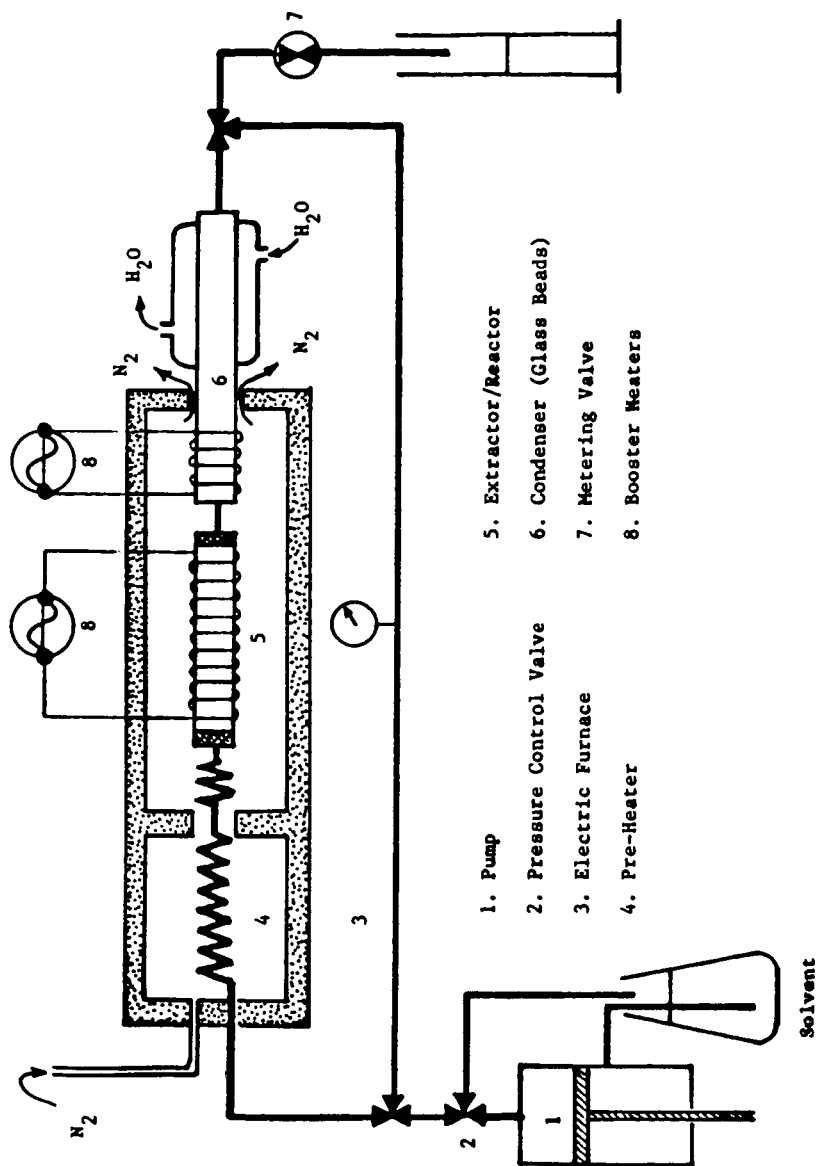
1. Pump
2. Pressure Control Valve
3. Electric Furnace
4. Pre-Heater

5. Extractor/Reactor
6. Condenser (Glass Beads)
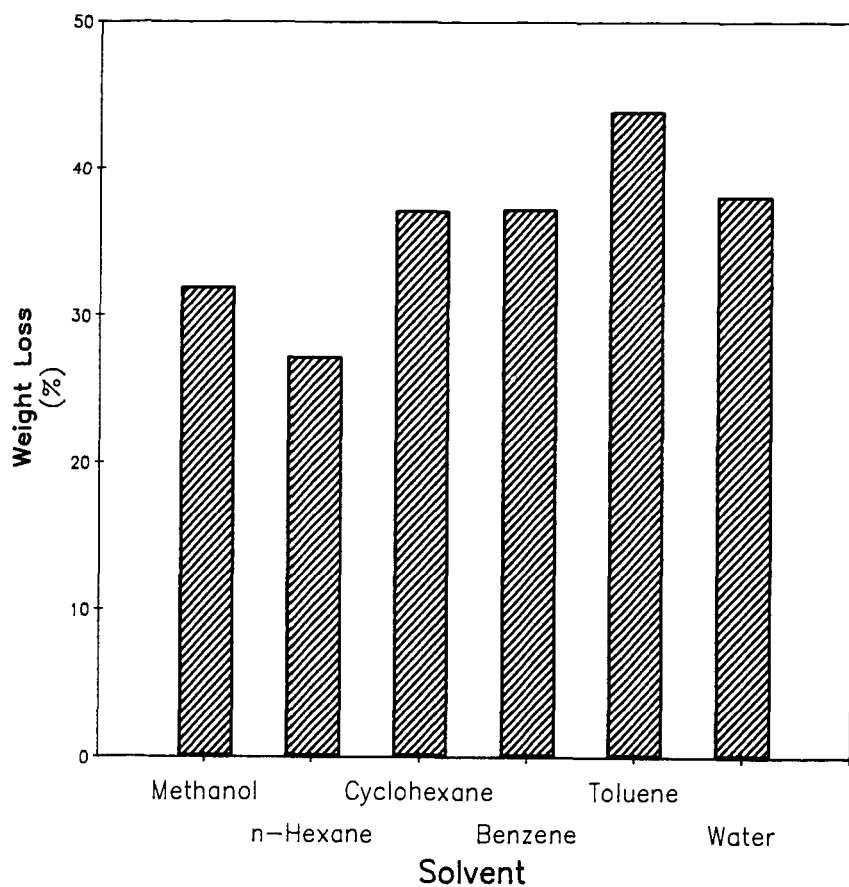7. Metering Valve
8. Booster Heaters

FIGURE 2. Solvent Extraction of Illinois No. 6 Coal at 420°C[a] and 3000 psi[a] (2 Hours[b])

a. Aqueous extraction conducted at 400°C, 3580 psi.

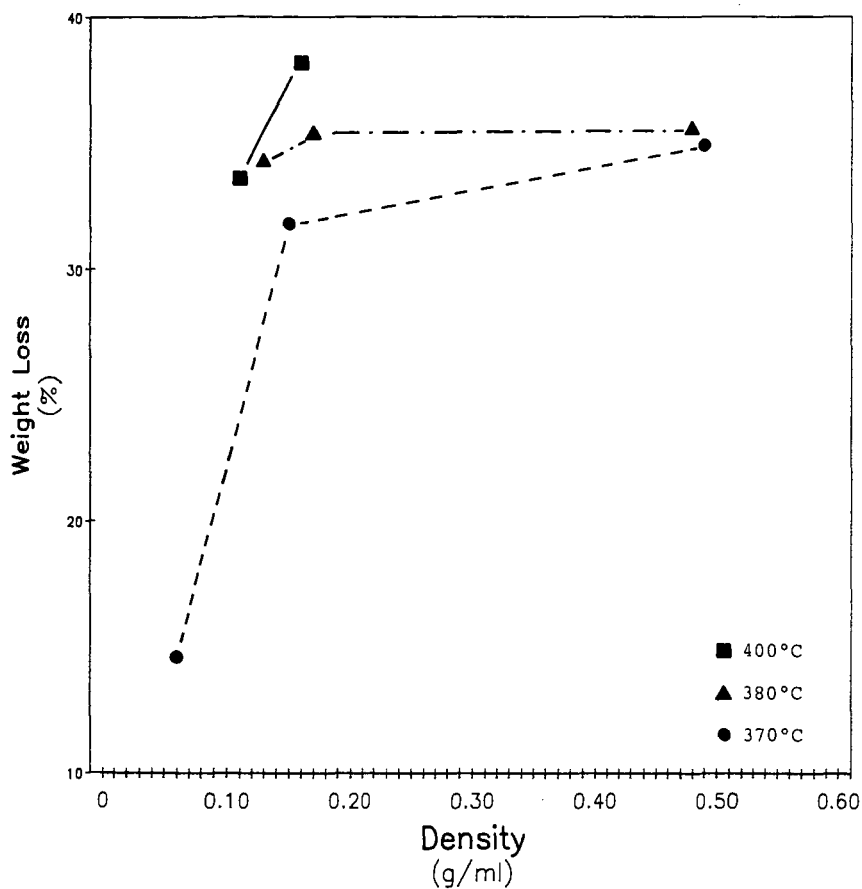b. Benzene and water extractions reported for 1 hour.

FIGURE 3.   Density and Temperature Effects in the Aqueous
            Extraction of Illinois No. 6 Coal